HSE
Health & Safety Executive

In vitro dermal absorption of liquids

Prepared by the
Skin Research Group
Department of Environmental
and Occupational Medicine
University of Newcastle
for the Health and Safety Executive

CONTRACT RESEARCH REPORT
350/2001

HSE
Health & Safety Executive

In vitro dermal absorption of liquids

Simon C Wilkinson PhD
and Faith M Williams PhD
Skin Research Group
Department of Environmental
and Occupational Medicine
University of Newcastle
Newcastle-upon-Tyne
NE2 4HH
United Kingdom

The absorption of several widely used solvents as neat liquids and in aqueous vehicles through dermatomed human skin was measured in vitro using flow through diffusion cells with tissue culture medium as receptor fluid. Butoxyethanol (BE) and ethoxyethanol (EE) exhibited higher apparent permeability coefficients (k_p) than more volatile (acetone, 1-methoxy-2-propanol, tetrahydrofuran, methyl ethyl ketone) or more lipophilic solvents (toluene and xylene) in both aqueous (200 μl) and neat finite (10.5 μl) vehicles. Pyridine showed comparable apparent k_p values to EE. The apparent k_p with aqueous 2-methyl pyridine was 2-3 fold greater than with aqueous pyridine, but was about 9-fold lower in neat, finite doses. Apparent k_p values with aqueous vehicles were much higher than with neat finite doses, as was the total percentage absorbed. Predictions of k_p were in good agreement with experimental data for neat, infinite doses of most solvents. There was a relation between log P and apparent k_p with aqueous doses for the more hydrophilic solvents (log P < 3). The relation between log P and apparent k_p for neat finite doses was complicated by the influence of volatility. Our findings have contributed significantly to risk assessment of liquid solvents.

This report and the work it describes were funded by the HSE. Its contents, including any opinions and/or conclusions expressed, are those of the authors alone and do not necessarily reflect HSE policy.

HSE BOOKS

First published 2001

ISBN 0 7176 2048 4

CONTENTS **Page**

Publications

Wilkinson SC and Williams FM (2000) Factors affecting dermal absorption of 2-ethoxyethanol from aqueous solution in vitro. Poster presentation at the British Toxicology Society Annual Congress, York University, April 2000. Toxicology Abstract in Press.

Williams FM and Wilkinson SC (2000) Factors affecting dermal absorption of ethoxyethanol *in vitro* - implications for risk assessment. In: Prediction of Percutaneous Penetration STS Publishing. In Press.

EXECUTIVE SUMMARY

Introduction

Dermal absorption of harmful substances in occupational and domestic environments is now a cause for concern. The importance of dermal absorption compared to exposure by inhalation for volatile compounds is increasing as steps such as improved respiratory protective equipment are taken to reduce inhaled dose by workers. *In vitro* dermal absorption experiments using excised human skin with intact barrier properties have a complimentary role to biological monitoring in refining risk assessment models. In the present study, the dermal absorption of selected occupationally relevant solvents (with a range of physicochemical properties) was studied *in vitro*. The effects of dose regime/vehicle and other experimental conditions on dermal absorption *in vitro* were investigated. Experimental findings were compared with predictions from the dermal knowledge based system, and the influence of physicochemical parameters such as vapour pressure and lipophilicity was examined.

Methods

Human breast skin (full thickness or dermatomed to about 330 μm) was mounted in Scott-Dick flow through diffusion cells. Tissue culture medium (MEM Eagle, pH 7.4) was used as receptor fluid (1.5 ml h^{-1}, 32˚C). Solvents were applied to the skin surface (0.64 cm^2) in three dose regimes/vehicles: neat finite (10.5 μl), aqueous infinite (200 μl) or neat infinite (200 μl). Charcoal filters were placed over the donor chamber to trap volatilized dose material. Levels of test compounds in receptor fluids were measured over 24 h. Levels in surface swabs, cell washes, stratum corneum (by tape stripping), skin tissue and charcoal filters were measured after 24 h. Levels of 2-ethoxyethanol (EE) and 2-butoxyethanol (BE) were measured using ^{14}C-labelled

analogues. Other test compounds (1-methoxy-2-propanol [M2P], methyl ethyl ketone [MEK], tetrahydrofuran [THF], acetone, toluene, *m*-xylene, *o*-xylene, pyridine, 2-picoline, 2,4-lutidine and 2,4,6-collidine) were determined using GC FID following solvent extraction. Steady state flux and time to steady state were derived from the linear region of cumulative absorption-time curves. Permeability coefficients were calculated by dividing the steady state flux by the donor concentration.

Results

The volatility of the test compounds was an important factor in determining dermal absorption. The majority of the dose (60-99%) was volatilized, depending on the dose regime or vehicle, and absorption into receptor fluid ceased after about 5 h for EE and BE, 1-2 h for MEK, THF and acetone, and 4 h for toluene and xylene. EE and BE were the most extensively absorbed test compounds. EE and BE had similar steady state fluxes (6.5 and 7.2 μmol cm^{-2} h^{-1} [584.1 and 852.1 μg cm^{-2} h^{-1}] respectively) in neat finite doses, though the absorption phase was longer for BE resulting in higher total absorption of BE (13.8% of the applied dose) than EE (3.7%). The steady state flux of M2P was much lower (0.7 μmol cm^{-2} h^{-1} [60.0 μg cm^{-2} h^{-1}]) and the steady state was short-lived, resulting in lower absorption (0.5%). Steady state fluxes for aqueous solutions of glycol ethers (3 mg ml^{-1}) were lower than for finite neat doses, but apparent k_p values for BE (0.0214 cm h^{-1}) and EE (0.0042 cm h^{-1}) were much higher in aqueous solution than in neat doses (0.0009 and 0.0006 cm h^{-1} respectively). Flux for aqueous M2P was again smaller than BE or EE. Steady state flux and absorption of aqueous EE was, surprisingly, greater from 100 μl applied than 200 μl. Furthermore, increasing the donor concentration of EE to 6 mg ml^{-1} resulted in a seven-fold increase in flux. These data suggested that there was concentration of dose solution with EE in an aqueous vehicle, possibly due to differential evaporation of the vehicle. Use of full thickness skin significantly reduced the time to steady state for EE and the steady state flux of BE. Addition of PEG 20 or BSA to receptor fluid approximately doubled the flux of all three glycol ethers from both aqueous and neat vehicles. Neat finite doses of EE and BE gave similar fluxes to neat infinite doses, though this was not the case with M2P, due to the volatility of this compound.

Absorption of the more volatile test compounds (MEK, THF, acetone) was markedly lower in finite neat doses (0.05-0.2% of the applied dose) than the glycol ethers, due to a much shorter absorption phase, though fluxes of MEK and THF were comparable with that of neat M2P. The steady state flux of neat finite acetone (178 nmol cm^{-2} h^{-1} [10.3 μg cm^{-2} h^{-1}]) was less than MEK (457 nmol cm^{-2} h^{-1} [33.0 μg cm^{-2} h^{-1}]) or THF (567 nmol cm^{-2} h^{-1} [40.9 μg cm^{-2} h^{-1}]). Again, the apparent k_p with aqueous solutions

was 70 to 150-fold higher than with neat finite doses. Steady state flux values from neat finite doses of MEK, THF and acetone were much lower than for neat infinite doses, due to rapid evaporation of the dose material. The was no significant effect of a neat finite application of these compounds on $^{3}H_2O$ absorption, hence there was no evidence of an occupationally relevant exposure resulting in barrier damage.

Steady state absorption of neat finite doses of toluene and xylenes was rapidly established but low (131, 242 and 182 nmol cm^{-2} h^{-1} [12.1, 25.7 and 19.5 μg cm^{-2} h^{-1}] for toluene, *m*-xylene and *o*-xylene respectively), probably due to low solubility of these compounds (log P 2.69 to 3.12) in the aqueous matrix of the epidermis and upper dermis. Again, the apparent k_p for these compounds in an aqueous vehicle was much higher than with neat doses. A much higher percentage absorption was observed (25 to 79%) with aqueous doses than with neat finite doses (0.2-0.6%).

Steady state absorption with pyridine (7.9 μmol cm-2 h-1 [0.63 mg cm-2 h-1]) was approximately ten-fold greater than with 2-picoline in neat finite applications. Addition of further methyl groups increased the temporal length of the absorption phase, the time to steady state and the flux and apparent kp. With aqueous applications, flux and apparent kp of 2-picoline were 2 to 3-fold higher than pyridine, but addition of further methyl groups did not further increase either parameter. Again, the apparent kp from aqueous applications exceeded that of neat applications ten- to 100-fold.

KBS predictions of k_p (based on an infinite dose of a saturated aqueous solution) were in good agreement for neat infinite doses of EE, BE, M2P and MEK, though values for acetone and THF were overestimated. Experimentally-determined k_p values for large volume aqueous solutions of glycol ethers, MEK, THF and acetone were greatly underestimated by the KBS. However, corresponding values for the aromatic compounds were well predicted by the KBS. KBS predictions generally overestimated absorption parameters for neat finite doses of test compounds, but this was not the case for BE and EE.

Conclusions

1. The length of the absorption phase was reduced for test compounds with higher vapour pressures (MEK, THF and acetone).

2. Steady state flux (and hence k_p) were influenced by log P and vapour pressure. A lower flux and k_p was measured with compounds with relatively low lipophilicities and high vapour pressures such as M2P and acetone whilst higher values were

measured with compounds with relatively higher lipophilicities and/or lower vapour pressures such as EE and BE. However, compounds with very high lipophilicities (toluene and xylenes) showed low flux and total absorption, due to low solubility in the aqueous matrix of the epidermis and dermis. In a neat, finite dose, the apparent k_p of pyridine exceeded that of 2-picoline, 2,4-lutidine and 2,4,6-collidine, though addition of methyl groups to 2-picoline increased apparent kp in a neat dose.

3. Flux and apparent k_p were markedly influenced by vehicle effects for all test compounds. In particular, apparent k_p values for dilute aqueous solutions were several fold higher than for neat finite doses. This is probably due to partitioning of the dose solution into the stratum corneum when aqueous vehicles were used, increasing the effective concentration gradient for diffusive flux. There was also an increase in the percentage of the dose solution absorbed with aqueous vehicles, indicating that there was less opportunity for the dose solution to be lost through evaporation. In contrast to neat finite applications, the apparent k_p of 2-picoline was 2-3 fold higher than pyridine when aqueous doses were used. Addition of methyl groups to 2-picoline did not further influence apparent kp, again contrasting the situation with neat finite doses.

4. Behaviour of EE was unusual in aqueous doses. Greater absorption from smaller volumes and a disproportionate increase in flux with donor concentration suggested that concentration of the dose solution occurred.

5. Absorption of EE and BE was markedly reduced with full thickness skin, indicating that the lower dermis presents a barrier to absorption *in vitro*. It is likely that dermatomed skin would give a better representation of the situation *in vivo*, since the vascular system in the upper dermis is not perfused *in vitro*.

6. Addition of PEG 20 or BSA to receptor fluid enhanced steady state flux of the glycol ethers in both aqueous and occupationally relevant neat doses. Inclusion of such materials in receptor fluid may reflect more closely the situation *in vitro*, and the case for including these materials for the study of hydrophilic test compounds should be considered.

7. Predictions of k_p were in good agreement with those obtained experimentally in neat infinite dose regimes for the glycol ethers and MEK, though they were overestimated for THF and acetone. However, predicted k_p values were much lower than those obtained for dilute aqueous donor solutions of EE, BE, M2P, MEK, THF, acetone and the pyridines*in vitro*, and use of predicted values to

calculate flux from aqueous solutions would greatly underestimate flux from these compounds. This was not the case with the aromatic compounds, for which good agreement between predicted and experimental values was observed with aqueous vehicles.

8. Predictions of absorption parameters were, as expected, overestimated for occupationally relevant doses of most test compounds, due to evaporation of the dose. However, reasonably good estimates were made of flux and k_p for EE and BE in neat finite doses. The k_p for neat pyridine was also reasonably predicted, though this was not the case for its methyl derivatives.

1.0 INTRODUCTION

This report details work carried out on the main project (including the core group of twelve solvents) between June 1999 and June 2000 and the supplementary project on pyridine and its derivatives, carried out between June 2000 and October 2000.

1.1 Aim of project

1. To assess the potential for solvents to penetrate skin using an *in vitro* approach in order to better appreciate the role of skin absorption in occupational exposure. To further validate the dermal knowledge based system (KBS) using solvents of occupational relevance and with a range of physicochemical properties.

1.2 Objectives

1. To study the absorption of a range of solvents through skin *in vitro* under different conditions.

2. For a series of solvents to compare absorption from a neat liquid application at finite and infinite dose and from an aqueous solution to assess effect on skin penetration.

3. To compare results from the *in vitro* system with predictions from QSAR strategies and the knowledge-based system to predict the influence of physicochemical parameters on dermal absorption.

1.3 Background to Project

Most substances are capable of penetrating skin to some degree so that the dermal absorption of harmful substances is now of concern. Consequently, skin has become increasingly important in our appreciation of the risk of occupational, domestic and environmental exposure to hazardous materials. In risk assessment it is important to determine the potential dermal absorption of chemicals to which there may be occupational exposure and to define the contribution of dermal uptake to the total body burden. The relative importance of dermal absorption compared to exposure by inhalation for volatile compounds is increasing as steps such as improved respiratory protective equipment are taken to reduce inhaled dose by workers. Parallel steps must be taken to determine dermal exposure and to reduce it with appropriate protection measures such as gloves to protect the hands and wearing of overalls. When the skin is

the primary route by which the chemical enters the body, dermal exposure measurements and biological monitoring play complimentary roles in defining exposure. These should be related to *in vitro* predictions of dermal absorption in order to refine risk assessment models.

The barrier properties of skin almost exclusively reside in its outermost layer, the stratum corneum, which is composed of essentially dead keratinocytes. Material absorbing from the surface of the skin crosses the stratum corneum by diffusion through the keratinocytes and upper dermis and is removed to the systemic circulation via the dermal capillaries. For some compounds follicular absorption may also be important. Isolated skin retains its barrier function and may be used in *in vitro* studies to predict absorption *in vivo*. *In vitro* techniques for studying absorption through the skin have been developed employing either static or flow-through diffusion cells that have been shown to reproduce *in vivo* dermal absorption (e.g. Scott and Ramsey 1987; Roper *et al*.,1995,1997,1998; Howes *et al*., 1996; Dick *et al*., 1997a,b). The flow-through cell, in which tissue culture medium was pumped continuously below the skin, was developed to maintain skin viability so that the potential for local metabolism during percutaneous absorption could be assessed. The absorption profile thus obtained may be closer to the *in vivo* situation than the static cell using ethanol/water as receptor (e.g. Bronaugh and Stewart, 1984,1985; Bronaugh *et al*., 1990; Clark *et al*. 1991, 1993; Clowes *et al*. 1994, Williams, 1998).

Predicting dermal uptake is particularly important for solvents which are widely used in industry. For a volatile liquid, dermal exposure normally occurs following immersion with direct contact to the substance either as the neat liquid or as a component of a liquid mixture. Immersion may occur in a large volume of liquid from which evaporation does not influence the dermal dose (such as hand immersion), or there may be contact with a small volume which will evaporate during exposure, such as a splash of solvent. There may also be direct absorption of the vapour through the skin although the relative importance of this route is unknown for most volatile chemicals.

Quantitative structure-activity relationships (QSAR) have been developed and used to predict the dermal absorption of a chemical on the basis of its physicochemical properties (Flynn, 1990; Potts and Guy, 1995; Barratt, 1995). Most published QSAR models and knowledge based systems have used data obtained with infinite doses in order to simplify the predictive algorithms. However occupational dermal exposure particularly of volatile solvents usually involves finite doses as the small volume of solvent that comes in contact with the skin rapidly evaporates (Payne, 1995). Results

from the *in vitro* system can be compared with predicted values in order to develop QSAR models and refine the knowledge-based system developed at HSE (Dick and Williams, 1998). The aim is to derive parameters relevant to absorption of chemicals through the skin in man therefore it is appropriate to consider *in vitro* values for absorption through human skin in the first instance if they can be derived.

1.4 Chemicals to be studied in in vitro dermal absorption experiments

Choice of solvents was influenced by the requirements of HSE for risk assessment and availability of human volunteer data and the requirement to investigate series of solvents to validate the knowledge based system.

Three groups of related solvents were selected for study (summarised in Table 1.1), each group consisting of structurally related compounds and a pair of isomers:

1. glycol ethers: 2-ethoxyethanol, 1-methoxy-2-propanol and 2-butoxyethanol;
2. methyl ethyl ketone, tetrahydrofuran and acetone; and
3. toluene, *m*-xylene and *o*-xylene.

This would enable measurements and predictions to be made on compounds with the same molecular weights but differing physical properties such as vapour pressure and lipophilicity (Table 1.1). The three groups represented a range of lipophilicities (3>2>1).

Table 1.1 Physicochemical properties of substances tested in flow through studies

Data on log P (log_{10} octanol:water partitioning coefficient) were obtained from Hansch *et al*. (1995), except for toluene (Chion *et al*., 1982) and 1-methoxy-2-propanol (Meylan and Howard, 1995). Skin irritancy data were obtained from safety information supplied with chemicals and from Croner's Substances Hazardous to Health (Kellard, 1999).

Substance	**Mol wt.**	**log P**	**Vapour Pressure (KPa @25˚C)**	**Water solubility**	**Skin irritancy**
2-butoxyethanol	118.18	0.83	0.12	$1x10^6$ mg/l	redness
2-ethoxyethanol	90.12	-0.32	0.71	Miscible	redness
1-methoxy-2-propanol	90.12	-0.55	1.60	Miscible	redness
methyl ethyl ketone	72.11	0.29	12.1	$3.53x10^5$ mg/l @ 10˚C	redness
tetrahydrofuran	72.11	0.46	21.6	Miscible	redness
acetone	58.08	-0.24	30.8	Miscible	none
toluene	92.15	2.69	3.89	700 mg/l @ 23˚C	redness
m-xylene	106.16	3.20	1.11	162 mg/l @ 25˚C	irritant
o-xylene	106.16	3.12	0.88	178 mg/l @ 25˚C	irritant

1.5 Dermal absorption data on the chemicals studied

The rapid absorption of volatile organic chemicals across skin has been demonstrated (e.g. Morgan *et al*., 1991). DiVincenzo *et al*. (1978) found that immersing the hands in methyl butyl ketone for 1 hour would provide twice the absorbed dose that would result from inhaling the vapour over the same period. Glycol ethers are versatile solvents that are miscible with both aqueous and organic media. Their chemical and physical properties have resulted in their widespread use in industrial and household applications. Glycol ethers penetrate skin rapidly (Kezic *et al*., 1997a,b; Filon *et al*., 1999) and dermal absorption of these compounds therefore presents a significant health

risk. Kezic *et al* (1997a) recently estimated the contribution of skin absorption to be around 55% and 42 % total uptake for 2-methoxyethanol and 2-ethoxyethanol respectively. They have investigated dermal absorption of both vaprous (Kezic *et al*., 1997 a,b; 1998; 2000a) and neat liquid applications (Kezic *et al*., 1997a,b; 2000b) and have shown it to relate to the physicochemical characteristics of the chemical. The ability to predict the dermal absorption profile of ethoxyethanol in the rat *in vivo* from *in vitro* studies with rat skin has recently been demonstrated (Lockley *et al*., 1999, Lockley, 2000). By inference, *in vitro* studies of human skin should be predictive of *in vivo* penetration in humans. However, the influence of some experimental conditions employed in *in vitro* models remains to be determined. A human volunteer study showed that dermal uptake of MEK and THF vapour contributed 3-3.5% and 1-2% of the total body burden respectively, including inhalation (Brooke *et al*., 1998), but no recent data on dermal absorption of these compounds from the liquid phase are available. Tsuruta (1996) showed that dermal penetration of liquid toluene in mice was enhanced by methanol, the k_p being 4.7 times higher in a 50% (v/v) mixture of toluene in methanol than in pure toluene. No such effect was measured in benzene:toluene mixtures. Dermal absorption of toluene vapour in human volunteers contributed 1-1.5% of the total body burden (including inhalation) (Brooke *et al*., 1998). Absorption of liquid toluene (neat, 200 or 300 µl) through split human skin amounted to 1.9 to 3.9% of the applied dose, depending on the skin donor in unventilated conditions (Boman and Maibach, 2000). Absorption depended upon lipophilicity and volatility (vapour pressure). Xylene is usually present as a mixture of three isomers, *ortho*- (1,2-dimethylbenzene), *para*- (1,4-dimethylbenzene) and *meta*- (1,3-dimethylbenzene). Acute exposure occurs primarily by inhalation, but xylene vapour can be absorbed through the skin (Engström *et al*., 1977; McDougal *et al*., 1990; Loizou *et al*. 1999). Percutaneous penetration of a technical grade mixture of xylene isomers (including 19% (v/v) ethylbenzene) in a neat infinite dose regime (10 cm^2, 4 h exposure) has been studied using a perfused pig ear model (De Lange *et al*., 1994). The degree of penetration of xylene into the perfusing medium was profoundly influenced by the protein content of the medium.

2.0 MATERIALS AND METHODS

2.1 Materials

2.1.1 Chemicals used

Table 2.1 Name, source and purity of solvents tested in flow through diffusion studies

Solvent	CAS number	Source	Purity (min. assay) and/or grade
1-methoxy-2-propanol	107-92-8	Aldrich	98%
2-ethoxyethanol	110-80-5	Aldrich	Spectrophotometric
2-butoxyethanol	111-76-2	BDH	98% GPR
methyl ethyl ketone	78-93-3	BDH	99-101% LabAR
tetrahydrofuran (stabilized with 0.1% quinol)	109-99-9	BDH	99.5% AR
acetone	67-64-1	Fisher	99.99% AR
toluene	108-88-3	Fisons	99.7% AR
m-xylene	108-38-3	Aldrich	99%
o-xylene	95-47-6	Aldrich	98.2% HPLC

Solvents used in dermal absorption studies are listed in Table 1. [2-^{14}C]-labelled analogues of 2-ethoxyethanol (205 KBq mg^{-1}) and 2-butoxyethanol (407 KBq mg^{-1}) were kind gifts from Unilever Research. Other solvents used for analytical techniques were: dichloromethane, methanol (both from Fisher, HPLC grade), carbon disulphide (Aldrich, Spectrophotometric grade, 99+%), 1,4 dioxan (BDH, special for chromatography, 99.7%), 2-isopropoxyethanol (Aldrich, 99%) and cyclohexane (BDH, AR, 99.5%). HiSafe 3 liquid scintillation fluid was obtained from Fisher Chemicals. Biolute S tissue solubiliser was from Zinser Analytic. All other chemicals (Sigma) were of at least reagent grade and used as supplied, unless indicated. Water was distilled and then purified by a Purite water polishing system that yielded a product of resistivity 18.2 $M\Omega\ cm^{-1}$.

2.1.2 Skin

Human breast skin was obtained after cosmetic surgery from a local hospital and stored at -70˚C until required. The procedure for obtaining skin was given approval by the University of Newcastle Medical and Dental Ethics committee.

2.1.3 Other materials

Dermatome blades (18 mm wide, gamma sterilised) were obtained from Adams Healthcare.

2.2 General methodology

2.2.1 Flow through diffusion studies

Skin was thawed at room temperature for 30 minutes and kept on ice until required. Skin was either used full thickness (after removal of any blood, subcutaneous fat or connective tissue) or dermatomed using a Davies Miniplex Seven small electric dermatome (blade width 18 mm) to prepare a membrane consisting of the stratum corneum, epidermis and upper dermis (approximately 330 μm thick), and mounted in Scott-Dick diffusion cells (n=4 or 5, skin from at least two donors). In selected experiments with 2-ethoxyethanol, skin was dermatomed and stored resting on the remaining skin at 4˚C overnight prior to use the next day. Receptor fluid (Eagle's Minimal Essential Medium, containing 2.2 g l^{-1} sodium hydrogen carbonate and 200 μg ml^{-1} gentamicin, pH 7.4 maintained by gassing with CO2/air) was pumped through at 1.5 ml h^{-1} using a peristaltic pump. The receptor fluid reservoir and cells were maintained at 32˚C using water jacket connected to a thermostatic circulating water bath. The lower (receptor) chamber of the Scott-Dick diffusion cells was continuously stirred using a magnetic stirrer bar. In some experiments, receptor fluid was supplemented with 2% (w/v) bovine serum albumin fraction V (BDH) (BSA) or 2% (w/v) or 6% (w/v) PEG 20 oleyl ether (Volpo). For aromatic compounds (toluene and xylenes), 2% (w/v) BSA was added to receptor fluid. However, there were availability problems with this material, and 2% PEG 20 Oleyl ether was added in place of BSA in certain studies. Receptor fluid was pumped through flow through cells containing mounted skin for at least 30 minutes prior to application of the dose solution to ensure rehydration of the skin. The dose solution was applied to the surface of the skin (0.64 cm^2) in three alternative doses for each chemical: a large volume (100 or 200 μl) of an aqueous solution (3 mg ml^{-1} unless otherwise stated); a finite dose of neat solvent (10.5

μl); or an infinite dose of neat solvent (200 μl). For experiments with 2-ethoxyethanol (EE) and 2-butoxyethanol (BE), [2-^{14}C] EE or [2-^{14}C] BE (58 KBq in each case) respectively were also added in aqueous solution and neat finite doses. Charcoal filters (2-5 per cell) were placed over the donor chamber to trap any volatilized dose solution. Silver foil was wrapped around the cell for infinite doses of neat solvent. Receptor fluid samples collected at time intervals for 24 h unless otherwise stated. Receptor fluid samples collected within in the first five hours of a study were frozen within two hours of collection. No observable decrease in analyte concentration was observed in this time (Chapter 3). Samples collected after this time were either frozen or analysed immediately at the beginning of the next day. Correction for the time spent at room temperature was possible from studies in Chapter 3, but this was not necessary in practice, as penetration of most compounds into receptor fluids ceased within 5 hours due to evaporation of the dose material. Those compounds in which the temperal length of the absorption phase was longer than this (EE, BE) were of sufficiently low vapour pressure and high water solubility to prevent loss if analyte from receptor fluids at room temperature over a 16 hour period.

2.2.2 Distribution analysis

After 24 h, the charcoal filters and/or foil were removed and the surface of the skin carefully swabbed with tissues soaked in 3% (w/v) aqueous Teepol to recover any remaining dose material. The diffusion cells were then disassembled and the cells swabbed as above. The stratum corneum was removed by sequential tape stripping (8-15 tape strips). The first tape strip was analysed separately. The remaining skin was retained.

In studies using radiolabelled compounds skin samples were minced with scissors and digested in 2 ml biolute until homogenous. Swabs, tape strips, and skin digests were mixed thoroughly with 10 ml HiSafe 3 prior to liquid scintillation counting using a Wallac 1410 beta counter. Dose material trapped on the charcoal filter was desorbed in dichloromethane:methanol 95:5 (v/v) (2.5 ml). Duplicate aliquots (100 μl) were taken for scintillation counting.

For experiments with methyl ethyl ketone (MEK), tetrahydrofuran (THF), toluene and xylenes, swabs, tape strips and skin samples (undigested) were mixed with 2 ml CS_2 containing a suitable internal standard (1,4-dioxan (1180 μM) for MEK and THF or cyclohexane (926 μM) for toluene, *m*-xylene and *o*-xylene), mixed thoroughly and stored at -20˚C for 72 h. An emulsion was formed in swab and wash samples after squeezing of tissues into glass vials. This was eliminated by freezing, thawing and

refreezing. An aliquot of each CS_2 phase (500 µl) was transferred to a crimp top vial for gas chromatography for determination of the parent compound as described below. Dose material collected on the charcoal filters was desorbed by addition of CS_2 with internal standard as above. After thorough mixing, filters were incubated at room temperature for 30 minutes before the desorbates were transferred to vials for GC for determination of the parent compound as described below.

For experiments with 1-methoxy-2-propanol (M2P), and studies with unlabelled EE and BE, swabs, tape strips and skin samples (undigested) were mixed with 2 ml dichloromethane:methanol 95:5 % (v/v) containing EE (1030 µM), M2P (1023 µM) or isopropoxyethanol (867 µM) respectively as internal standards, mixed thoroughly and stored at -20˚C for 72 h. After freezing, thawing and refreezing of swabs and washes as above, an aliquot of the organic phase (500 µl) was transferred to a crimp top vial for gas chromatography for determination of the parent compound as described below. Dose material from filters was desorbed with 2.5 ml dichloromethane:methanol 95:5 % (v/v) containing an appropriate internal standard, thoroughly mixed and incubated at room temperature for 30 minutes before transferring to vials for GC as described below.

The methods described above were assessed for efficiency of recovery by addition of known concentrations of parent materials to swabs, tape strips and skin samples and compared with recovery from control vials containing only the standards. Recovery was over 95% of the control value in each case.

2.2.3 Analysis of receptor fluid samples

In studies using radiolabelled compounds, levels were measured by liquid scintillation counting of aliquots (200 µl) in HiSafe 3 scintillation fluid as described above. Aliquots of the dose solution (10-50 µl) were also counted to enable recovery to be determined.

For experiments with M2P and unlabelled EE and BE, aliquots of receptor fluid (0.5 to 1.0 ml) were mixed with an equal volume of aqueous 1,4-dioxan (1173 µM), M2P (1023 µM) or isopropoxyethanol (867 µM) respectively as internal standards in polypropylene tubes (5 ml capacity). Dichloromethane:methanol 95:5 (v/v) was added (0.75 ml), and the tubes were stoppered and agitated on a rotary shaker (45 rpm) for 30 minutes. Standard solutions of the parent compounds were prepared in receptor fluid (0 to 205 µM) and treated as for receptor fluid samples. Curves were plotted of standard concentration against apparent parent compound concentration. Sample

concentrations were determined by interpolation. The concentration in the dose solutions was also measured in this way for aqueous doses. The concentration for neat doses was calculated from density values in the literature.

For experiments with MEK, THF and acetone, aliquots of receptor fluid (0.5 to 1.0 ml) were mixed with an equal volume of aqueous 1,4-dioxan (1173 μM) as an internal standard in polypropylene tubes as above. CS_2 (0.75 ml) was added and tubes were stoppered and agitated on a rotary shaker (45 rpm) for 30 minutes. Concentrations in samples and dose standards were determined from standard curves prepared in the corresponding receptor fluid or from density values as above.

For experiments with toluene, *m*-xylene and *o*-xylene, aliquots (1.0 ml) of receptor fluid were mixed with cyclohexane (926 μM) in aqueous solution containing 0.1% (v/v) methanol (1.0 ml) as an internal standard in polypropylene tubes as above. For receptor fluids containing 2% (w/v) BSA, 0.75 ml CS_2 was added and tubes agitated as above. For receptor fluids containing PEG 20 Oleyl ether, dichloromethane:methanol 95:5% (v/v) (0.75 ml) was used in place of CS_2. Concentrations in samples and dose standards were determined from standard curves prepared in the corresponding receptor fluid as above.

2.2.4 Gas chromatography column and conditions

GC was carried out using a Hewlett Packard 5890 Series II chromatograph, equipped with an Ultra 1 (cross linked methyl siloxane) column (50 m, 0.32 mm i.d., 0.52 μm film thickness). A split ratio of 10:1 was employed. The injector temperature was 200˚C. Detection was by flame ionisation detection using hydrogen (130 KPa) and air (270 KPa) with nitrogen (150 KPa) as auxiliary gas. Helium was used as a carrier gas (column head pressure 75 KPa). The detector temperature was 250˚C. An injection volume of 1 μl was used. M2P, EE, acetone, MEK and THF were eluted isothermally at 35˚C. BE, toluene, *m*-xylene and *o*-xylene were eluted using the following temperature program: 40˚C for 3 minutes; 20˚C/min to 80˚C. Hold for 3 minutes. Details of methods development are given in section 3.1. Peak area measurement was done using a Hewlett Packard HP3396A integrator.

2.2.5 Calculation of absorption parameters

Steady state flux (J) values were calculated from the slope of the linear region of cumulative absorption-time curves (Fig 2.1). Apparent permeability coefficient (k_p) was calculated by dividing the flux rate (in mol cm^{-2} h^{-1}) by the concentration of the test

compound in the donor solution in mol cm^{-3}. The time to steady state was obtained from the intercept of cumulative absorption time curves on the time axis. The total amount of compound absorbed was calculated from the maximum of the absorption time curve and expressed both in absolute terms and as a percentage of the applied dose. Absorption parameters were compared using one-way ANOVA.

2.2.6 Prediction of absorption parameters using knowledge based system

Predicted values for flux, permeability coefficient and time to steady state were generated from physical properties using the Dermal KBS knowledge-based system at the Health and Safety Executive, Magdalene House, Bootle, by Ms Elanor Ball. A full list of the output (including input parameters used) is given in the Appendix.

2.2.7 Studies with tritiated water

In one flow through study, the effect of application of acetone, MEK and THF in neat finite (10.5 µl) doses on the integrity of the stratum corneum was assessed by pre- and post-application measurement of tritiated water absorption. After mounting the skin and pumping through receptor fluid for at least 30 minutes, tritiated water (50 µl, about 100000 DPM per cell) was applied and receptor fluid samples collected at intervals of 30 minutes over the next 4 h. After this time, any remaining water was carefully removed with a pasteur pipette, and the dose solutions were applied. After 24 h from application of the dose solutions, a second dose of tritiated water was applied (as above) and the process repeated. Aliquots of receptor fluid (0.5 ml) were mixed with 1 ml HiSafe 3 in eppendorf tubes and tritium activity was measured by liquid scintillation counting using a Wallac 1410 beta counter. Permeability coefficients (k_p) for water were calculated from the steady state region of cumulative absorption-time curves for each cell pre-and post-application of the solvent dose solution. Cells with a pre-application of 1.5×10^{-2} cm h^{-1} or greater were considered damaged during dermatoming and were rejected.

2.3 Flow through studies carried out

1. Absorption of EE, BE and M2P in aqueous vehicle through dermatomed skin
2. Absorption of EE and BE in different volumes in aqueous vehicle through dermatomed skin
3. Absorption of EE and BE in aqueous vehicle through full thickness skin

4. Absorption of EE in aqueous vehicle through dermatomed skin with BSA and PEG 20 in receptor fluid
5. Absorption of aqueous EE through freshly and previously stored dermatomed skin
6. Absorption of EE and BE in aqueous vehicle at high concentration through dermatomed skin
7. Absorption of neat finite doses of EE, BE and M2P through dermatomed skin
8. Absorption of neat finite doses of EE, BE and M2P through dermatomed skin with PEG 20 in receptor fluid
9. Absorption of neat infinite doses of EE, BE and M2P through dermatomed skin
10. Absorption of neat finite doses of MEK, THF and acetone through dermatomed skin
11. Absorption of MEK, THF and acetone in aqueous vehicle through dermatomed skin
12. Absorption of neat infinite doses of MEK, THF and acetone through dermatomed skin
13. Absorption of neat finite doses of toluene, *m*-xylene and *o*-xylene through dermatomed skin
14. Absorption of toluene, *m*-xylene and *o*-xylene in aqueous vehicle through dermatomed skin

3.0 DEVELOPMENT OF ANALYTICAL METHODS

3.1 Quantitation of M2P, EE and BE in receptor fluids

Quantitation of M2P, EE and BE in receptor fluid samples was carried out by solvent extraction followed by gas chromatography. Isothermal elution at 35˚C separated M2P (rt = 2.21 min) and EE (rt = 2.77 min) from the solvent front. Increasing the oven temperature to 80˚C eluted BE (rt = 6.91 min). The glycol ethers studied here did not partition successfully into CS_2, so extraction with dichloromethane:methanol 95:5 (v/v) was used. A volume of MEM containing the parent compound (0 to 205 μM) was mixed with an equal volume of internal standard (as a solution in high purity water) and 0.75 ml of CH_2Cl_2:MeOH added. After mixing on a rotary mixer for 30 minutes and settling, 0.5 ml of the lower layer was removed for analysis by GC. Standard curves were prepared of each parent compound and the apparent concentration of the parent compound plotted against the actual concentration (Fig 3.1-3.3). A linear regression line was fitted to the data and the equation derived was used to calculate actual concentrations in unknown samples. A variety of internal standards were assessed for M2P measurement (Fig 3.1), EE measurement (Fig 3.2) and BE measurement (Fig 3.3). 1,4-dioxan (1173 μM) was selected as the internal standard for use in M2P detection (r-squared = 0.9915, $P<0.001$, Fig 3.1). 2-methoxyethanol gave a highly linear response (r-squared = 0.9993) but was not integrated reproducibly because it eluted closely to the solvent peak. M2P (1023 μM) was selected as an internal standard for EE (r-squared = 0.9910, $P<0.001$, Fig 3.2) whilst isopropoxyethanol (867 μM) was selected as an internal standard for BE (r-squared = 0.9779, $P<0.001$, Fig 3.3). The detection limit was 5 μM in each case.

3.2 Quantitation of MEK, THF and acetone in receptor fluids

Quantitation of MEK, THF and acetone in receptor fluid samples was carried out by solvent extraction followed by gas chromatography. These compounds were successfully separated by isothermal elution at 35˚C when CS_2 was used as a solvent though acetone was not detected when CH_2Cl_2:MeOH 95:5 (v/v) was used and hence use of this solvent for extraction of MEK, THF and acetone was discontinued. Analysis of parent compounds was carried out essentially as in section 3.1, with CS_2 was used as the extracting solvent. Standard curves of each parent compound were prepared as in section 3.1 (Fig 3.4). 1,4-dioxan (1173 μM) was an effective internal standard for MEK (r-squared = 0.9919, $P<0.001$) and THF (r-squared = 0.9913, $P<0.001$) whilst MEK (1116 μM) was selected as an internal standard for acetone (r-

squared = 0.9444, P<0.001). The detection limit for MEK (rt = 1.62 min) and THF (rt = 1.93 min) was 1 μM; that for acetone (rt = 1.17 min) was 10 μM.

3.3 Quantitation of toluene, *m*-xylene and *o*-xylene in receptor fluids

Quantitation of toluene, *m*-xylene and *o*-xylene in receptor fluid samples was carried out by solvent extraction followed by gas chromatography. In receptor fluids supplemented with 2% (w/v) bovine albumen fraction V, both CS_2 and CH_2Cl_2:MeOH 95:5 (v/v) were successfully used to extract parent compounds. However, CS_2 also extracted PEG 20 oleyl ether. Hence CH_2Cl_2:MeOH 95:5 (v/v) was used to extract receptor fluids supplemented with PEG 20 oleyl ether. A temperature program of : 40˚C for 3 minutes; 20˚C/min to 80˚C; hold for 3 minutes, successfully separated toluene (rt = 3.82 min), *m*-xylene (rt = 5.53 min) and *o*-xylene (5.93 min). Analysis of these compounds in receptor fluids and preparation of standard curves were carried out as in section 3.1. Cyclohexane (926 μM) in water containing 0.1% (v/v) methanol was a suitable internal standard for all three parent compounds (Fig 3.5). Detection limits for all three compounds were 1 μM.

3.4 Measurement of analyte loss during sample collection in a flow through study

It appeared likely that the volatile parent compounds may be lost by evaporation and/or other processes from receptor fluid samples collected during a flow through study (cooling the autosampler was not practicable). It was important, therefore, to measure levels of losses of the parent compounds during collection. Standard solutions of M2P, EE, MEK, THF, toluene and xylene (mixed isomers) were prepared and dispensed in 1.5 ml aliquots into 4 ml polystyrene tubes (the standard fraction size) and either capped or left uncapped for up to 24 h at room temperature. Concentrations of parent compounds were measured at time intervals using the methods described in section 2.2.3.

M2P concentrations in MEM decreased from 30.2 μM at time zero to 24.3 ± 0.8 μM in uncapped tubes and to 25.3 ± 0.7 μM in capped tubes after 4 hours (Fig 3.6) (P<0.05 in both cases). In a separate overnight study, M2P concentrations decreased from 18.1 μM at time zero to 14.4 ± 0.7 μM in uncapped tubes, compared with 14.3 ± 0.3 μM in capped tubes (P<0.05 in both cases). In contrast, EE levels in MEM did not decrease significantly from initial levels over 24 h (Fig 3.6). MEK concentrations increased slightly from initial levels (44.9 μM) after 2 h incubation at room temperature to 52.5 ± 0.9 μM in uncapped tubes and 51.4 ± 5.7 μM in capped tubes (Fig. 3.7). There was a

marked decrease in MEK concentration to about 50% of initial levels after overnight storage in uncapped tubes ($P<0.01$). This decrease was numerically lower in capped tubes, but capping did not significantly reduce loss of MEK. THF concentrations in MEM did not fall significantly from initial levels (24.6 μM) after 2 h incubation, regardless of capping. As with MEK, THF levels decreased markedly after overnight incubation in uncapped tubes to 9.1± 0.3 μM ($P<0.001$), though the decrease in capped tubes was almost completely reversed (main plot and interaction $P<0.001$). Both toluene and xylene concentrations decreased dramatically after overnight incubation in uncapped tubes ($P<0.001$) (Fig 3.8), though again, this decrease was reduced with capping ($P<0.01$).

It was clear from these studies that evaporation of EE was not a practical problem during sample collection. For other compounds, however, it was clear that receptor fluid samples required freezing as soon as was practicable after collection. In practise, samples were frozen two hours after collection for initial samples (0 to 5 h), well within the limit for any observable decrease in analyte concentration. Samples taken after this time were not frozen until the next day, or for radiolabelled compounds, were sampled and analysed at the beginning of the next day.

4.0 PERCUTANEOUS PENETRATION OF 1-METHOXY-2-PROPANOL, 2-ETHOXYETHANOL AND 2-BUTOXYETHANOL

4.1 Percutaneous penetration of EE, BE and M2P from large volumes of aqueous solution

All three glycol ethers applied to dermatomed human skin in aqueous solution (200 µl, 3 mg ml^{-1}) were absorbed into receptor fluid (Fig 4.1). Although the rate and extent of absorption differed markedly between compounds, no further absorption into receptor fluid was measured after about 5 h in each case, probably because of evaporation of the dose material. Steady state absorption of BE was rapidly established with a time to steady state of 0.30 ± 0.03 h being measured. The steady state flux for BE was 544 ± 64 nmol cm^{-2} h^{-1}, giving a corresponding apparent k_p of 0.0214 ± 0.0025 cm h^{-1} (Table 4.1). Absorption increased linearly to a maximum of 1.39 ± 0.17 µmol (27.3 ± 0.3 % of the applied dose). The absorption time curve for EE was more sigmoidal than for BE (Fig 4.1) with a longer time to steady state (1.67 ± 0.14 h) and a much lower flux and apparent k_p (143 ± 19 nmol cm^{-2} h^{-1} and 0.0042 ± 0.0006 cm h^{-1} respectively, Table 4.1). The final level of absorption for EE (0.34 ± 0.06 µmol, corresponding to 5.1 ± 0.9 % of the applied dose) was also much lower than for BE. The rate and extent of absorption of M2P was lower than both EE and BE (Fig 4.1). Whilst the time to steady state for M2P (0.68 ± 0.09 h) was shorter than for EE, the steady state flux (48 nmol cm^{-2} h^{-1}) and apparent k_p (0.0014 ± 0.0002 cm h^{-1}) for M2P were both much lower than for EE (Table 4.1). The final level of absorption was also correspondingly lower (0.15 ± 0.02 µmol, 2.3 ± 0.2% of the applied dose).

Distribution analysis of glycol ethers from large volume aqueous doses (Table 4.2) showed that very little material was detected in surface swabs, cell washes, tape strips or skin digests for any of the three compounds studied. Levels were especially low in the tape strips, suggesting that the stratum corneum did not contain a reservoir of these compounds 24 hours after application. Slightly more EE than BE or M2P was recovered from cell washes and swabs, whilst slightly more BE than EE or M2P was detected in skin digests. The remainder of the material from all three compounds that was not absorbed into the receptor fluid was mainly detected in the charcoal filters following volatilization. Total recovery was somewhat lower with BE than with M2P and EE, possibly because of breakthrough from the charcoal filters.

4.2 Percutaneous penetration of 2-ethoxyethanol and 2-butoxyethanol in aqueous solution from different application volumes and donor concentrations

Reducing the application volume of aqueous 2-ethoxyethanol (3 mg ml-1) to 100 µl had an unexpected effect on the rate and extent of EE absorption (Fig 4.2). Steady state absorption was established more rapidly with the smaller volume (1.36 ± 0.29 h). The steady state flux and the apparent k_p were approximately doubled compared with 200 µl (Table 4.3) ($P<0.01$). The final level of absorption was higher in both absolute terms and as a percentage of the dose ($P<0.01$), and reached a maximum somewhat earlier with 100 µl. In contrast, the steady state flux for BE absorption and the apparent k_p were approximately halved with the smaller application volume ($P<0.001$), whilst the time to steady state was slightly higher than with 200 µl ($P<0.05$). Maximum absorption was reached after about 3 h compared to 5 h with 200 µl. The final level of BE absorption was markedly reduced in both absolute and percentage terms. The proportions of both compounds recovered from surface swabs and cell washes were slightly higher than with 200 µl, though again, proportions were less than 1% of the applied dose in total, and very little material was recovered in the tape strips. Recovery of volatilized BE from charcoal filters was higher than with 200 µl, as was total recovery.

Increasing the concentration of the donor solution to 6 mg ml^{-1} resulted in an increase of about 60% in the steady state flux for BE (Fig 4.3, Table 4.3), and the apparent k_p was only slightly reduced compared to 3 mg ml^{-1}. The percentage of the dose absorbed after 24 h was also similar. In contrast, the steady state flux for EE was over seven-fold higher with 6 mg ml^{-1}, whilst the apparent k_p was about four-fold higher ($P<0.001$). Similarly, the proportion of the applied dose absorbed after 24 h was greatly increased with the higher donor concentration ($P<0.01$). These data, taken together with the increase in flux and absorption of EE at lower application volumes, suggest that concentration of the dose solution occurred on the surface of the skin, probably due to differential evaporation of water. Apart from the differences in absorption of the dose into receptor fluid, the only influence of higher donor concentration on EE distribution was a concomitant decrease in the proportion of dose material volatilized (Table 4.4). There was very little influence of donor concentration on BE distribution expressed in percentage terms.

4.3 Influence of skin thickness on the absorption profile of 2-ethoxyethanol and 2-butoxyethanol

There was a marked increase in the time to steady state ($P<0.01$), in EE absorption through full thickness skin (Fig 4.4, Table 4.5) compared with dermatomed skin, although the steady state flux was not significantly affected. This indicates that the lower dermis present in full thickness skin but absent in dermatomed skin presented a significant barrier to diffusion of EE. The upper dermis is vascularised *in vivo*, and it is not easy to recreate this *in vitro*. It is likely therefore that material applied to the surface of the skin would enter the systemic circulation earlier than the time to steady state measured with full thickness skin would suggest. The time to steady state measured with dermatomed skin probably represents a better estimation of that measured *in vivo*. There was a small decrease in the final level of absorption, possibly resulting from the increased opportunity for the EE to be volatilized due to the increase in path length between the donor solution and the receptor fluid (Fig 4.4, Table 4.5). The time to steady state for BE absorption was also significantly increased ($P<0.01$) will full thickness skin, but in contrast to EE, the steady state flux for BE was significantly decreased ($P<0.01$, Fig 4.4 Table 4.5). The final level of absorption was also significantly reduced compared with dermatomed skin ($P<0.001$). It is clear that the presence of the dermis has a more marked effect on the higher molecular weight, more lipophilic compound.

4.4 Influence of receptor fluid additions on percutaneous penetration of aqueous 2-ethoxyethanol

Materials such as BSA and PEG 20 Oleyl ether are added to physiological receptor fluids such as saline and tissue culture media in order to increase the solubility of lipophilic compounds in the receptor fluid where this parameter might limit absorption *in vitro*. Although the glycol ethers tested in the present study are highly soluble in water, there was a clear influence of addition of materials to receptor fluid on the absorption of 2-ethoxyethanol from aqueous solution (Fig 4.5, Table 4.6). The presence of BSA (2% (w/v)) or PEG 20 oleyl ether (2% or 6% (w/v)) resulted in an approximate doubling of the steady state flux (and hence apparent k_p) ($P<0.01$) as well as an increase in the final level of absorption ($P<0.01$), when compared with unmodified receptor fluid. There was no significant difference between the BSA and the PEG 20 , or between the different concentrations of PEG 20, however. The cumulative absorption-time curve was also affected, with absorption continuing until 8 h with PEG 20 and 10 h with BSA (Fig 4.5), though the time to steady state was not

significantly altered (Table 4.6). Apart from the degree of absorption into receptor fluid, there was little influence of receptor fluid additions on distribution (Table 4.7). Increased absorption into receptor fluid was accompanied by a concomitant decrease in the proportion of the dose volatilized. There was a small but not statistically significant increase in EE in skin when 2% (w/v) BSA or 6% (w/v) PEG 20 Oleyl ether were present in receptor fluid. These findings show that, even for materials with high aqueous solubility and relatively low lipophilicity (log P = -0.32 for ethoxyethanol, 0.83 for butoxyethanol), the presence of materials such as BSA in receptor fluid can significantly modulate penetration *in vitro*. It is possible that these findings have relevance to *in vitro*/*in vivo* scaling.

4.5 Effects of dermatoming and cold storage on 2-ethoxyethanol absorption

There were no significant effects of dermatoming and cold storage overnight prior to a flow through study on absorption or distribution of 2-ethoxyethanol from 100 µl of 3 mg ml^{-1} aqueous solution (Table 4.8). This enables the prior dermatoming and storage of skin, and its transport in cold conditions to other sites and research groups without the facility to dermatome, without effects on 2-ethoxyethanol penetration.

4.6 Penetration of glycol ethers through dermatomed human skin from a neat finite dose

The absorption of glycol ethers from finite (10.5 µl) neat doses (Fig 4.6, Table 4.9) showed similar trends to those observed with aqueous solutions, i.e. BE absorption was greater than EE absorption, which was in turn greater than M2P absorption. In contrast to the aqueous vehicle, the steady state flux of neat EE was not greatly different to that with BE, though the steady state for EE absorption was brief and no further absorption into receptor fluid was measured after 2 h. The steady state for BE absorption was more prolonged, with absorption continuing until 5 h, resulting in a much higher level of total absorption for BE. M2P absorption was also short-lived, and the final level of M2P absorption was approximately a tenth of that for EE. These findings suggest that M2P is the least absorbed of the glycol ethers studied here and presents the lowest risk in an occupational situation, probably because of its low lipophilicity (log P = -0.55) and high vapour pressure (1.57 KPa). Flux values (Table 4.9) were, as expected, considerably higher than for aqueous solutions (Table 4.1), especially for EE. Apparent k_p values, however, were ten- to twentyfold lower in neat finite doses than in aqueous doses, indicating the importance of vehicle effects in glycol ether absorption. The time to steady state for neat EE was reduced compared with

aqueous EE, though there was little difference in this parameter for BE and M2P between neat and aqueous vehicles.

Addition of 6% (w/v) PEG 20 oleyl ether to receptor fluid also modulated the absorption of finite neat doses of glycol ethers (Fig 4.7, Table 4.9). The steady state flux of all three compounds was approximately doubled with PEG 20 oleyl ether, as was the apparent k_p. Steady state flux for EE was more rapidly established with PEG 20 oleyl ether ($P<0.01$), though this parameter was not greatly affected with M2P and EE. There was an approximate doubling of the final level of absorption into receptor fluid with EE and M2P, whilst BE absorption increased by about 50% with PEG 20 oleyl ether. These data show that PEG 20 can influence absorption of glycol ethers in occupationally relevant doses as well as in large volume aqueous doses.

4.7 Experimentally determined and predicted absorption parameters for neat infinite doses of glycol ethers

Steady state flux and apparent k_p values determined *in vitro* with infinite (200 µl) doses of neat solvent (Table 4.10) were similar to those for finite doses for EE and BE (Table 4.9), though the steady state flux and apparent k_p for M2P were considerably higher for the infinite dose, suggesting that the high vapour pressure (1.57 KPa) of this compound limited absorption in the finite dose experiment. The predicted steady state flux values for EE and BE are similar to those determined experimentally. There was some discrepancy between experimental and predicted flux values for M2P, though this is not unexpected, since the model is based on an infinite dose of a saturated aqueous solution; solubility data for M2P were not available and were calculated by the KBS system from other parameters. Predicted and experimental k_p values (which are theoretically constant for all concentrations) were very similar. The time to establish the steady state was somewhat underestimated by the KBS system for EE. The experimentally determined value for time to steady state with an infinite dose of neat EE was closer to that measured with the large volume aqueous dose, whilst the predicted value was closer to the time to steady state for neat finite EE (Table 4.9). In the case of EE and especially BE, the predicted and experimentally determined k_p values were (as with finite neat doses) much lower than the apparent k_p values measured for infinite aqueous doses. Hence, application of the model to predict absorption from more dilute aqueous solutions of glycol ethers will underestimate the flux rate for BE and EE. This was not the case with M2P, however.

Table 4.1 Absorption parameters measured for 2-ethoxyethanol, 1-methoxy-2-propanol and 2-butoxyethanol through dermatomed human skin from aqueous solution (200 µl, 3 mg ml^{-1}, 0.6 mg). Figures are mean ± SEM (n=4/5)

Compound and Dose	**Flux (nmol cm^{-2} h^{-1}) [µg cm^{-2} h^{-1}]**	**Apparent k_p (cm h^{-1})**	**Time to steady state (h)**	**Total absorption (µmol) [µg]**	**Total absorption (% of dose)**
EE 200 µl (33.3 mM) (6.7 µmol)	143 ± 19 [12.9 ± 1.7]	0.0042 ± 0.0025	1.67 ± 0.14	0.34 ± 0.06 [30.6 ± 5.4]	5.1 ± 0.9
M2P 200 µl (33.3 mM) (6.7 µmol)	48 ± 6 [4.3 ± 0.5]	0.0014 ± 0.0002	0.68 ± 0.09	0.15 ± 0.02 [13.5 ± 1.8]	2.3 ± 0.2
BE 200 µl (25.4 mM) (5.1 µmol)	544 ± 64 [64.3 ± 7.6]	0.0214 ± 0.0025	0.30 ± 0.03	1.39 ± 0.17 [164.3 ± 20.1]	27.3 ± 0.3

Table 4.2 Distribution of 2-ethoxyethanol, 1-methoxy-2-propanol and 2-butoxyethanol through dermatomed human skin from aqueous solution (200 µl, 0.6 mg, 3 mg ml^{-1}) as percentage of the applied dose (nd = none detected). Figures are mean ± SEM (n=4/5)

	EE 200 µl (33.3 mM) (6.7 µmol)	**M2P 200 µl (33.3 mM) (6.7 µmol)**	**BE 200 µl (25.4 mM) (5.1 µmol)**
Surface swabs	0.25 ± 0.05	nd	0.07 ± 0.01
Cell washes	0.28 ± 0.04	nd	0.13 ± 0.02
1st Tapes	0.02 ± 0.00	nd	0.00 ± 0.00
Tape strips	0.03 ± 0.00	nd	0.02 ± 0.01
Skin	0.08 ± 0.04	nd	0.24 ± 0.16
Receptor fluid	5.09 ± 0.83	2.29 ± 0.26	27.39 ± 3.32
Charcoal	96.60 ± 2.30	91.62 ± 3.90	60.60 ± 2.70
TOTAL	102.40 ± 1.60	94.10 ± 3.80	88.45 ± 3.40

Table 4.3 Absorption parameters measured for 2-ethoxyethanol and 2-butoxyethanol - influence of application volume and donor concentration (3 or 6 mg ml^{-1}). Figures are mean ± SEM (n=4/5)

Compound and Dose	**Flux (nmol cm^{-2} h^{-1}) [µg cm^{-2} h^{-1}]**	**Apparent k_p (cm h^{-1})**	**Time to steady state (h)**	**Total absorption (µmol) [µg]**	**Total absorption (% of dose)**
EE 200 µl (33.3 mM) (6.7 µmol, 0.6 mg)	143 ± 19 [12.9 ± 1.7]	0.0042 ± 0.0025	1.67 ± 0.14	0.34 ± 0.06 [30.6 ± 5.4]	5.1 ± 0.9
BE 200 µl (25.4 mM) (5.1 µmol, 0.6 mg)	544 ± 64 [64.3 ± 7.6]	0.0214 ± 0.0025	0.30 ± 0.03	1.39 ± 0.17 [164.3 ± 20.1]	27.3 ± 0.3
EE 100 ul (33.3 mM) (3.4 µmol, 0.3 mg)	280 ± 23 [25.2 ± 2.1]	0.0084 ± 0.0007	1.36 ± 0.29	0.47 ± 0.06 [42.4 ± 5.4]	14.1 ± 1.8
BE 100 µl (25.4 mM) (2.5 µmol, 0.3 mg)	261 ± 23 [30.8 ± 2.7]	0.0103 ± 0.0009	0.36 ± 0.01	0.40 ± 0.05 [47.3 ± 5.9]	15.8 ± 2.0
EE 200 µl (66.6 mM) (13.3 µmol, 1.2 mg)	1084 ± 74 [97.7 ± 6.7]	0.0163 ± 0.0011	2.64 ± 0.10	2.37 ± 0.32 [213.6 ± 28.8]	17.80 ± 2.40
BE 200 µl (50.8 mM) (10.2 µmol, 1.2 mg)	894 ± 217 [105.7 ± 25.6]	0.0176 ± 0.0043	0.52 ± 0.11	2.34 ± 0.44 [276.5 ± 52.0]	23.05 ± 4.33

Table 4.4 Distribution of 2-ethoxyethanol, and 2-butoxyethanol through dermatomed human skin from aqueous solution as percentage of the applied dose - influence of application volume (100 or 200 µl) and donor concentration (3 or 6 mg ml^{-1}). Figures are mean ± SEM (n=4/5)

	EE 200 µl (33.3 mM) (6.7 µmol, 0.6 mg)	**BE 200 µl (25.4 mM) (5.1 µmol, 0.6 mg)**	**EE 100 µl (33.3 mM) (3.4 µmol, 0.3 mg)**	**BE 100 µl (25.4 mM) (2.5 µmol, 0.3 mg)**	**EE 200 µl (66.6 mM) (13.3 µmol, 1.2 mg)**	**BE 200 µl (50.8 mM) (10.2 µmol, 1.2 mg)**
Surface swabs	0.25 ± 0.05	0.07 ± 0.01	0.52 ± 0.08	0.21 ± 0.03	0.22 ± 0.04	0.03 ± 0.01
Cell washes	0.28 ± 0.04	0.13 ± 0.02	0.43 ± 0.08	0.40 ± 0.06	0.24 ± 0.03	0.10 ± 0.01
1st Tapes	0.02 ± 0.00	0.00 ± 0.00	0.01 ± 0.00	0.01 ± 0.01	0.01 ± 0.00	0.00 ± 0.00
Tape strips	0.03 ± 0.00	0.02 ± 0.01	0.00 ± 0.00	0.00 ± 0.00	0.03 ± 0.01	0.01 ± 0.00
Skin	0.08 ± 0.04	0.24 ± 0.16	0.28 ± 0.24	0.14 ± 0.03	0.44 ± 0.31	0.15 ± 0.04
Receptor fluid	5.09 ± 0.83	27.39 ± 3.32	14.12 ± 1.80	15.76 ± 2.00	17.80 ± 2.40	23.05 ± 4.36
Charcoal	96.60 ± 2.30	60.60 ± 2.70	81.37 ± 5.12	86.47 ± 4.22	89.97 ± 4.39	85.00 ± 3.37
TOTAL	102.40 ± 1.60	88.45 ± 3.40	96.29 ± 4.20	106.21 ± 4.71	109.34 ± 4.36	108.36 ± 2.27

Table 4.5 Absorption parameters measured for 2-ethoxyethanol and 2-butoxyethanol (3 mg ml^{-1} in each case) - influence of skin thickness. Figures are mean ± SEM (n=4/5)

Compound and Dose thickness	**Flux (nmol cm^{-2} h^{-1}) [μg cm^{-2} h^{-1}]**	**Apparent k_p (cm h^{-1})**	**Time to steady state (h)**	**Total absorption (μmol) [μg]**	**Total absorption (% of dose)**
EE 200 μl (33.3 mM) (6.7 μmol, 0.6 mg) dermatomed	143 ± 19 [12.9 ± 1.7]	0.0042 ± 0.0025	1.67 ± 0.14	0.34 ± 0.06 [30.6 ± 5.4]	5.1 ± 0.9
BE 200 μl (25.4 mM) (5.1 μmol, 0.6 mg) dermatomed	544 ± 64 [64.3 ± 7.6]	0.0214 ± 0.0025	0.30 ± 0.03	1.39 ± 0.17 [164.3 ± 20.1]	27.3 ± 0.3
EE 200 μl (33.3 mM) (6.7 μmol, 0.6 mg) full thickness	124 ± 24 [11.2 ± 2.2]	0.0037 ± 0.0007	3.33 ± 0.19	0.25 ± 0.04 [22.5 ± 3.6]	3.8 ± 0.2
BE 200 μl (25.4 mM) (5.1 μmol, 0.6 mg) full thickness	135 ± 5 [16.0 ± 0.6]	0.0053 ± 0.0002	1.14 ± 0.06	0.34 ± 0.01 [40.2 ± 1.2]	6.7 ± 0.2

Table 4.6 Absorption parameters measured for aqueous 2-ethoxyethanol (200 µl, 33.3 mM [3 mg ml^{-1}], 6.7 µmol [0.6 mg]) - influence of receptor fluid. Figures are mean ± SEM (n=5/6)

Receptor fluid	**Flux (nmol cm^{-2} h^{-1}) [µg cm^{-2} h^{-1}]**	**Apparent k_p (cm h^{-1})**	**Time to steady state (h)**	**Total absorption (µmol) [µg]**	**Total absorption (% of dose)**
MEM plus 2% PEG 20 Oleyl ether	342 ± 18 [30.8 ± 1.6]	0.0103 ± 0.0005	2.52 ± 0.38	0.75 ± 0.01 [67.6 ± 0.9]	11.3 ± 0.2
MEM plus 6% PEG 20 Oleyl ether	281 ± 19 [25.3 ± 1.7]	0.0084 ± 0.0006	2.04 ± 0.34	0.89 ± 0.07 [80.2 ± 6.3]	13.4 ± 1.0
MEM plus 2% BSA	270 ± 38 [24.3 ± 3.4]	0.0081 ± 0.0012	2.25 ± 0.09	0.77 ± 0.08 [69.4 ± 7.2]	11.6 ± 1.3
MEM	143 ± 19 [12.9 ± 1.7]	0.0042 ± 0.0025	1.67 ± 0.14	0.34 ± 0.06 [30.6 ± 5.4]	5.1 ± 0.9

Table 4.7 Distribution of aqueous 2-ethoxyethanol (200 µl, 33.3 mM [3 mg ml^{-1}], 6.7 µmol [0.6 mg]) - influence of receptor fluid
Figures are mean ± SEM (n=5)

	MEM plus 2% (w/v) PEG 20 Oleyl ether	**MEM plus 6% (w/v) PEG 20 Oleyl ether**	**MEM plus 2% (w/v) BSA**	**MEM**
Surface swabs	0.73 ± 0.06	0.26 ± 0.05	0.23 ± 0.11	0.25 ± 0.05
Cell washes	0.02 ± 0.01	0.38 ± 0.04	0.50 ± 0.15	0.28 ± 0.04
1st Tapes	0.04 ± 0.00	0.02 ± 0.02	0.01 ± 0.00	0.02 ± 0.00
Tape strips	0.06 ± 0.02	0.02 ± 0.01	0.03 ± 0.02	0.03 ± 0.00
Skin	0.08 ± 0.04	0.52 ± 0.34	0.42 ± 0.24	0.08 ± 0.04
Receptor fluid	11.26 ± 0.15	13.37 ± 1.01	11.56 ± 1.26	5.09 ± 0.83
Charcoal	74.26 ± 7.91	93.83 ± 9.60	93.20 ± 7.30	96.60 ± 2.30
TOTAL	87.17 ± 8.79	106.50 ± 8.50	106.60 ± 7.10	102.40 ± 1.60

Table 4.8 Distribution (as percentage of applied dose) of 2-ethoxyethanol (100 µl, 33.33 mM [3 mg ml^{-1}], 3.4 µmol [0.3 mg]) and absorption parameters measured with freshly dermatomed skin and previously dermatomed and stored skin. Figures are mean ± SEM (n=4/5)

	Freshly dermatomed skin	**Previously dermatomed skin at 4˚C overnight**
Surface swabs	0.54 ± 0.06	0.36 ± 0.05
Cell washes	0.32 ± 0.06	0.28 ± 0.06
1st Tapes	0.00 ± 0.00	0.00 ± 0.00
Tape strips	0.01 ± 0.00	0.01 ± 0.01
Skin	0.26 ± 0.15	0.19 ± 0.15
Receptor fluid	10.68 ± 1.40	11.32 ± 1.57
Charcoal	83.22 ± 3.50	77.35 ± 4.74
TOTAL	95.05 ± 3.37	89.51 ± 4.15
steady state flux (nmol cm^{-2} h^{-1})	280 ± 23	237 ± 36
steady state flux (µg cm^{-2} h^{-1})	25.2 ± 2.1	21.4 ± 3.2
Apparent k_p (cm h^{-1})	0.0084 ± 0.0007	0.0071 ± 0.0011
time to steady state (h)	1.36 ± 0.29	1.34 ± 0.07

Table 4.9 Absorption parameters of glycol ethers (10.5 µl, neat) through dermatomed human skin *in vitro*. Figures are mean ± SEM (n=4/5)

Compound and concentration/dose	**Flux ($nmol\ cm^{-2}\ h^{-1}$) [$\mu g\ cm^{-2}\ h^{-1}$]**	**Apparent k_p ($cm\ h^{-1}$)**	**Time to steady state (h)**	**Total absorption (µmol) [µg]**	**Total absorption (% of dose)**
EE 10.3 M 108.5 µmol [9.8 mg]	6481 ± 1079 [584.1 ± 97.2]	0.0006 ± 0.0001	0.60 ± 0.04	4.03 ± 0.82 [363.2 ± 73.9]	3.7 ± 0.8
BE 7.6 M 80.1 µmol [9.5 mg]	7210 ± 1552 [852.1 ± 183.4]	0.0009 ± 0.0002	0.51 ± 0.05	12.63 ± 2.07 [1492.6 ± 244.6]	15.8 ± 2.6
M2P 10.6 M 112.1 µmol [10.1 mg]	666 ± 219 [60.0 ± 19.7]	6.2x10-5 ± 2.1x10-5	0.42 ± 0.01	0.49 ± 0.16 [44.2 ± 14.4]	0.5 ± 0.2
EE 10.3 M 108.5 µmol [9.8 mg] 6% (w/v) PEG 20	13248 ± 1321 [1193.9 ± 119.0]	0.0013 ± 0.0001	0.38 ± 0.05	8.95 ± 1.51 [806.6 ± 136.1]	7.98 ± 1.4
BE 7.6 M 80.1 µmol [9.5 mg] 6% (w/v) PEG 20	13160 ± 2006 [1555.2 ± 237.1]	0.0017 ± 0.0003	0.55 ± 0.02	18.33 ± 3.88 [2166.2 ± 458.5]	22.9 ± 4.8
M2P 10.6 M 112.1 µmol [10.1 mg] 6% (w/v) PEG 20	1577 ± 338 [142.1 ± 30.5]	14.8x10-5 ± 3.2x10-5	0.49 ± 0.07	1.01 ± 0.28 [91.0 ± 25.2]	0.9 ± 0.3

Table 4.10 Absorption parameters of glycol ethers (200 µl, neat) through dermatomed human skin *in vitro* (no PEG 20 in receptor fluid) and predicted values from the Dermal KBS (based on an infinite dose of a saturated aqueous solution). Figures are mean ± SEM (n=4/5)

Compound and concentration	**Flux (nmol cm^{-2} h^{-1}) [mg cm^{-2} h^{-1}]**	**Flux (mg cm^{-2} h^{-1})**	**Apparent or predicted k_p (cm h^{-1})**	**Time to steady state (h)**
EE 10.3 M experimental (186.7 mg)	12590 ± 4038	1.13 ± 0.36	0.0012 ± 0.0004	1.63± 0.17
EE 10.3 M predicted	13316	1.2	0.0010	0.88
BE 7.6 M experimental (181.0 mg)	8536 ± 3906	1.01 ± 0.35	0.0011 ± 0.0005	1.04 ± 0.39
BE 7.6 M predicted	11906	1.41	0.0014	1.29
M2P 10.6 M experimental (192.4 mg)	6623 ± 2424	0.60 ± 0.22	0.0006 ± 0.0002	1.21 ± 0.16
M2P 10.6 M predicted	22614	2.04	0.0010	0.88

5.0 PERCUTANEOUS PENETRATION OF METHYL ETHYL KETONE, TETRAHYDROFURAN AND ACETONE

5.1 Absorption of MEK, THF and acetone from neat finite doses and infinite dose aqueous solutions

Steady state absorption of MEK, THF and acetone from finite neat doses (10.5 µl) was rapidly established (Fig 5.1) but short-lived compared to EE and BE (Fig 4.7). The steady state fluxes (and hence apparent k_p values) measured for MEK and THF were similar (Table 5.1), but were an order of magnitude lower than the corresponding values for EE and BE in neat finite doses. This is probably a reflection of the higher vapour pressure of MEK and THF (12.1 KPa and 21.6 KPa respectively compared with 0.12 KPa for BE and 0.71 KPa for EE). THF steady state absorption was slightly more long-lived than MEK and acetone, though absorption of all three compounds into receptor fluid ceased after about 2h. Acetone was the least well absorbed compound, probably because of its more hydrophilic nature (log P = -0.24) and high vapour pressure (30.8 KPa at 25 C). Final levels of absorption for all three compounds were again considerably lower than for EE and BE.

Absorption of MEK, THF and acetone from large volume (200 µl) aqueous solutions (3 mg ml^{-1}) (Fig 5.2, Table 5.1) followed similar trends to absorption from neat doses (Fig 5.1). Steady state absorption was again rapidly established and short-lived, with absorption ceasing after about 2 h. Steady state flux values were, as expected, lower than for finite neat doses, though the difference was not as marked as with EE and BE (Tables 4.6 and 4.9), and indeed, fluxes for aqueous MEK and THF were similar to those measured with EE in aqueous solution at the same concentration. Apparent k_p values were, again, much higher with aqueous solutions than with neat doses, and over 100 fold higher with THF and acetone, illustrating the importance of vehicle effects for these compounds. A higher proportion of the applied dose was absorbed into receptor fluid with aqueous doses, but again, the overall level of absorption was low (0.4 - 1.7%) compared with glycol ethers, due to the short-lived absorption phase.

Attempts to study distribution and total recovery of MEK, THF and acetone in dermal absorption experiments were hampered by low efficiency of charcoal filters to trap these compounds. After 24 h, for example, only 25.4 ± 0.7% of the applied dose from a neat finite application of MEK was recovered from the charcoal filters, compared with 11.9 ± 0.6% with THF and 1.5 ± 0.0% with acetone. Subsequent experiments with shorter contact times (4 h) showed that MEK, THF and acetone were not stably retained

by the charcoal filters. Levels of MEK, THF and acetone in swabs, washes, tape strips and skin samples were not detectable by GC.

5.2 Absorption of MEK, THF and acetone from neat infinite doses and predictions from the KBS

Steady state flux values (and hence apparent k_p values) measured for MEK, THF and acetone in infinite neat dose conditions (Table 5.2) were several-fold higher than those measured with finite doses (Table 5.1), illustrating the limiting effect of volatilization of dose material on flux rates in finite dose conditions . Predictions of k_p from the KBS system overestimated experimental values for THF and acetone by a factor of 10, though the prediction for MEK was within acceptable limits. Again, predictions of k_p were great underestimates of values determined experimentally for aqueous solutions.

5.3 Influence of neat finite doses of MEK, THF and acetone on barrier integrity as measured by tritiated water absorption

There was no significant effect of application of single, neat, finite doses of MEK, THF or acetone on the apparent k_p or time to steady state of tritiated water before and after application (Table 5.3). There was no significant effect of tritiated water pre-treatment on dermal absorption of the test compounds when compared with cells without pre-treatment.

Table 5.1 Absorption parameters measured for MEK, THF and acetone in neat (10.5 µl) and aqueous (200 µl, 3 mg ml^{-1}) doses. Figures are means ± SEM (n=4/5)

Compound and concentration/dose	**Flux (nmol cm^{-2} h^{-1}) [µg cm^{-2} h^{-1}]**	**Apparent k_p (cm h^{-1})**	**Time to steady state (h)**	**Total absorption (µmol) [µg]**	**Total absorption (% of dose)**
MEK 11.2 M 117.2 µmol [8.5 mg]	457 ± 74 [33.0 ± 5.3]	4.1x10-5 ± 0.7x10-5	0.33 ± 0.00	0.15 ± 0.01 [10.8 ± 0.7]	0.13 ± 0.01
THF 12.3 M 129.5 µmol [9.3 mg]	567 ± 113 [40.9 ± 8.1]	4.6x10-5 ± 0.9x10-5	0.33 ± 0.00	0.24 ± 0.06 [17.3 ± 4.3]	0.19 ± 0.05
Acetone 13.6 M 142.8 µmol [8.3 mg]	178 ± 39 [10.3 ± 2.3]	1.3x10-5 ± 0.3x10-5	0.31 ± 0.00	0.06 ± 0.01 [3.5 ± 0.6]	0.05 ± 0.01
MEK 41.6 mM 8.3 µmol [0.6 mg]	117 ± 37 [8.4 ± 2.7]	0.0028 ± 0.0009	0.35 ± 0.02	0.06 ± 0.02 [4.3 ± 1.4]	0.77 ± 0.24
THF 41.6 mM 8.3 µmol [0.6 mg]	254 ± 98 [18.3 ± 7.1]	0.0061 ± 0.0023	0.35 ± 0.02	0.14 ± 0.05 [10.1 ± 3.6]	1.68 ± 0.61
Acetone 51.6 mM 10.3 µmol [0.6 mg]	73 ± 15 [4.2 ± 0.9]	0.0014 ± 0.0003	0.38 ± 0.03	0.04 ± 0.02 [2.3 ± 1.2]	0.41 ± 0.16

Table 5.2 Absorption parameters for MEK, THF and acetone determined from infinite (100 µl) neat doses *in vitro* and predicted values from the Dermal KBS (based on an infinite dose of a saturated aqueous solution). Figures are means ± SEM (n=4/5)

Compound and concentration	**Flux (nmol cm^{-2} h^{-1})**	**Flux (mg cm^{-2} h^{-1})**	**Apparent or predicted k_p (cm h^{-1})**	**Time to steady state (h)**
MEK 11.2 M experimental	8822 ± 1853	0.63 ± 0.13	7.9x10-4 ± 1.7x10-4	0.57 ± 0.02
MEK 11.2 M predicted	3633	0.26	11.1x10-4	0.68
THF 12.3 M experimental	3737 ±1464	0.27 ± 0.11	3.0x10-4 ± 1.2x10-4	0.34 ± 0.02
THF 12.3 M predicted	3244	0.23	14.7x10-4	0.68
Acetone 13.6 M experimental	1749 ± 446	0.10 ± 0.03	1.3x10-4 ± 0.3x10-4	0.51 ± 0.08
Acetone 13.6 M predicted	11074	0.80	10x10-4	0.24

Table 5.3 Apparent k_p and time to steady state for tritiated water before and after application of neat finite doses of MEK, THF and acetone. Figures are means ± SEM (n=4)

Compound and concentration	**Pre/post application**	**Apparent k_p (cm h^{-1})**	**Time to steady state (h)**
MEK 11.2 M 117.2 µmol	Pre	0.0057 ± 0.0007	0.36 ± 0.03
MEK 11.2 M 117.2 µmol	Post	0.0081 ± 0.0026	0.34 ± 0.05
THF 12.3 M 129.5 µmol	Pre	0.0059 ± 0.0010	0.32 ± 0.10
THF 12.3 M 129.5 µmol	Post	0.0070 ± 0.0019	0.26 ± 0.07
Acetone 13.6 M 142.8 µmol	Pre	0.0066 ± 0.0006	0.48 ± 0.05
Acetone 13.6 M 142.8 µmol	Post	0.0051 ± 0.0012	0.32 ± 0.08

6.0 PERCUTANEOUS PENETRATION OF TOLUENE, *m*-XYLENE AND *o*-XYLENE

6.1 Percutaneous penetration of toluene, *m*-xylene and *o*-xylene in neat finite (10.5 μl) doses

Absorption of toluene from a neat finite dose was at its highest flux during the first hour of contact (Fig 6.1), steady state flux being established very rapidly. Thereafter, the rate of absorption decreased gradually, until 8 h. No further absorption was measured after this time. In contrast, the maximum flux for *m*- and *o*-xylene occurred later (times to steady state were 0.22 ± 0.14 h and 0.28 ± 0.12 h respectively) and, again, the rate of absorption decreased gradually until about 6 h, the decrease being more rapid in *o*-xylene. The prolonged absorption phases measured with these compounds contrast with those measured for MEK, THF and acetone, and are at least partly related to the lower vapour pressures of the aromatic compounds (3.89, 0.88 and 1.11 KPa for toluene, *m*-xylene and *o*-xylene, respectively). The steady state fluxes (and hence apparent k_p values) of *m*- and *o*-xylene were similar and numerically greater than that of toluene in a neat finite dose regime but the difference was not statistically significant (P=0.08) (Table 6.1). Overall, flux and k_p values for the aromatic compounds were comparable with those for acetone but considerably lower than those measured for the glycol ethers in comparable doses (section 4.0). The more prolonged absorption phase observed with *m*-xylene resulted in a higher level of total absorption for this compound (Fig 6.1, Table 6.1). Levels of total absorption (both absolute and as a proportion of the dose absorbed) were comparable with those measured for MEK, THF and acetone (section 5.0). It is likely, therefore, that occupationally-related doses of these compounds would result in very low absorption. Recovery of the applied aromatics from the surface swabs, cell washes, tape strips or skin samples was very low, less than 0.01% of the applied dose in most cases, in neat finite doses. The majority of the applied dose was recovered in the charcoal filter, but this accounted for only 48.0 ± 1.8% of the applied toluene, 58.7± 2.7% of the applied *m*-xylene and 58.8 ± 0.9% of the applied *o*-xylene, suggesting that, as with MEK, THF and acetone, the volatilized aromatics were not stably or not efficiently retained by the charcoal filters.

6.2 Percutaneous penetration of toluene, *m*-xylene and *o*-xylene in infinite (200 μl) aqueous doses

In contrast to the neat finite dose regime (Fig 6.1, Table 6.1), the steady state flux of aqueous toluene (infinite dose) was significantly greater than *m*-xylene ($P<0.001$), which was in turn significantly greater than *o*-xylene under the same dose conditions ($P<0.001$) (Fig 6.2, Table 6.1). A similar trend was observed for apparent k_p values. Furthermore, absorption continued for 4 h in all three cases (Fig 6.2). However, the greatest steady state flux for toluene occurred within the first hour, whilst that for the xylenes occurred later, as with the finite neat dose study. Indeed, times to steady state for the three compounds were not greatly influenced by the dose regime. Flux rates for aqueous solutions of aromatics were, as expected, approximately a tenth of those measured with neat finite doses. However, the apparent k_p values for the aqueous dose regime were, again, several orders of magnitude higher than the corresponding neat finite doses. The absolute amounts of total absorption were lower in aqueous dose conditions than in neat finite dose conditions, but the percentage of the applied dose absorbed was much higher, almost 80% in the case of toluene. The proportion of toluene absorbed was significantly greater than *m*-xylene, which was in turn significantly greater than *o*-xylene ($P<0.001$). Predictions of k_p from the dermal KBS were very close to the experimental values for aqueous solutions (Table 6.1). Flux values were overestimated by the KBS, but this is expected as the program assumes a saturated aqueous solution, and solubility of toluene in water was calculated, since no figures were available. Times to steady state were clearly overestimated, however.

Table 6.1 Absorption parameters measured and predicted from Dermal KBS (based on an infinite dose of saturated aqueous solution) for toluene, *m*-xylene and *o*-xylene. Figures are means ± SEM (n=4/5)

Compound and Dose/ Vehicle	**Flux (nmol cm^{-2} h^{-1}) [μg cm^{-2} h^{-1}]**	**Apparent k_p (cm h^{-1})**	**Time to steady state (h)**	**Total absorption (μmol) [μg]**	**Total absorption (% of dose)**
toluene 10.5 μl neat (98.7 μmol [9.1 mg])	131 ± 24 [12.1 ± 2.2]	1.40 x 10-5 ± 0.26 x 10-5	0.001 ± 0.008	0.21 ± 0.02 [19.4 ± 1.8]	0.22 ± 0.02
m-xylene 10.5 μl neat (85.9 μmol [9.1 mg])	242 ± 37 [25.7 ± 3.9]	2.96 x 10-5 ± 0.46 x 10-5	0.22 ± 0.14	0.51 ± 0.04 [54.1 ± 4.2]	0.59 ± 0.05
o-xylene 10.5 μl neat (87.0 μmol [9.2 mg)	184 ± 21 [19.5 ± 2.2]	2.22 x 10-5 ± 0.25 x 10-5	0.28 ± 0.12	0.31 ± 0.05 [32.9 ± 5.3]	0.35 ± 0.06
toluene 200 μl aq. (211.8 μM [19.5 μg ml^{-1}], 0.042 μmol [3.9 μg])	18 ± 2 [1.7 ± 0.2]	0.083 ± 0.007	0.00 ± 0.00	0.03 ± 0.00 [2.8 ± 0.0]	79.26 ± 6.89
m-xylene 200 μl aq. (244.1 μM [25.9 μg ml^{-1}], 0.049 μmol [5.2 μg])	14 ± 1 [1.5 ± 0.1]	0.059 ± 0.006	0.18 ± 0.10	0.03 ± 0.00 [3.2 ± 0.0]	57.58 ± 7.10
o-xylene 200 μl aq. (295.8 μM [31.4 μg ml^{-1}], 0.059 μmol [6.3 μg])	10 ± 1 [1.1 ± 0.1]	0.035 ± 0.004	0.27 ± 0.15	0.02 ± 0.00 [2.1 ± 0.0]	25.29 ± 4.12
toluene (predicted)	552 [50.9]	0.042	0.90		
m-xylene (predicted)	122 [13.0]	0.080	1.10		
o-xylene (predicted)	118 [12.5]	0.070	1.10		

7.0 DISCUSSION

7.1 Influence of physicochemical properties on absorption - interaction with vehicle and dose

The total amount of a compound absorbed through the skin is determined by two factors: the steady state flux of the compound and the temporal length of the steady state absorption phase. The data obtained in this study showed a clear inverse relationship between the vapour pressure of the solvent applied and the extent of the absorption phase in cumulative absorption time curves for neat finite doses and for aqueous doses. This suggests that the length of the absorption phase was limited by evaporation of the dose. For the glycol ethers, the absorption phase for BE (vapour pressure 0.12 KPa) was about 5 h, followed by EE (0.71 KPa), with M2P (1.6 KPa) having the shortest absorption phase (2-3 h). Similarly, acetone (30.8 KPa), THF (21.6 KPa) and MEK (12.1 KPa) followed this trend, having absorption phases of less than 2 h. Absorption of neat toluene (3.89 KPa) ceased earlier than the xylenes (0.88-1.11 KPa respectively). Furthermore, the absorption phases for the neat xylenes were comparable in length with those for ethoxyethanol. The relationship between evaporation of volatile solvents and the rate and/or degree of absorption is well described in the literature (Boman and Maibach, 2000). However, this relationship was modified by dose regime in the present study. For example, an "infinite" dose of aqueous EE had a slightly longer absorption phase than neat EE, despite the lower absolute dose in the former case, though EE showed unexpected behaviour in aqueous solution (see below). The absorption phase of toluene was also prolonged in aqueous solution. This suggests that, for compounds with high or moderate solubility in water, the dose was retained in the aqueous solution for longer than in a neat dose, giving a greater opportunity for penetration.

For the more hydrophilic compounds studied in previous sections of this report (log P < 1), there was some relationship between log P and flux (and apparent k_p) for neat finite doses. Apparent k_p increased with log P (i.e. increasing lipophilicity) (see Fig S.4.1 in the Supplement to this report), reaching a peak with BE. Compounds with low (and especially negative) log P exhibited low steady state flux, though EE was an obvious exception. The log P of a compound reflects the ability of the compound to penetrate the stratum corneum, and hence diffuse through the epidermis and upper dermis and be absorbed into the receptor fluid. The relationship appears to be complicated by volatility, however. The high volatility of acetone, MEK and THF would have limited the flux in a neat finite application, whilst the lower volatility of EE and BE contributed to their apparent k_p.

There was a more gradual increase in apparent k_p with log P with aqueous applications (Fig S.4.2). Furthermore, apparent k_p values were considerably higher with aqueous solutions than with neat doses (both finite and infinite). This was especially the case for the glycol ethers. Steady state flux and k_p of EE increased (and time to steady state decreased) with a smaller application volume, and doubling the concentration in the aqueous donor solution resulted in an eight-fold increase in flux. This suggests that concentration of the dose solution occurred in aqueous solutions, possibly due to preferential evaporation of water, and the actual k_p (dependent on concentration) cannot therefore be determined. However, the marked increase in apparent k_p in aqueous solution compared with neat solvent was also measured with BE, M2P, acetone, MEK and THF. The difference in k_p was generally larger with more lipophilic compounds such as BE and THF and smaller for compounds with negative log P values (though acetone did not follow this trend). These findings suggest that partitioning of the dose compound into the stratum corneum occurred in aqueous solution, resulting in a proportionately higher concentration gradient, which hence drove steady state flux. The influence of vehicles in the dermal absorption of compounds is well described in the literature for certain compounds but less so for solvents. For example, the permeability coefficients for dibromomethane and bromochloromethane (for *in vivo* rat skin) were approximately 73- and 40-fold higher, respectively, in a water vehicle than in corn oil, though the permeability coefficient, when normalized for the skin:vehicle matrix partition coefficient, varied by less than a factor of 2 (Jepson and McDougal, 1999). Although the effects of co-solvents such as acetone (Filon *et al*., 1999) toluene and n-butanol (Tsuruta 1996, Boman and Maibach, 2000) have been researched, and the influence of aqueous vehicles on a range of compounds has been investigated (Hilton *et al*., 1994; Rawlings *et al*., 1994; Dick and Williams, 1998), there has been very little work on aqueous solutions of volatile solvents (Williams and Wilkinson, 2000). This is a surprising given that the glycol ethers are equally miscible with aqueous and organic media.

For the more lipophilic compounds (toluene and xylenes) however, the relationship between log P is complicated by the low water solubility of the parent compounds (from 700 mg l^{-1} to 162 mg l^{-1}). Although the high log P results in high ability to penetrate stratum corneum (evidenced by short times to steady state), low solubility in the aqueous matrix of the epidermal and subepidermal tissues limits the steady state flux (Elsisi *et al*., 1989). Hence the flux and apparent k_p of these compounds was much lower than that measured for equivalent doses of the glycol ethers (which have comparable vapour pressure) (Fig S.4.1). In aqueous solutions, the apparent k_p values for the aromatic compounds were again much higher than those measured with neat

doses. This is again easily explained by partitioning into the stratum corneum from the aqueous vehicle, resulting in a proportionately higher concentration gradient, hence driving flux at a greater rate. The flux and apparent k_p of toluene in neat finite dose was the lowest of the three compounds tested, whilst in aqueous solution it was the highest. This may be due to the higher solubility of toluene in aqueous media (700 mg l^{-1} at 23˚C compared with 178 mg l^{-1} and 162 mg l^{-1} at 25˚C for *o*-xylene and *m*-xylene respectively), combined with the effect of dissolving toluene in an aqueous solution on evaporation of the dose as mentioned above. Consequently, toluene exceeded the trend established by other solvents for apparent k_p and log P in Fig S.4.2. However, it should be stressed that the concentration of the donor solution is difficult to measure accurately, since evaporation of the parent compounds may result in an underestimate of the donor concentration, so apparent k_p values may be overestimated.

As discussed above, vapour pressure may also have influenced the relationships between log P and flux/apparent k_p, e.g. neat acetone, MEK and THF. The influence of application volume for aqueous solutions is more difficult to explain. In the present study, there was greater penetration from 100 µl of EE at 3 mg ml^{-1} than from 200 µl, possibly due to concentration of the dose solution resulting from evaporation of the vehicle. However, the flux and apparent k_p of BE were both significantly reduced with a smaller application volume, despite the lower vapour pressure of BE. Hilton *et al*. (1994) reported higher absorption rates for fluazifop butyl (10 mg ml^{-1} or 35 mg ml^{-1} in propylene glycol) through human epidermis from larger volumes of the dose material. There was an approximately threefold increase in absorption rate when the dose volume was increased from 10 µl cm^{-2} to 200 µl cm^{-2} for the 35 mg ml^{-1} donor. The authors believed that this was due to the presence on the skin of a permeable surface layer of loose skin cells and sebum. After application, some of the penetrant distributes out of the application vehicle into this surface layer, reducing the effective donor concentration and hence the concentration gradient to drive flux. A greater reduction in effective donor concentration would be observed with low application volumes. Incorporating this surface layer into a model greatly improved prediction of experimental penetration rates. With regard to the present investigation, it is possible that BE is more soluble in this surface layer (especially in sebum) than EE. With an aqueous dose regime, a greater proportion of BE than EE may have partitioned into the surface layer, hence reducing the amount of BE available to drive flux. The lower solubility of EE in the surface layer may have resulted in a lower proportionate decrease in the effective donor concentration of EE with the smaller application volume. However, this does not explain why absorption-time curves for aqueous EE become sigmoidal, suggesting concentration of the dose solution due to preferential evaporation of water, whilst curves for BE are almost linear. BE has a lower vapour pressure than EE and may also

be expected to exhibit such concentration effects. Further research is needed to clarify this point.

It is clear, therefore, that the degree of dermal absorption of a liquid chemical (and hence the contribution of dermal absorption from a liquid dose to the overall body burden) depends on a combination of vapour pressure, lipophilicity and vehicle/dose. Low vapour pressure and a log P between zero and unity favour absorption. Apparent k_p from an aqueous vehicle will be proportionately higher than from a neat dose for compounds with a log P higher than zero.

7.2 Influence of receptor fluid and skin thickness

The nature of the receptor fluid used in the present study markedly affected glycol ether absorption in both aqueous doses and occupationally relevant, neat finite doses. There was no marked effect on other aspects of the distribution such as surface swabs or stratum corneum. The effects of receptor fluid on penetration are well researched for lipophilic compounds. DeLange *et al*. (1994) showed that penetration of xylene in a perfused pig ear organ model was dependent on the protein content of the receptor fluid, though the influence of the receptor fluid depends on the penetrating compound (Bast and Kampffmeyer, 1996; Pelling et al., 1998). It is unexpected, however, to find such an effect for relatively hydrophilic compounds such as EE and BE. The draft OECD guidelines for the testing of chemicals by the skin absorption *in vitro* method (OECD, 2000) state that "the precise composition of the receptor fluid should be justified. Adequate solubility of the test chemical in the receptor fluid should be demonstrated so that it does not act as a barrier to absorption." The data from the present study indicate that there are factors other than solubility in the receptor fluid that need to be investigated, and the importance of clearly defining the composition of the receptor fluid is illustrated. There may be a case for inclusion of PEG 20 or BSA in receptor fluid at all times, even for hydrophilic molecules, since this may better represent the situation *in vivo* (e.g. proteins in circulatory fluid). Lockley (2000) showed that *in vitro* absorption through occluded dermatomed rat skin using tissue culture medium without protein or PEG 20 underestimated BE (and to a much lesser degree EE) absorption from a topical dose *in vivo*.

Experiments with full thickness skin in the present study show that the dermis clearly presents a barrier to absorption of EE and BE. It is recommended in the OECD guidelines that epidermal membranes or split thickness skin (200 to 400 μm) be used.

It is likely that split skin would give a better representation of the situation in vivo, since the perfused capillary system in the upper dermis is not maintained *in vitro*. A physiological receptor fluid such as tissue culture medium or saline should be used with dermatomed skin, whether skin viability is important or not, as ethanol:water increases permeability of epidermal membranes to tritiated water (Pelling *et al*, 1998).

7.3 Comparison with predictions and *in vivo* data

There was good agreement between predictions of permeability coefficients from the KBS (based on an infinite dose of a saturated aqueous solution) and apparent k_p values obtained from *in vitro* experiments dosed with an infinite neat dose, especially for the glycol ethers. Discrepancy between flux predictions and experimental findings are expected due to the difference in dose regime. However, these *in vitro* experiments were conducted without PEG 20 or BSA in receptor fluid. If further research shows that the inclusion of PEG 20 etc. in receptor fluid results in a better prediction of absorption *in vivo*, then a correction factor will need to be included in the KBS, though this will depend on the test compound. Prediction of k_p for THF and acetone (neat infinite dose) was overestimated, probably due to the high volatility of these compounds. For the relatively hydrophilic test compounds (the glycol ethers, acetone, MEK and THF), the predicted k_p grossly underestimated the apparent k_p when a dilute (3 mg ml^{-1}) aqueous solution was used *in vitro*. This indicates that flux would be greatly underestimated if the KBS were used to derive predictions from more dilute aqueous solutions (i.e. if the dose concentration were entered rather than calculated from solubility data or other physiochemical parameters), and suggests that vehicle effects are not well corrected by the KBS for relatively hydrophilic compounds. For the aromatic compounds, however, there was very good agreement between predicted and apparent k_p values for dilute aqueous solutions. This is expected as the aqueous solubility of the aromatic compounds is low, so a dilute aqueous solution is a close approximation to the conditions assumed by the KBS. Times to steady state showed reasonable agreement between prediction and experiment for the more hydrophilic test compounds, though predictions of time to steady state appear to be based on molecular weight. There were some differences in observed times to steady state between isomers (e.g. between THF and MEK in neat infinite doses) which were not predicted by the KBS. The time to steady state for EE in aqueous solution is also complicated by the apparent concentration effect, resulting in the fastest linear rate being measured later than with neat doses. The time to steady state for the aromatic compounds was overestimated by the KBS. Apart from EE and BE, apparent k_p values for neat finite doses were lower than those predicted, suggesting that evaporation from smaller,

occupationally-relevant dose volumes limits absorption, which ceased in most cases after less than 5 h, even in infinite doses of aqueous solutions.

There have been few controlled human *in vivo* studies of dermal absorption of the test compounds from a liquid application described in the present study. Kesic *et al*. (1997a) reported a penetration rate of 0.7 ± 0.3 mg cm^{-2} h^{-1} ($= 7.76 \pm 3.32$ μmol cm^{-2} h^{-1}) for EE (neat liquid applied to human forearm 27 cm^2 for 15 minutes). This is in good agreement with data obtained in the present study from a neat finite application. There have been some studies of dermal absorption of vapours, notably Brooke *et al*. (1998) and Loizou *et al*. (1998). These studies showed that dermal uptake of xylene, toluene and THF from the vapour phase was unlikely to contribute greatly to the overall body burden, though dermal absorption for glycol ethers could be an important contributor to total uptake. The data obtained in the present study are supported by these findings.

7.4 Reservoir effects and barrier damage

There was little evidence of reservoir effects from cumulative absorption-time curves of the test compounds. Absorption into receptor fluid of most of the test compounds ceased after about 5 h or less (especially for finite doses), suggesting that the supply of dose material was exhausted by this time (probably due to evaporation). Very little material was recovered from surface swabs or tape strips, or from the skin itself, even in short term (4 h) experiments with MEK and THF. There was some evidence of the development of a reservoir in the skin with EE penetration in an aqueous dose when 2% (w/v) BSA or 6% (w/v) PEG 20 was included in the receptor fluid. Absorption into receptor fluid continued for longer in these experiments than in the absence of BSA or PEG 20. Addition of these materials may have altered the equilibrium between the dose material and the receptor fluid, thus encouraging more diffusion into the aqueous matrix of the dermis. This effect was not reproduced in occupationally relevant doses, however, though the flux itself was enhanced by additions to receptor fluid. The great majority of all compounds tested appeared to be volatilized, though recovery of volatilized material was poor for MEK, THF and acetone, since these compounds were not stably retained by the charcoal filters. There were no apparent effects of occupationally relevant doses of MEK, THF or acetone on the permeability of human skin to tritiated water, suggesting that single application dose not result in barrier damage.

7.5 Conclusions

7.5.1 Best systems for studying dermal absorption of liquid solvents *in vitro*

From the present study, it is recommended that dermatomed skin or epidermal membranes should be used for *in vitro* studies. The receptor fluid should be clearly defined, and experimenters should quantify the effect of the addition of PEG 20 or BSA for all compounds, regardless of their solubility in the receptor fluid. Other conditions such as dose volume should be clearly defined.

7.5.2 *In vitro* findings and predictions

Both EE and BE exhibited a high degree of dermal absorption due to a high flux and prolonged absorption phase in both aqueous and neat doses. Exposure to these compounds represented the highest dermal absorption hazard of all the test compounds. Dermal absorption of the other test compounds was markedly lower, especially in occupationally relevant (neat, finite) doses, due to high vapour pressure influencing flux and/or the degree of absorption, and/or due to an adverse log P for dermal absorption. Test compounds with high vapour pressure and negative log P exhibited the lowest dermal absorption hazard. However, apparent k_p values for dermal absorption from aqueous solutions were higher than those measured for neat doses for all compounds, illustrating the importance of vehicle effects. Absorption from large volume aqueous solutions was also more prolonged than from neat finite doses, even for highly volatile compounds. The importance of these findings for occupational exposure (especially for the glycol ethers) should not be underestimated.

KBS predictions of k_p (and flux) were very good for neat infinite doses of the glycol ethers and for MEK, though k_p was overestimated for THF and acetone. However, k_p was greatly underestimated for large doses of dilute aqueous solutions for these compounds; hence flux would be underestimated if predicted k_p values were used for dilute aqueous solutions. KBS predictions for aqueous solutions of toluene and xylene were good however. *In vitro* findings for neat finite doses (flux, k_p) were in reasonable agreement with KBS predictions for EE and BE. For other compounds, however, KBS predictions overestimated these parameters for neat, finite doses.

8.0 OUTCOMES OF THE PROJECT

- We have expanded the use of *in vitro* dermal prediction techniques for the study of absorption of liquid solvents

- We have further evaluated the *in vitro* dermal absorption techniques and related results to theoretical predictions

- We have contributed to the knowledge base on dermal absorption of solvents in the workplace under a range of conditions, and have highlighted similarities and differences between *in vitro* findings and predictions for the test compounds.

9.0 REFERENCES

Bast GE and Kampffmeyer HG (1996) No effect of albumin on the dermal absorption rate of hydrocortisone 21-butyrate, permethrin or diflusinal in the isolated, single-pass perfused rabbit ear. Skin Pharmacology 9, 327-333

Barratt MD (1995) Quantitative structure activity relationships for skin permeability. Toxicology *in Vitro* 9, 27-37

Boman A and Maibach HI (2000) Influence of evaporation and solvent mixtures on the absorption of toluene and *n*-butanol in human skin *in vitro*. Annals in Occupational Hygiene 44, 125-135

Bronaugh RL and Stewart RF (1984) Methods for *in vitro* percutaneous absorption studies III: hydrophobic compounds. Journal of Pharmacological Sciences 73, 1255-1258

Bronaugh RL and Stewart RF (1985) Methods for *in vitro* percutaneous absorption studies IV: the flow-through diffusion cell. Journal of Pharmacological Sciences 74, 64-67

Bronaugh RL, Collier SW, Storm JE, Nathan DL and Stewart RF (1990) *In vitro* absorption/metabolism studies in human and animal skin. In: Prediction of percutaneous penetration Vol 1 (Scott RC, Guy RH and Hadgraft J, Eds) IBC Technical Services, London pp 58-73

Brooke I, Cocker J, Delic JI, Payne M, Jones K, Gregg NC and Dyne D (1998) Dermal uptake of solvents from the vapour phase: an experimental study in humans. Annals of Occupational Hygiene 42, 531-40

Chion *et al*. (1982) Environmental Science and Technology 16, 4-10

Clark NWE, Scott RC, Blain PG and Williams FM (1991) Maintenance of skin viability in skin absorption systems. In: Prediction of percutaneous penetration Vol 2 (Scott RC, Guy RH, Hadgraft J and Boddé HE, Eds) IBC Technical Services, London pp 541-554

Clark NWE, Scott RC, Blain PG and Williams FM (1993) Fate of fluazifop butyl in rat and human skin *in vitro*. Archives of Toxicology 67, 44-48

Clowes HM, Scott RC and Heylings JR (1994) Skin absorption: flow through or static diffusion cells. Toxicology *in Vitro* 8, 827-830

DeLange J, Vaneck P, Bruijnzeel PLB, Elliott GR (1994) The rate of percutaneous permeation of xylene, measured using the perfused pig ear model, is dependent on the effective protein-concentration in the perfusing medium. Toxicology And Applied Pharmacology 127, 298-305

Dick I, Blain PG, Williams FM (1997a) The percutaneous absorption and skin distribution of lindane in man (1) In vivo studies. Human and Experimental Toxicology 16, 645-651

Dick I, Blain PG, Williams FM (1997b) The percutaneous absorption and skin distribution of lindane in man (2) In vitro studies. Human and Experimental Toxicology 16, 652-657

Dick I, Williams FM (1998) HSL Research Report In vitro models for the prediction of dermal absorption of chemicals

Di Vincenzo GD, et al. (1978) Studies on the respiratory uptake and excretion and the skin absorption of methyl n-butyl ketone in humans and dogs. Toxicology and Applied Pharmacology 44, 593-604

Elsisi AE, Carter DE and Sipes IG (1989) Dermal absorption of phthalate diesters in rats. Fundamental and Applied Toxicology 12, 70-77

Ensgtröm K, Husman K and Riihimäki V (1977) Percutaneous absorption of m-xylene in man. International Archives of Occupational and Environmental Health 38, 181-189.

Filon FL, Fiorito A, Adami G, Barbieri P, Coceani N, Bussani R and Reisenhofer E (1999) Skin absorption in vitro of glycol ethers. International Archives Of Occupational And Environmental Health 72, 480-484 OCT

Flynn GL (1990) Physicochemical determinants of skin absorption In: Principles of route to route extrapolation for risk assessment (Gerrity TR and Henry CJ, Eds). Elsevier Science Publishing. 93-127

Hansch C *et al*. (1995) Exploring QSAR - hydrophobic, electronic and steric constants. American Chemical Society, Washington DC

Hilton J, Woollen BH, Scott RC, Auton TR, Trebilcock KL And Wilks MF (1994) Vehicle effects on in-vitro percutaneous-absorption through rat and human skin. Pharmaceutical Research 11, 1396-1400

Howes D, Guy R, Hadgraft J, Heylings J, Hoeck U, Kemper F, Maibach H, Marty J-P, et al. (1996) Methods for assessing percutaneous absorption. ATLA (Alternatives to laboratory animals) 24, 81-106

Jepson GW and McDougal JN (1999) Predicting vehicle effects on the dermal absorption of halogenated methanes using physiologically based modeling. Toxicological Sciences 48, 180-188

Kelland B (1999) Chemical Hazards In: Croner's substances hazardous to health (Kelland B ed). 1999 update. Croner Publications Ltd, New Malden. 620 pp

Kezic S, Mahieu K, Monster AC and de Wolff FA (1997a) Dermal absorption of vaprous and liquid 2-methoxyethanol and 2-ethoxyethanol in volunteers. Occupational and Environmental Medicine 54, 38-43

Kezic S, Monster AC, Opdam JJG and de Wolff FA (1997b) Dermal exposure to vaprous and liquid organic solvents in volunteers. Fundamental and Applied Toxicology 36, 190

Kezic S, Monster AC, Kruse J and Verbeck MM (2000a) Dermal absorption of vaprous organic solvents in volunteers. Accepted for publication in International Archives of Occupational and Environmental Health

Kezic S, Monster AC, van de Gevel AC, Kruse J and Verbeck MM (2000b) Dermal absorption of neat liquid solvents in volunteers. Accepted for publication in American Hygiene Association Journal

Kezic S, van Dorth S, Monster AC, Kruse J and de Wolff FA (1998) Dermal absorption of vaprous 2-butoxyethanol in volunteers. The Toxicologist 42, 390

Lockley DJ (2000) Percutaneous absorption and metabolism of glycol ethers: prediction by an *in vitro* approach. PhD Thesis, University of Newcastle

Lockley DJ, Howes D and Williams FM (1999) Percutaneous penetration of 2-ethoxyethanol and 2-butoxyethanol through rat and human skin in vitro: prediction of in vivo penetration. Human and Experimental Toxicology 18, 537

Loizou GD, Jones K, Akrill P, Dyne D, Cocker J (1999) Estimation of the dermal absorption of m-xylene vapor in humans using breath sampling and physiologically based pharmacokinetic analysis. Toxicological Sciences 48, 170-179

McDougal JN et al (1990) Dermal absorption of organic chemical vapors in rats and humans. Fundamental and Applied Toxicology 14, 299-308

Meylan WM, Howard PH (1995) Atom fragment contribution method for estimating octanol-water partition-coefficients. Journal of Pharmaceutical Sciences 84, 83-92

Morgan DL et al (1991) Dermal absortion of neat and aqueous volatile organic chemicals in the Fischer 344 rat. Environmental Research 55, 51-63

Organisation for Economic Cooperation and Development (OECD) (2000) OECD Draft guideline for the testing of chemicals - skin absorption: *in vitro* method. OECD Paris.

Payne MP (1995) Prediction of skin penetration potential form physicochemical and toxicological properties: SARs for a knowledge-based system. HSE Project Report

Pelling D, Phillips JC and Cunninghame ME (1998) Absorption of hydrophilic and lipophilic compounds thorough epidermal and subepidermal strata of rat skin in vitro. Toxicology *in Vitro* 12, 47-55

Potts RO and Guy RH (1995) A predictive algorithm for skin permeability: the effects of molecular size and hydrogen bond activity. Pharmaceutical Research 12, 1628-1633

Rawlings JM, Hilton J, Trebilcock KL, Woollen BH, Wilks MF (1994) Effect of dosing vehicle on the dermal absorption of fluazifop-butyl and fomesafen in rats in-vivo. Fundamental And Applied Toxicology 23, 93-100

Roper CS, Howes D, Blain PG, Williams FM (1995) Prediction of the percutaneous penetration and metabolism of dodecyldecaethoxylate in rats. Archives of Toxicology 69, 649-654

Roper CS, Howes D, Blain PG, Williams FM (1997) Percutaneous penetration of 2-phenoxyethanol through rat and human skin. Food and Chemical Toxicology 35, 1009-1016

Roper CS, Howes D, Blain PG, Williams FM (1998) A comparison of the absorption of a series of ethoxylates through rat skin *in vitro*. Toxicology *in Vitro* 12, 57-65

Scott RC and Ramsey JD (1987) Comparison of the *in vivo* and *in vitro* percutaneous absorption of a lipophilic molecule (Cypermethrin, a pyrethroid insecticide). Journal of Investigative Dermatology 89, 142-146

Tsuruta H (1996) Skin absorption of solvent mixtures - Effect of vehicles on skin absorption of toluene. Industrial Health 34, 369-378

Williams FM (1998) The role of skin metabolism in percutaneous absorption. In: Perspectives of Percutaneous Penetration Vol 5b. (Brain, James and Waters Eds) STS Publishing, Cardiff 41-44

Williams FM and Wilkinson SC (2000) Factors affecting dermal absorption of ethoxyethanol *in vitro* - implications for risk assessment. In: Prediction of Percutaneous Penetration. In Press.

In Vitro Dermal Absorption of Liquids

SUPPLEMENT

Dermal absorption of pyridine and its derivatives

Investigators: Simon C. Wilkinson, PhD and Faith M.Williams, PhD

Department of Environmental and Occupational Medicine,
University of Newcastle

S.1 INTRODUCTION

Pyridine and its derivatives, picoline (methyl pyridine), lutidine (dimethyl pyridine) and collidine (trimethyl pyridine) are widely used in chemical industry, as solvents in manufacturing processes and as chemical reagents, both starting materials and intermediates. Pyridine is miscible in water, alcohol and ether (Windholz, 1983) and water solubility and vapour pressure decrease with increasing molecular weight (Table S.1). Pyridine and the above derivatives are listed as skin irritants, as well as severe eye and/or respiratory irritants (Kelland, 1999; manufacturers chemical safety data sheets). Little detailed information about skin absorption of these compounds is available (though all are listed as being absorbed through skin), and little is known about the toxicity of di- and tri-methyl derivatives to man.

Studies carried out on the dermal absorption of solvents detailed in previous sections of this report have resulted in a better understanding of the role of physicochemical parameters in determining the degree of dermal absorption. The aims of the present study were to determine the degree of dermal absorption of pyridine and its derivatives from neat and aqueous vehicles using human skin in an *in vitro* system, and to use the resulting data to further investigate the influence of molecular weight, vapour pressure, water solubility and lipophilicity on dermal absorption.

Table S.1 Physicochemical properties of pyridine and its derivatives

Log P data were obtained from Hansch *et al*. (1995), except for 2,4-lutidine (estimated, from Meylan and Howard, 1995). Data on vapour pressure and water solubility were obtained from the Environmental Sciences Centre database (available through www.chemfinder.com).

Compound	CAS No.	water solubility (mg l^{-1})	vapour pressure (KPa at 25˚C)	log P	MW
pyridine	110-86-1	1 x 106	2.77	0.65	79.1
2-picoline	109-06-8	1 x 106	1.49	1.11	93.13
2,4-lutidine	108-47-4	3.5 x 105	0.42	1.90	107.15
2,4,6-collidine	108-75-8	3.5 x 104	0.26	1.88	121.18

S.2 MATERIALS AND METHODS

S.2.1 Materials

Pyridine (AR, 99.5%) was obtained from BDH. 2-picoline (Approx. 95%) was obtained from GD Searle. 2,4-lutidine (99%) and 2,4,6-collidine (99%) were obtained from Aldrich. Other materials used were as in sections 2.1.2 and 2.1.3.

S.2.2 Methods

S.2.2.1 Flow through diffusion studies

Flow through diffusion studies were carried out as in section 2.2.1. Briefly, human breast skin was dermatomed to produce a section containing the stratum corneum, epidermis and upper dermis (approx. 330 μm). Squares of dermatomed skin (approx. 1.5 cm^2) were mounted in Scott-Dick flow through diffusion cells. Receptor fluid (Eagle's Minimal Essential Medium, pH 7.4, maintained with CO_2/air) was pumped beneath the skin at 1.5 ml h^{-1} for 21 h, and the system was maintained at 32˚C. Test compounds were applied to the skin surface (0.64 cm^2) in either a finite neat dose (10 μl) or an aqueous dose (200 μl, 3 mg ml^{-1}). Charcoal filters were placed above the donor chamber to trap any volatilized dose material.

S.2.2.2 Distribution analysis

Distribution analysis was carried out for selected studies after 21 h. The donor chamber of the diffusion cell was carefully swabbed with tissue paper soaked in 3% (v/v) aqueous teepol H and blotted with dry tissue paper. The skin surface was swabbed alternately with tissue paper squares soaked in aqueous teepol H and dry tissue paper squares as above (three of each). The inner parts of the diffusion cell were also swabbed in this way. The stratum corneum was removed by tape stripping with 3M tape (the first tape strip was analysed separately). The remaining skin was cut into strips with scissors. Test compounds were desorbed in all samples with CH_2Cl_2:MeOH (95:5 v/v) for 24 h at -20˚C. Desorbates were subjected to GC as described in S.2.2.4.

S.2.2.3 Analysis of receptor fluids

Aliquots of receptor fluid (0.5 to 1.0 ml) were pipetted into polypropylene tubes (3 ml capacity). An equal volume of internal standard was added. 1,4-dioxan (1180 μM in deionised water) was used as an internal standard for pyridine determination. Pyridine (1236 μM in deionised water) was used as an internal standard for the other compounds. CH_2Cl_2:MeOH (95:5 v/v) was added (0.75 ml), the tubes stoppered and mixed on a rotary shaker for 30 minutes. After settling, 500 μl of the lower phase was collected and transferred to septum sealed vials for GC/FID as described below. Standard curves of all compounds were plotted using standards prepared in MEM (R-squared values 99% or greater). Concentrations in receptor fluid samples were determined by interpolation from standard curves. The detection limit for each compound was 10 μM in receptor fluids. The micromolar response factor for pyridine was 1.31×10^7.

S.2.2.4 Gas chromatography column and conditions

GC was carried out using a Hewlett Packard 5890 Series II chromatograph, equipped with an Ultra 1 (cross linked methyl siloxane) column (50 m, 0.32 mm i.d., 0.52 μm film thickness). A split ratio of 10:1 was employed. The injector temperature was 200˚C. Detection was by flame ionisation detection using hydrogen (130 KPa) and air (270 KPa) with nitrogen (150 KPa) as auxiliary gas. Helium was used as a carrier gas (column head pressure 75 KPa). An injection volume of 1 μl was used. The temperature program used was 50˚C for 3 minutes; 50˚C/min to 100˚C; hold for 3 minutes.

S.2.3 Flow through studies carried out

Study 1	Dermal absorption of aqueous pyridine in different donor concentrations
Study 2	Dermal absorption of neat pyridine
Study 3	Dermal absorption of aqueous 2-picoline, 2,4-lutidine and 2,4,6-collidine (3 mg ml^{-1})
Study 4	Dermal absorption of neat 2-picoline, 2,4-lutidine and 2,4,6-collidine

S.3 RESULTS

S.3.1 Dermal absorption of aqueous pyridine - effect of dose concentration on absorption through dermatomed human skin into receptor fluid

The temporal length of the steady state phase of pyridine absorption through dermatomed human skin was short and not affected by dose concentration. Absorption from both dose concentrations ceased after 2 h (Fig S.3.1). The steady state flux from aqueous pyridine (200 μl applied) was approximately doubled ($P<0.05$) when the dose concentration was increased from 3 to 6 mg ml^{-1} (Fig S.3.1, Table S.3.1). The apparent k_p was not significantly affected by the dose concentration (Table S.3.1), nor was the time to steady state (Fig S.3.1). The total absorbed was again approximately doubled with the higher dose concentration ($P<0.05$), whilst the proportion of the dose absorbed was unaffected ($P>0.05$) (Table S.3.1).

S.3.2 Distribution of pyridine in dermatomed human skin following application of aqueous pyridine

No pyridine was detected in surface swabs, cell washes, tape strips of skin tissue. About 84% of the dose material was recovered from the charcoal filters in both dose concentrations. The total recovery was about 85% in both cases.

S.3.3 Comparison of absorption through dermatomed human skin into receptor fluid of aqueous pyridine, 2-picoline, 2,4-lutidine and 2,4,6-collidine (200 μl dose)

There was an apparent increase in the temporal length of the absorption phase of the pyridine derivatives with increasing molecular weight (and decreasing vapour pressure). Pyridine absorption into receptor fluid ceased after 100 minutes, whilst absorption of 2,4,6-collidine continued until 3 h. The time to establish steady state flux also increased numerically, but this effect was not significant statistically (Fig S.3.2, Table S.3.2). The steady state flux of the methyl derivatives was two to three-fold greater than that of pyridine, as was their apparent k_p ($p<0.001$ in each case). However, there was no significant difference in steady state flux or apparent k_p between 2-picoline, 2,4-lutidine and 2,4,6-collidine (Fig S.3.2, Table S.3.2). The final proportion of the dose absorbed was again higher with the methyl derivatives than with

pyridine ($P<0.01$), though there was no statistically significant difference between the proportions of 2-picoline, 2,4-lutidine and 2,4,6-collidine absorbed.

S.3.4 Comparison of absorption through dermatomed human skin into receptor fluid of pyridine, 2-picoline, 2,4-lutidine and 2,4,6-collidine in a neat finite dose (10 μl)

There was a similar increase in the temporal length of the absorption phase with molecular weight with neat, finite doses (Fig S.3.3) as that observed with aqueous doses (Fig S.3.2). There was also a significant increase in time to steady state with molecular weight ($P<0.05$). However, a very different response of flux to molecular weight was observed when neat doses were applied. The greatest steady state flux (and apparent k_p) was measured with pyridine, whilst significantly lower fluxes were measured with the methyl derivatives ($P<0.001$ in each case) (Table S.3.3). In contrast to aqueous doses, flux ($P<0.01$) and apparent k_p ($P<0.01$) for neat 2-picoline, 2,4-lutidine and 2,4,6-collidine increased significantly with molecular weight. This finding, coupled with the increase in temporal length of the absorption phase for neat 2,4,6-collidine, resulted in a significantly ($P<0.01$) higher total absorption for 2,4,6-collidine (2.62 ± 0.57 μmol) than for 2-picoline (0.50 ± 0.15 μmol) and 2,4-lutidine (0.90 ± 0.04 μmol). The proportion of the applied dose absorbed of neat 2,4-lutidine and 2,4,6-collidine was not significantly different that of neat pyridine ($P>0.05$).

S.4 DISCUSSION

There were some similarities in the dermal absorption profile through human skin *in vitro* of pyridine, and its derivatives, and the solvents reported in previous sections. A large proportion of the dose solution was volatilized in each case (50 to 99%), and this depended on the dose regime. The apparent k_p values for absorption from aqueous solutions were much higher than from neat finite doses, as was the case with all solvents examined. This is probably due to the solvent partitioning into the stratum corneum when applied in an aqueous vehicle, thus increasing the effective concentration to drive the flux. The differences in apparent k_p values for aqueous and neat finite doses of pyridine followed the pattern established for other solvents and described in previous sections. The apparent k_p of neat pyridine was similar to that for THF and lower than that for butoxyethanol, suggesting a relationship between apparent k_p and log P in which k_p is maximum for a log P of around 0.9 (Fig S.4.1). It is likely that vapour pressure limits the k_p of certain highly volatile solvents following application in a small volume of neat solvent, however. A different relationship was found between log P and apparent k_p in an aqueous dose (S.4.2). There was an increase in apparent k_p

with log P, although the highly lipophilic compounds studied in section 6 (toluene and xylenes) did not follow the trend established by the more hydrophilic compounds. Again, pyridine followed the pattern established for the other solvents applied in aqueous doses. Addition of a single methyl group to pyridine resulted in a marked increase in flux (and apparent k_p) when an aqueous vehicle was used. This could be predicted from the increase in log P. However, addition of further methyl groups did not further increase the flux or the apparent k_p. This suggests that factors other than lipophilicity influenced the rate of absorption from aqueous vehicles. Aqueous solubility, which decreases with increasing molecular weight, may have limited the diffusion of the higher methyl derivatives out of the stratum corneum and into the aqueous matrix of the epidermis and upper dermis. Absorption-time curves for the pyridine derivatives became increasingly sigmoidal as methyl groups were added. This suggests that concentration of the dose solution may have occurred for derivatives with high molecular weight (and hence low vapour pressure) when aqueous doses were employed, possibly because of preferential evaporation of water from the dose solution. A similar effect was previously observed with aqueous ethoxyethanol in section 4. Addition of methyl groups to pyridine had a very different effect on flux and apparent k_p from neat doses. Addition of one methyl group resulted in a marked decrease in both flux and apparent k_p. Addition of further methyl groups increased these parameters with respect to picoline, though none achieved the flux and apparent k_p of pyridine in neat doses.

There was a clear relationship between molecular weight of the pyridine derivatives and the temporal length of the absorption phase for both aqueous and neat dose regimes. This is likely to be related to vapour pressure, which decreases with increasing molecular weight of the pyridine derivatives. Decreasing vapour pressure is likely to influence the evaporation of the solvent from the dose, particularly in the finite, neat dose regime. This effect had been previously observed, particularly with butoxyethanol (and to a lesser extent ethoxyethanol) as discussed in previous sections. In neat, finite doses, the steady state phase became more distinct as more methyl groups were added to the pyridine skeleton. Conversely, compounds previously examined which had a high vapour pressure had a much less defined steady state phase when applied in neat, finite doses, particularly acetone and THF. In support of our findings, Boman *et al*. (1995) found that the amount of n-butanol, toluene and 1,1,1-trichloroethane absorbed percutaneously by guinea pigs *in vivo* from neat doses was inversely related to the vapour pressure of the solvent.

The total absorption was influenced by the temporal length of the absorption phase and the steady state flux. Addition of methyl groups to the pyridine skeleton thus resulted in higher levels of total absorption with the aqueous dose regime, both in absolute terms and as a percentage of the dose applied. The situation for neat finite doses did not follow this pattern in absolute terms, as the steady state flux and apparent k_p measured with pyridine decreased markedly when picoline was used. Addition of further methyl groups did result in an increase in final absorption with respect to picoline, however. The high steady state flux measured with neat pyridine resulted in a significantly higher level of total absorption than 2-picoline (about sixfold) and 2,4-lutidine (about fourfold) in absolute terms, despite the temporal length of the steady state phase being approximately one hour. The time taken to establish steady state flux also increased significantly with molecular weight, and was somewhat longer for picoline, lutidine and collidine in a neat dose than in an aqueous dose (though there was very little difference with pyridine). The decrease in aqueous solubility with molecular weight is also likely to influence the time taken to establish steady state flux.

The high apparent k_p and low time to steady state flux measured with neat pyridine clearly illustrate the high dermal absorption risk from exposure to this compound as a liquid in an occupational situation. The data presented here suggest that neat 2-picoline and 2,4-lutidine present a comparatively lower risk, though the long steady state phase of 2,4,6-collidine resulted in higher level of absorption into receptor fluid than 2-picoline and 2,4-lutidine when neat doses were used. The fact that these compounds are skin irritants may encourage a worker to wash off rapidly any dose material from a liquid splash before significant levels of compound are absorbed. However, the same may not apply to aqueous doses of pyridine and its derivatives. It is unlikely that dilute aqueous doses would cause the same level of irritation as neat doses, though a splash of an aqueous solution (10-20 μl) would dry more rapidly on the skin than the doses used in the present study. The lower vapour pressure of the higher methyl derivatives may result in concentration of such a dose to an extent that a significant dose is absorbed, though this may result in some irritation. Furthermore, occlusion of an aqueous dose, for example under latex gloves, may impede evaporation of the dose and hence prolong contact. The greater apparent k_p, and in the case of collidine, temporal length of the absorption phase, of aqueous doses of methyl derivatives increase the dermal absorption risk of these compounds relative to pyridine when an aqueous vehicle is employed.

Prediction of permeability coefficient by the Dermal KBS is carried out using the following equation:

$$\log k_p = -2.72 + 0.71\log P - 0.0103\ MW$$

where k_p is the permeability coefficient (cm h^{-1}), log P is $\log_{10}$ octanol:water partitioning coefficient and MW is the molecular weight. This allows us to calculate the following predicted values for k_p (cm h^{-1}): pyridine: 0.00084; 2-picoline: 0.00128; 2,4-lutidine: 0.00335; and 2,4,6-collidine: 0.00233. These predictions differ from experimental findings in two ways. Firstly, the equation did not predict the insensitivity of apparent k_p to log P for picoline, lutidine and collidine in aqueous solution (and greatly underestimated apparent k_p for all compounds in aqueous solution, as was the case with solvents studied in previous sections). Secondly and surprisingly, the prediction for apparent k_p of neat pyridine, the most volatile of the compounds tested was very close to that found experimentally, whilst there was large disparity between predicted and apparent k_p values from neat dose experiments with less volatile compounds, namely 2-picoline, 2,4-lutidine and 2,4,6-collidine.

Although the dermal absorption of pyridine-based compounds (particularly pharmaceuticals) has been studied, there are apparently no published reports of the absorption of pyridine or its derivatives from liquid applications through human skin. This study therefore provides important quantitative information on the dermal absorption risk of pyridines as well as valuable data on the influence of physicochemical properties on dermal absorption of a series of structurally related solvents.

Table S.3.1 Dermal absorption parameters for pyridine in aqueous vehicle (200 µl) - influence of donor concentration. Figures are means ± SEM (n=4/5)

Donor concentration ($mg\ ml^{-1}$) [dose (mg)]	Flux ($nmol\ cm^{-2}\ h^{-1}$) [$\mu g\ cm^{-2}\ h^{-1}$]	Apparent k_p ($cm\ h^{-1}$)	Time to steady state (h)	Final absorption (µmol) [µg]	Final absorption (% applied dose)
3 [0.6]	**238 ± 62** **[18.8 ± 4.9]**	**0.0063 ± 0.0016**	**0.37 ± 0.02**	**0.15 ± 0.04** **[11.9 ± 3.2]**	**1.99 ± 0.55**
6 [1.2]	**444 ± 37** **[35.1 ± 2.9]**	**0.0058 ± 0.0005**	**0.43 ± 0.05**	**0.28 ± 0.02** **[22.1 ± 1.6]**	**1.82 ± 0.16**

Table S.3.2 Dermal absorption parameters for pyridine and its derivatives in aqueous vehicle (200 µl, 3 mg ml^{-1}, 0.6 mg)
Figures are means ± SEM (n=4/5)

Compound and concentration, dose	Flux (nmol cm^{-2} h^{-1}) [µg cm^{-2} h^{-1}]	App k_p (cm h^{-1})	time to steady state (h)	Amount absorbed (µmol) [µg]	Amount absorbed (% applied dose)
pyridine (37.9 mM, 7.6 µmol)	**238 ± 62 [18.8 ± 4.9]**	**0.0063 ± 0.0016**	**0.37 ± 0.02**	**0.15 ± 0.04 [11.9± 3.2]**	**1.99 ± 0.55**
2-picoline (32.2 mM, 6.4 µmol)	**686 ± 129 [63.9 ± 12.0]**	**0.021 ± 0.004**	**0.39 ± 0.04**	**0.36 ± 0.08 [33.5 ± 7.5]**	**5.56 ± 1.18**
2,4-lutidine (28.0 mM, 6.0 µmol)	**559 ± 191 [59.9 ± 20.5]**	**0.020 ± 0.007**	**0.41 ± 0.03**	**0.33 ± 0.10 [35.4 ± 10.7]**	**5.87 ± 1.74**
2,4,6-collidine (24.8 mM, 5.0 µmol)	**508 ± 80 [61.6 ± 9.7]**	**0.021 ± 0.003**	**0.50 ± 0.06**	**0.35 ± 0.05 [42.4 ± 6.1]**	**7.01 ± 0.98**

Table S.3.3 Dermal absorption parameters for neat pyridine and its derivatives in finite doses (10 µl)
Figures are means ± SEM (n=4/5)

Compound and concentration, dose	Flux (nmol cm^{-2} h^{-1}) [µg cm^{-2} h^{-1}]	App k_p (cm h^{-1})	time to steady state (h)	Amount absorbed (µmol) [µg]	Amount absorbed (% applied dose)
pyridine (123.6 µmol, 9.8 mg)	**7907 ± 1055 [625 ± 83.5]**	**6.4×10^{-4} ± 0.9×10^{-4}**	**0.36 ± 0.05**	**3.67 ± 0.54 [290.3 ± 42.7]**	**2.96 ± 0.44**
2-picoline (101.3 µmol, 9.4 mg)	**822 ± 222 [76.6 ± 20.7]**	**8.1×10^{-5} ± 2.2×10^{-5}**	**0.55 ± 0.15**	**0.50 ± 0.15 [46.6 ± 14.0]**	**0.49 ± 0.14**
2,4-lutidine (86.5 µmol, 9.3 mg)	**1685 ± 137 [180.5 ± 14.7]**	**1.9×10^{-4} ± 0.2×10^{-4}**	**0.65 ± 0.01**	**0.90 ± 0.04 [96.4 ± 4.3]**	**1.04 ± 0.04**
2,4,6-collidine (75.7 µmol, 9.2 mg)	**2305 ± 286 [279.3 ± 34.7]**	**3.0×10^{-4} ± 0.4×10^{-4}**	**0.76 ± 0.06**	**2.62 ± 0.57 [317.5 ± 69.1]**	**3.46 ± 0.75**

S.5.0 REFERENCES

Boman A, Hagelthorn G, Magnusson K (1995) Percutaneous-absorption of organic solvents during intermittent exposure in guinea-pigs. Acta Dermato-Venereologica 75, 114-119

Hansch C *et al*. (1995) Exploring QSAR - hydrophobic, electronic and steric constants. American Chemical Society, Washington DC

Kelland B (1999) Chemical Hazards In: Croner's substances hazardous to health (Kelland B ed). 1999 update. Croner Publications Ltd, New Malden. 620 pp

Meylan WM, Howard PH (1995) Atom fragment contribution method for estimating octanol-water partition-coefficients. Journal of Pharmaceutical Sciences 84, 83-92

Windholz M. (1983) Merck Index 10th Edition Merck and Co., Rahway, NJ. USA.

APPENDIX

Fig 3.1 Standard curves of M2P in MEM using a range of internal standards

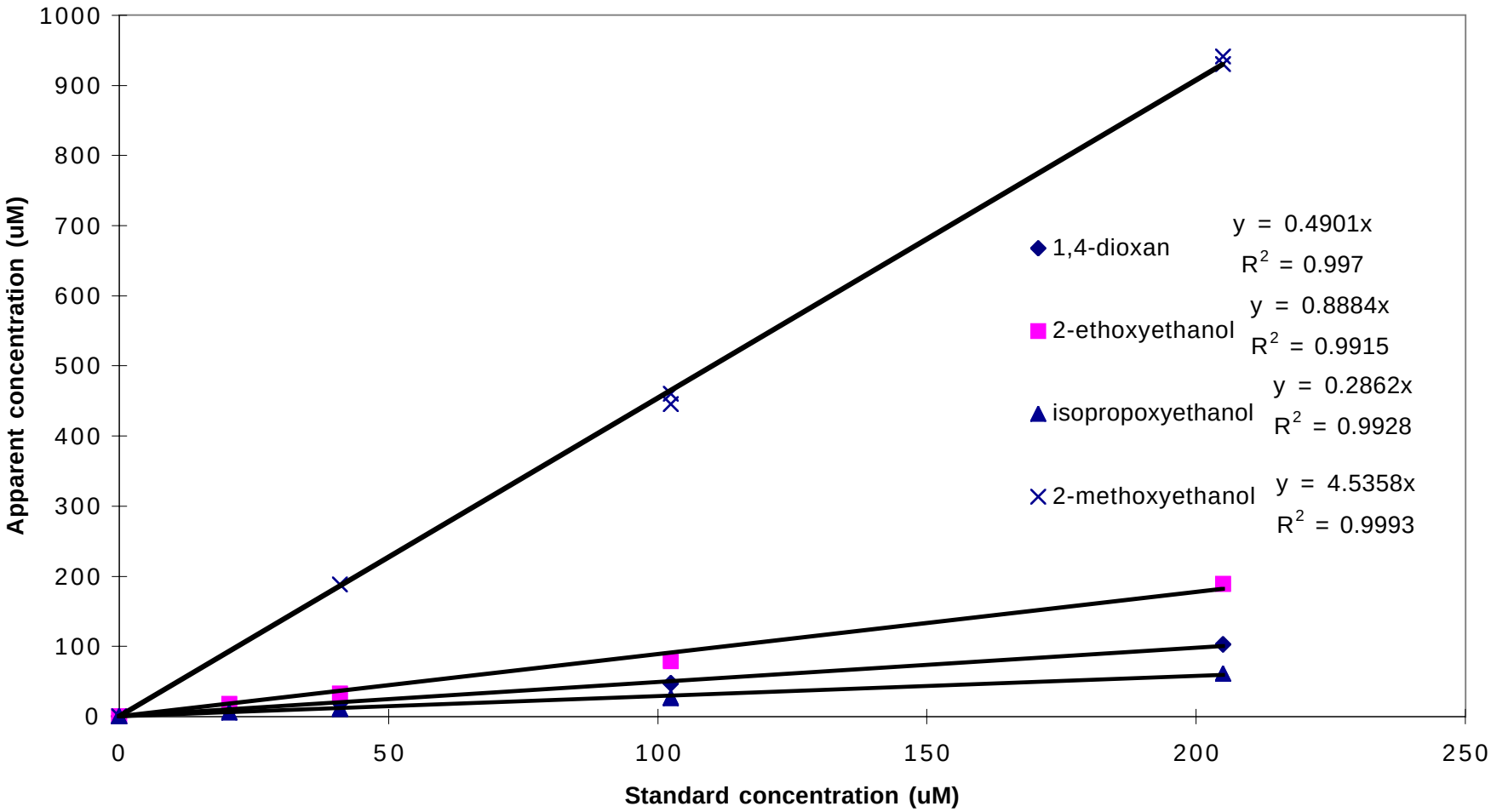

Fig 3.2 Standard curve for 2-ethoxyethanol in MEM using 1-methoxy-2-propanol as an internal standard

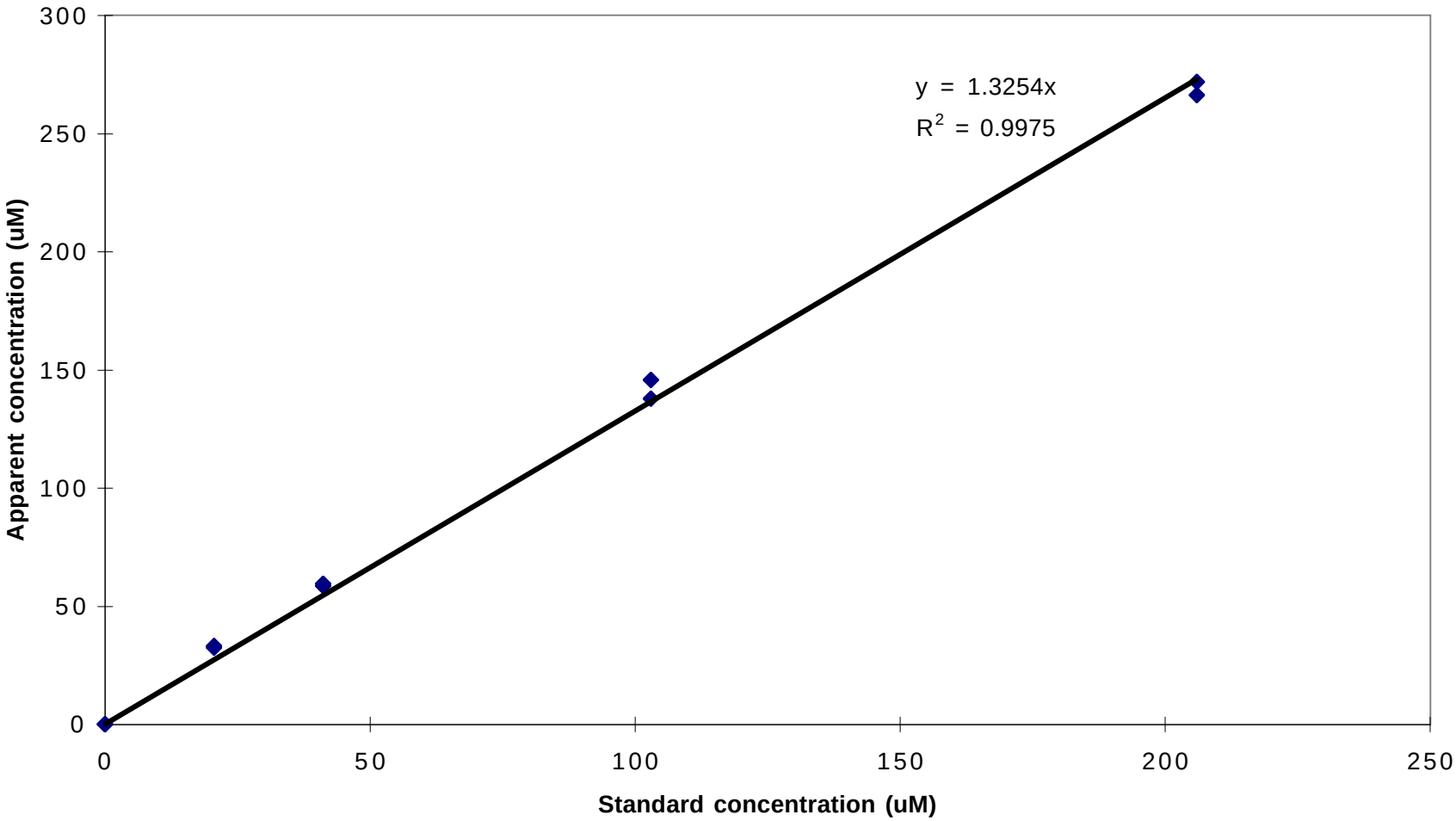

Fig 3.3 Standard curve for 2-butoxyethanol in MEM using isopropoxyethanol as an internal standard

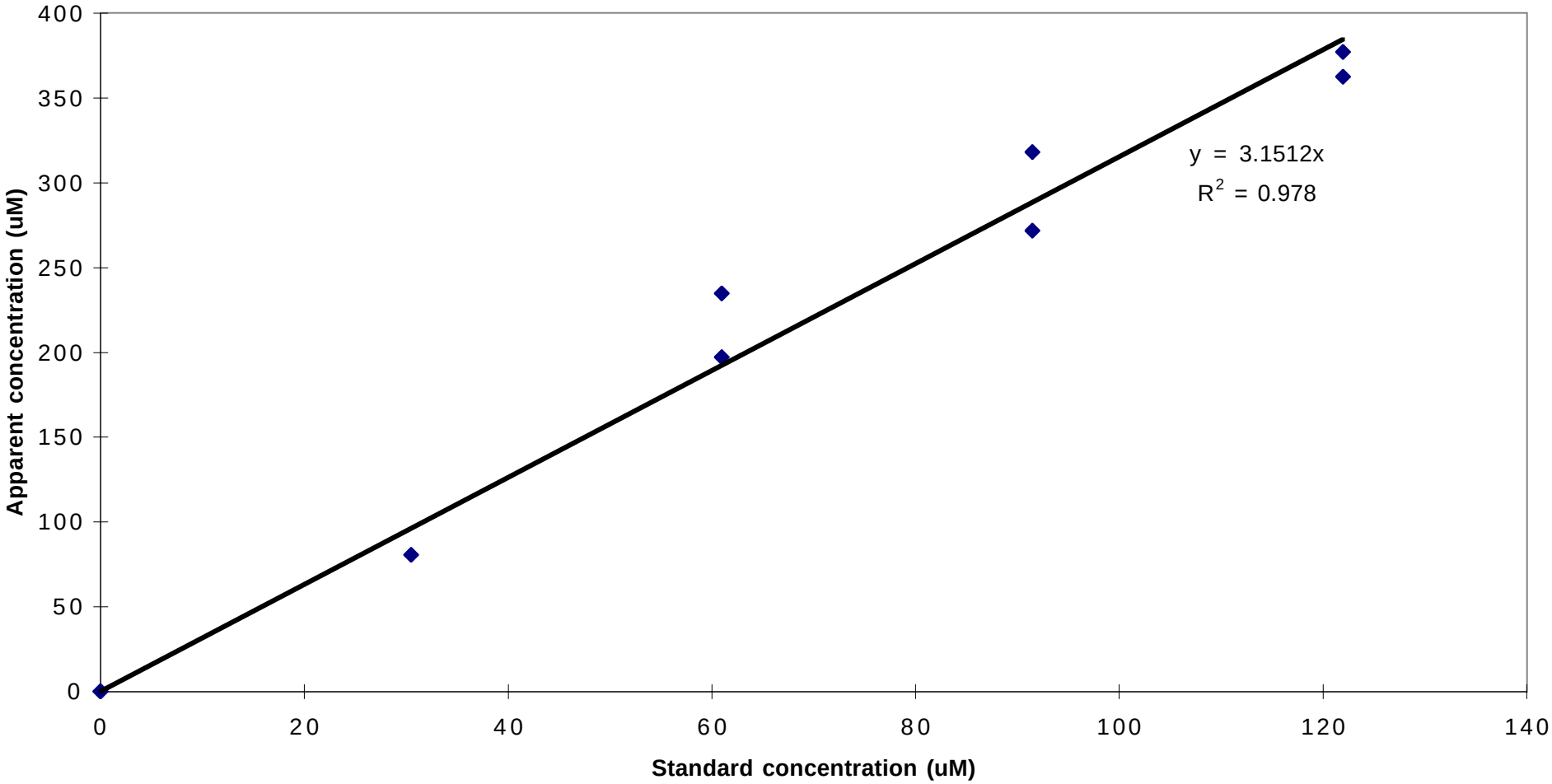

Fig 3.4 Standard curves for MEK,THF and acetone in MEM

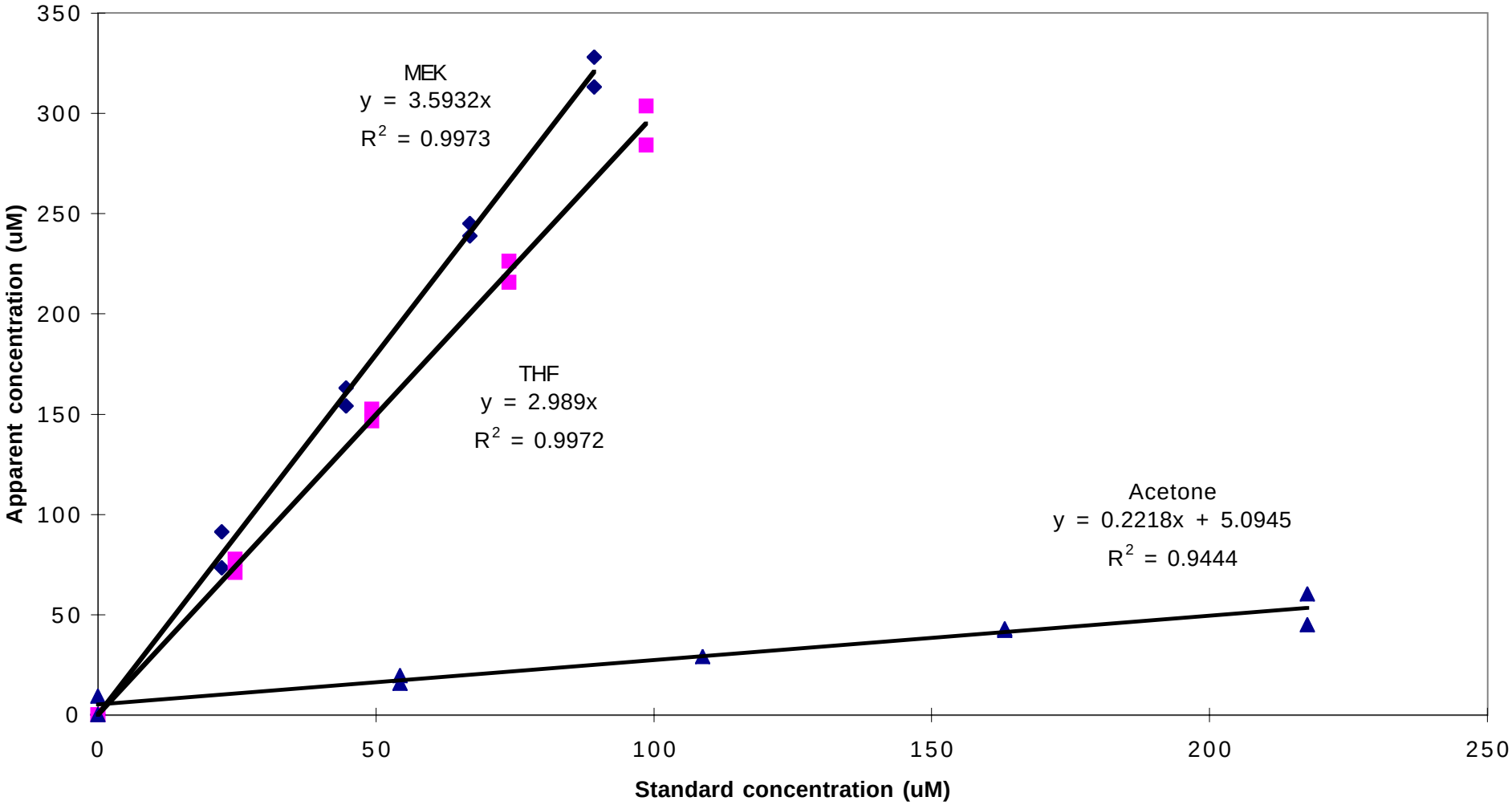

Fig. 3.5 Standard curves for toluene, m-xylene and o-xylene in MEM

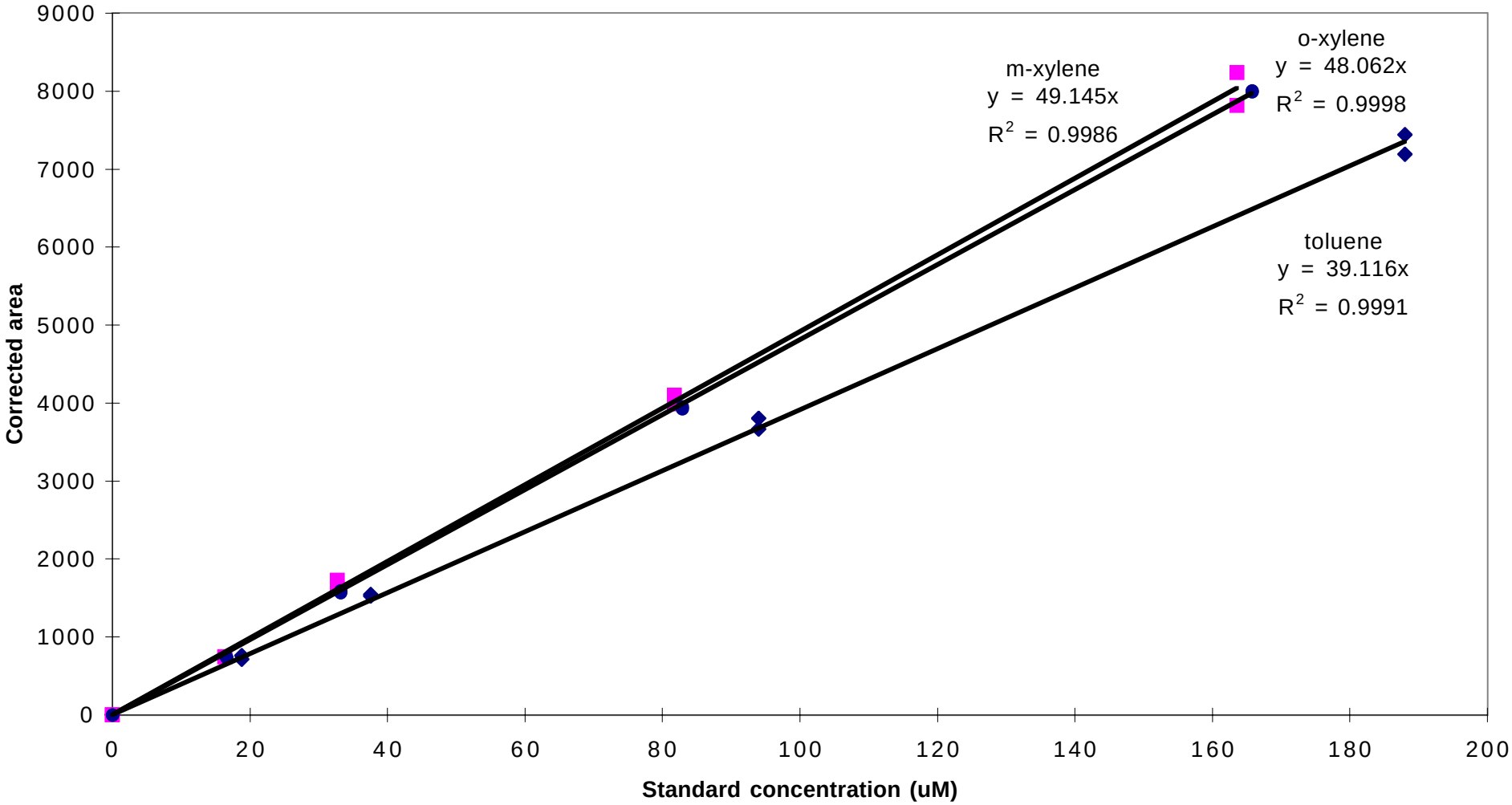

Fig 3.6 Loss of 2-ethoxyethanol and 1-methoxy-2-propanol from MEM at room temperature

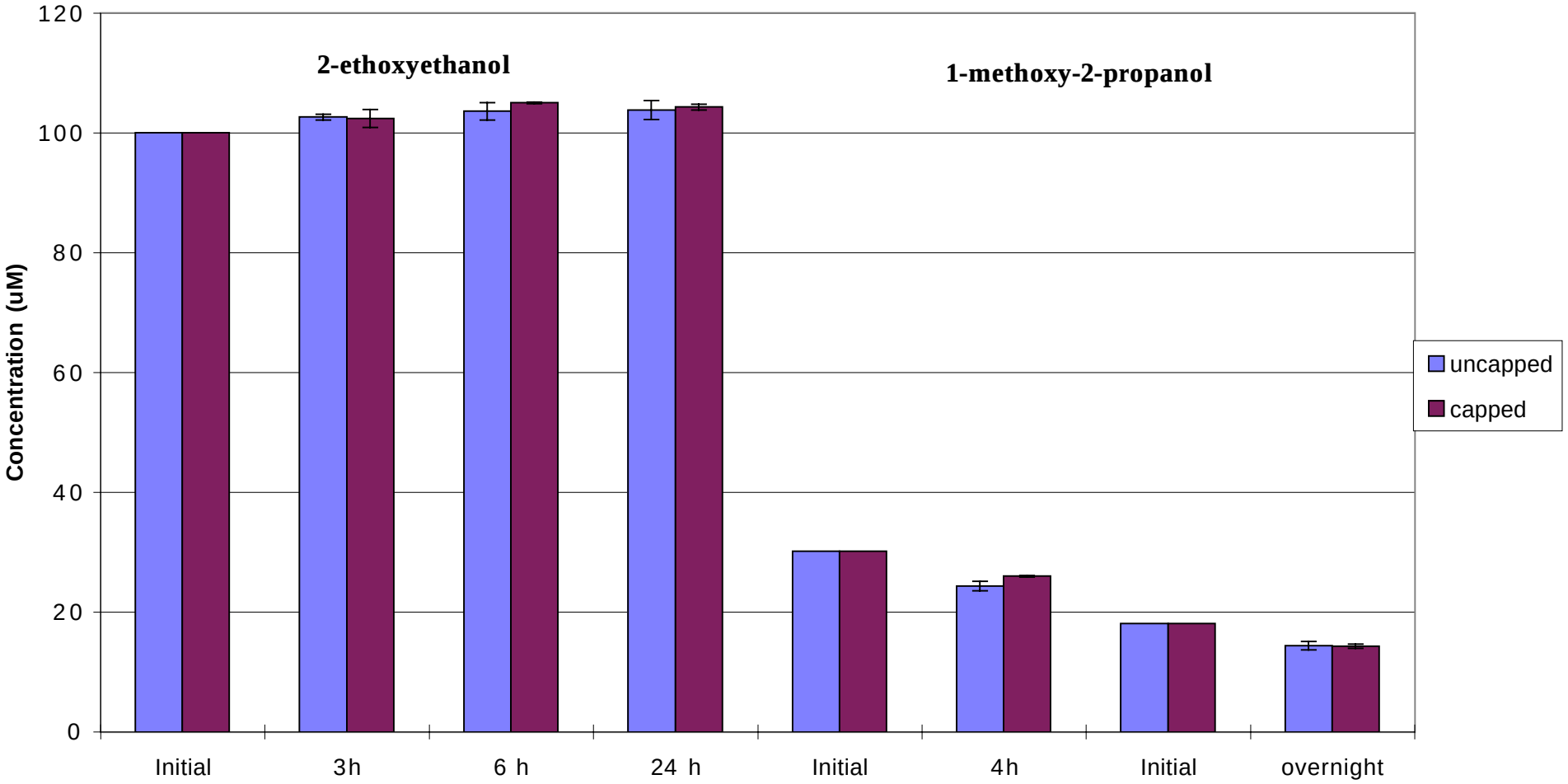

Points are means +/- SEM (n=3)

Fig 3.7 Loss of MEK and THF from MEM at room temperature

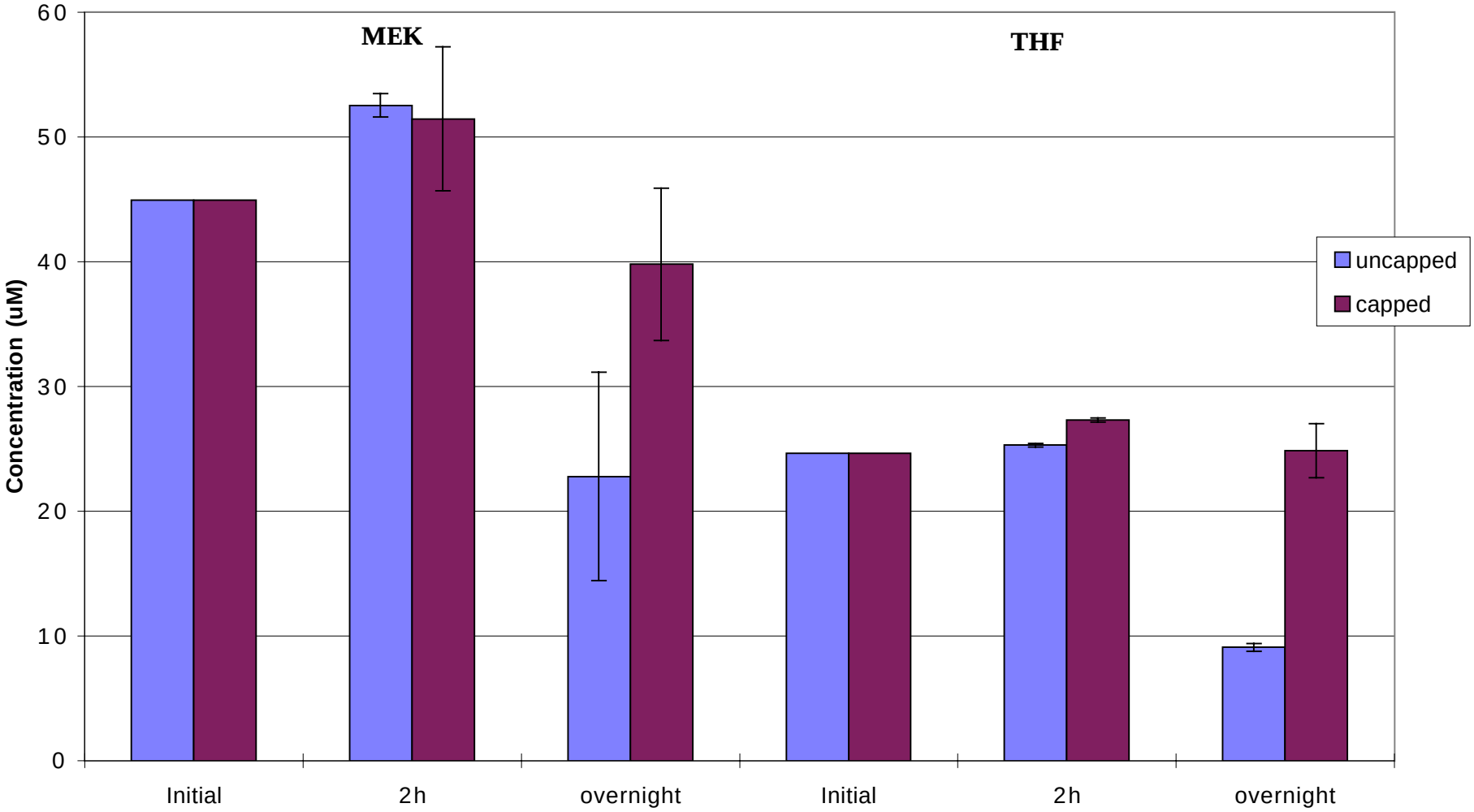

Points are means +/- SEM (n=3)

Fig 3.8 Loss of toluene and xylene (mixed isomers) from MEM at room temperature

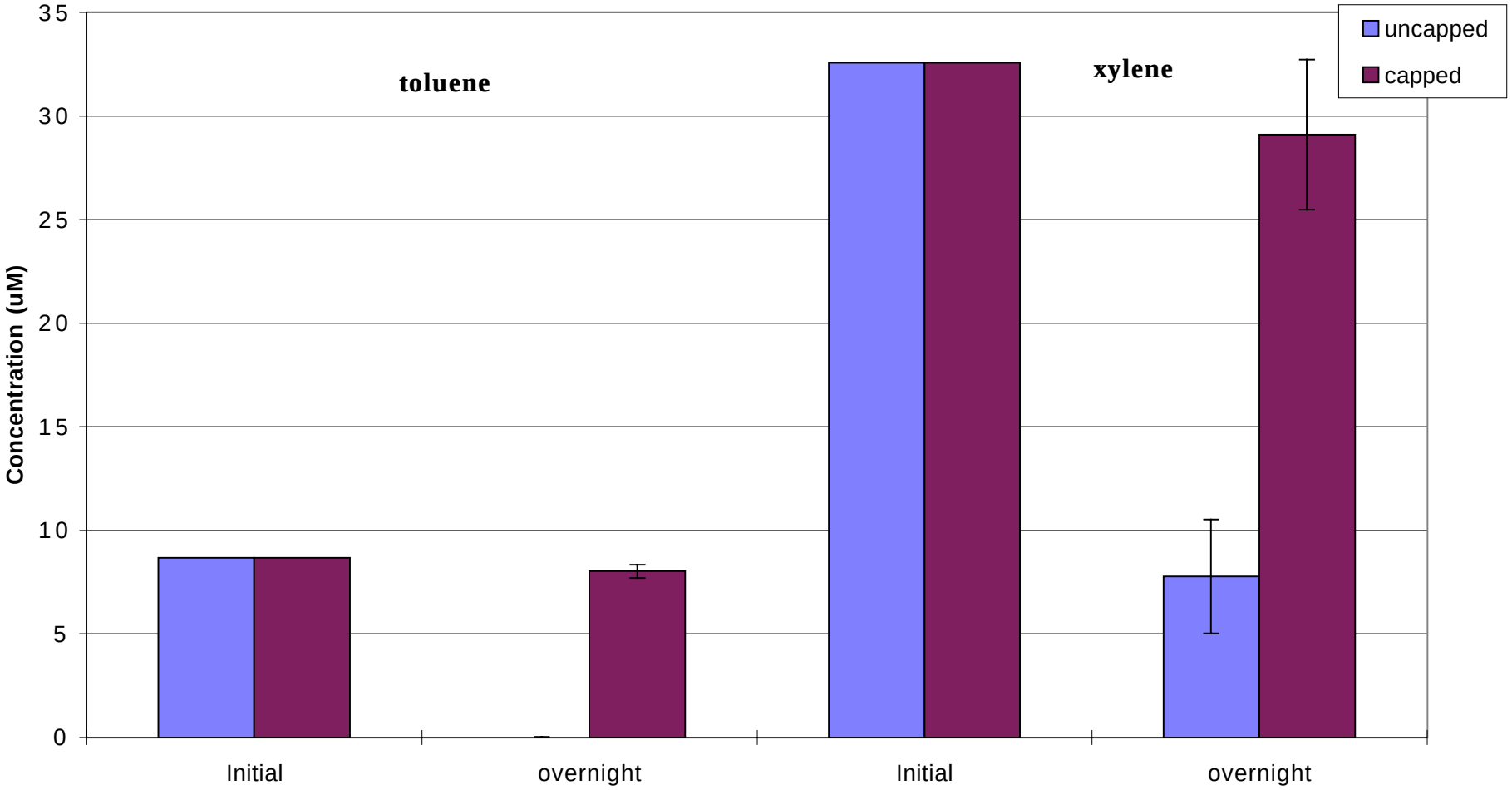

Points are means +/- SEM (n=3)

Fig 4.1 Penetration of glycol ethers through dermatomed human skin in aqueous solution (3 mg/ml, 200 ul of each) in flow through experiments

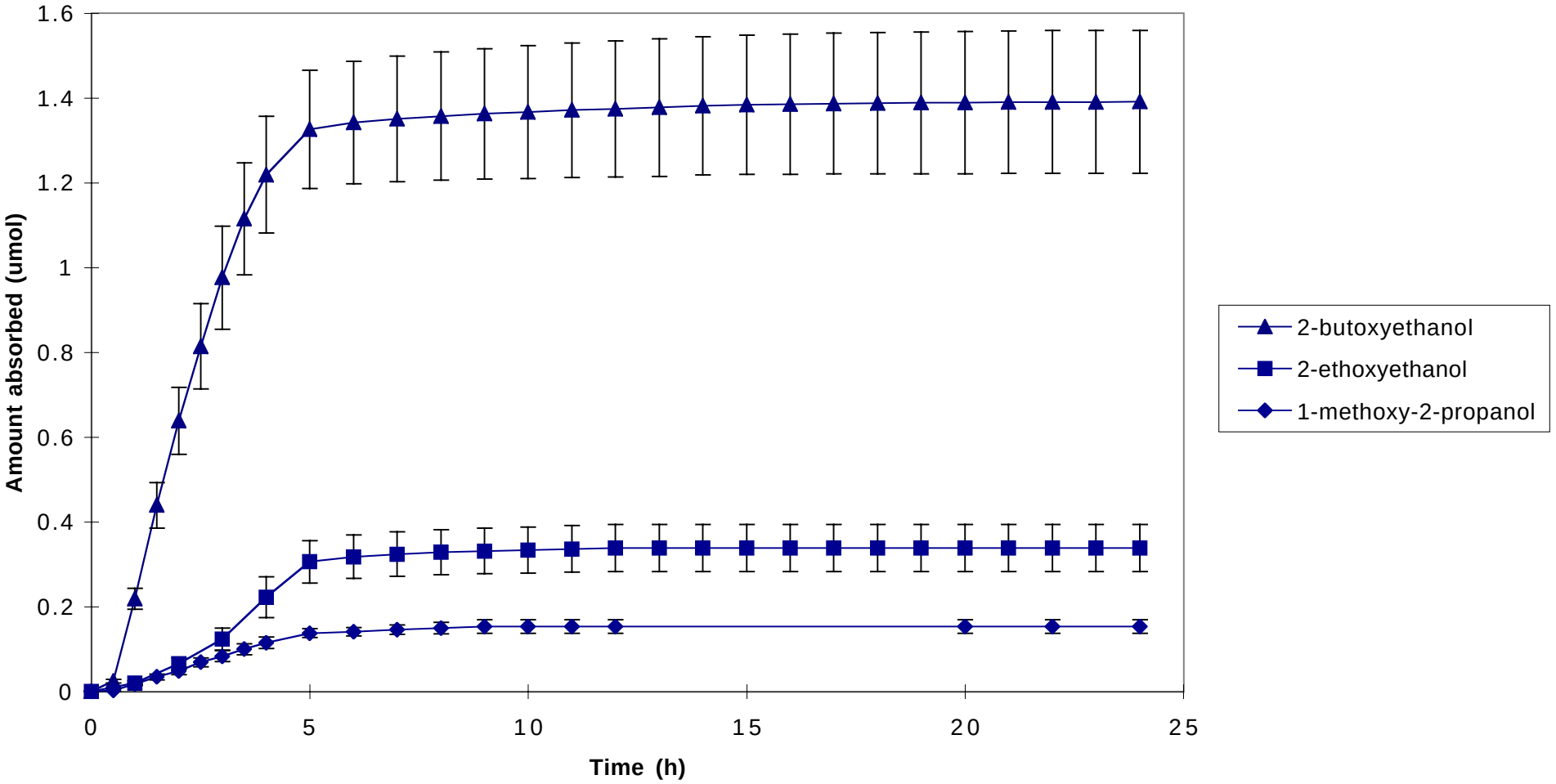

Points are means ± SEM (n=5)

Fig 4.2 Penetration of glycol ethers (3 mg/ml) through dermatomed human skin in aqueous solution - effect of application volume

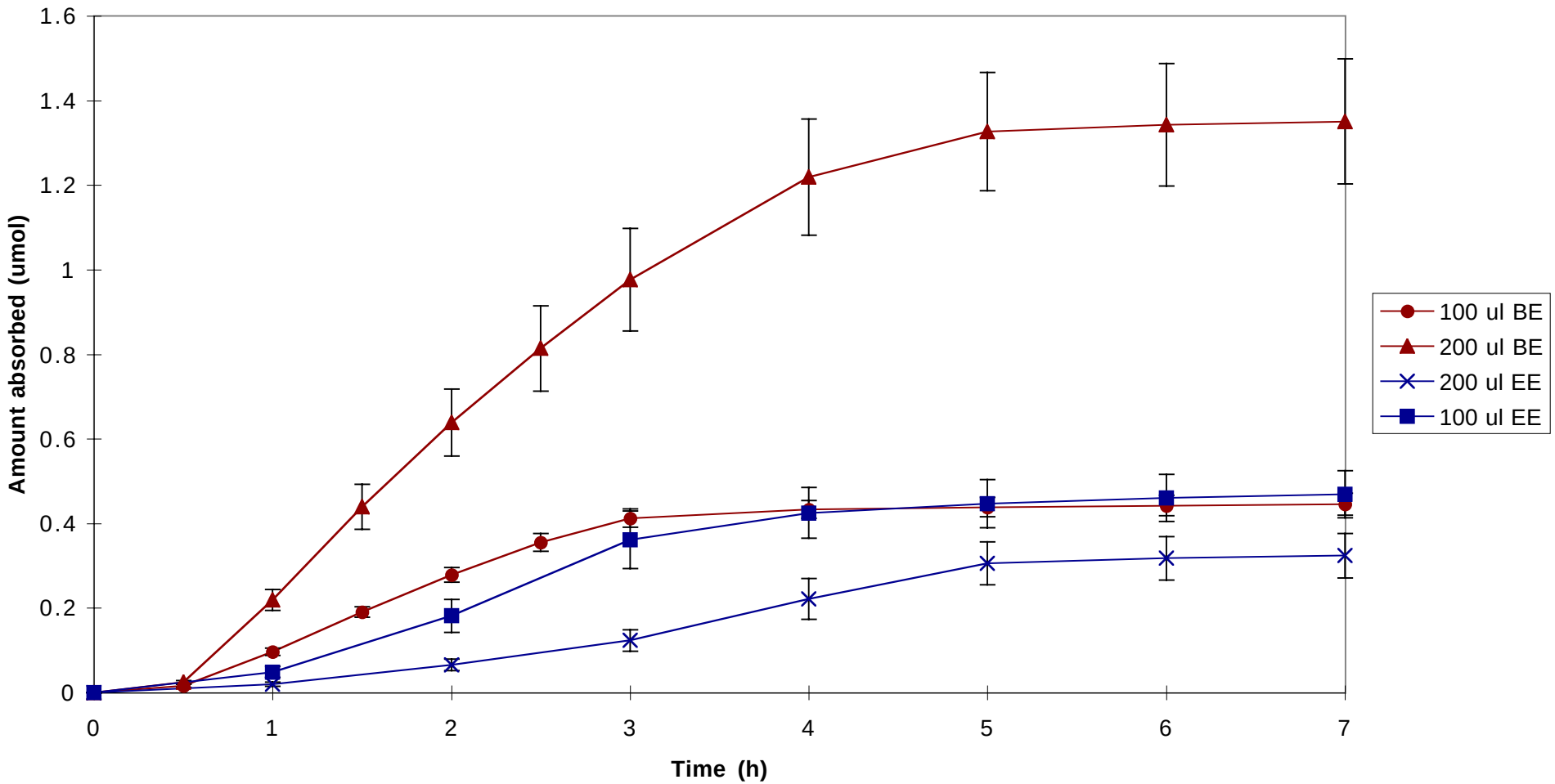

Points are means +/- SEM (n=4/5)

Fig 4.3 Effect of dose concentration on penetration of glycol ethers (200 ul aqueous solution) through dermatomed human skin in vitro

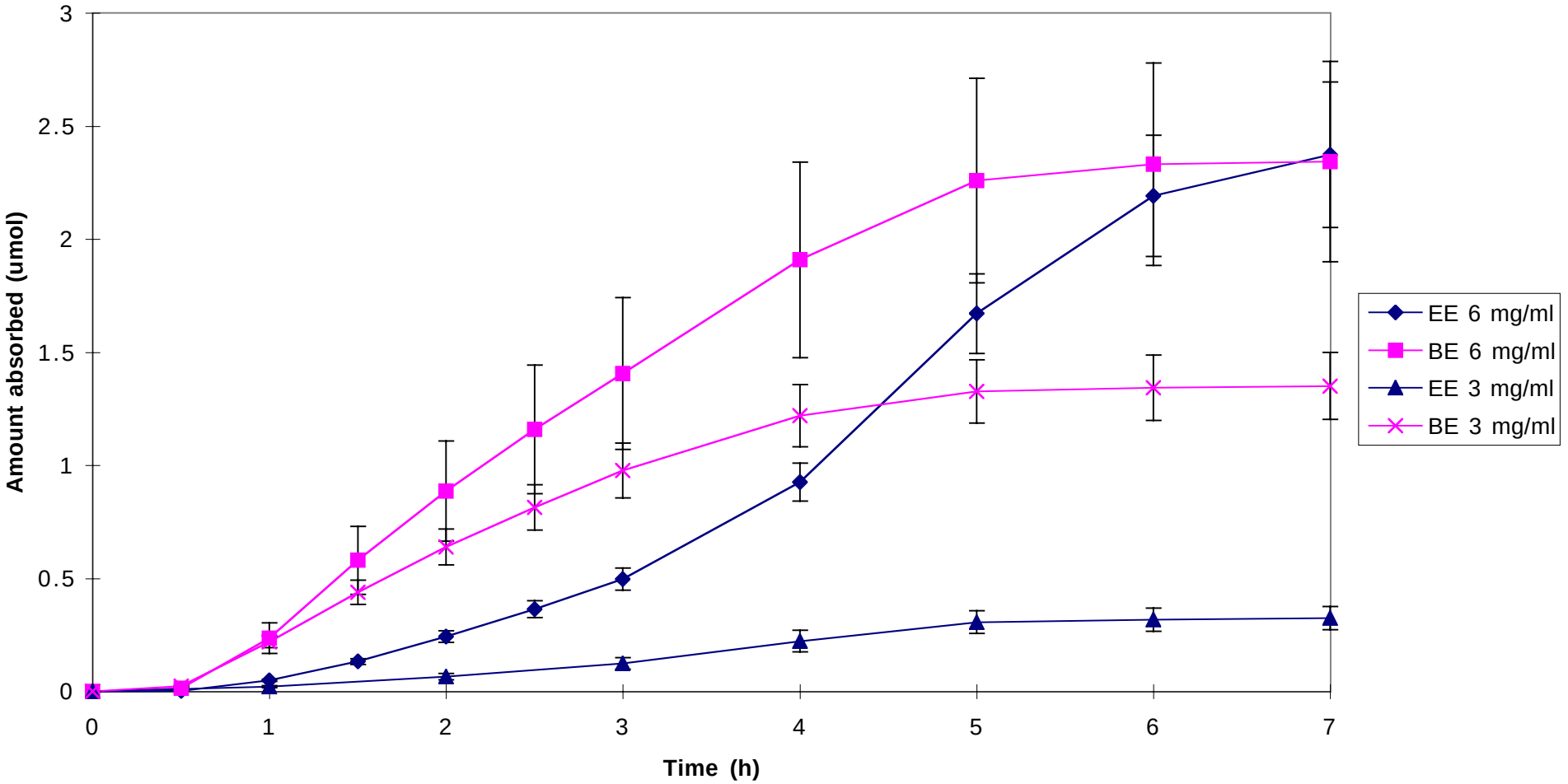

Points are means +/- SEM (n=5)

Fig 4.4 Penetration of glycol ethers (200 ul aqueous solution, 3 mg/ml) through full thickness and dermatomed human skin in vitro

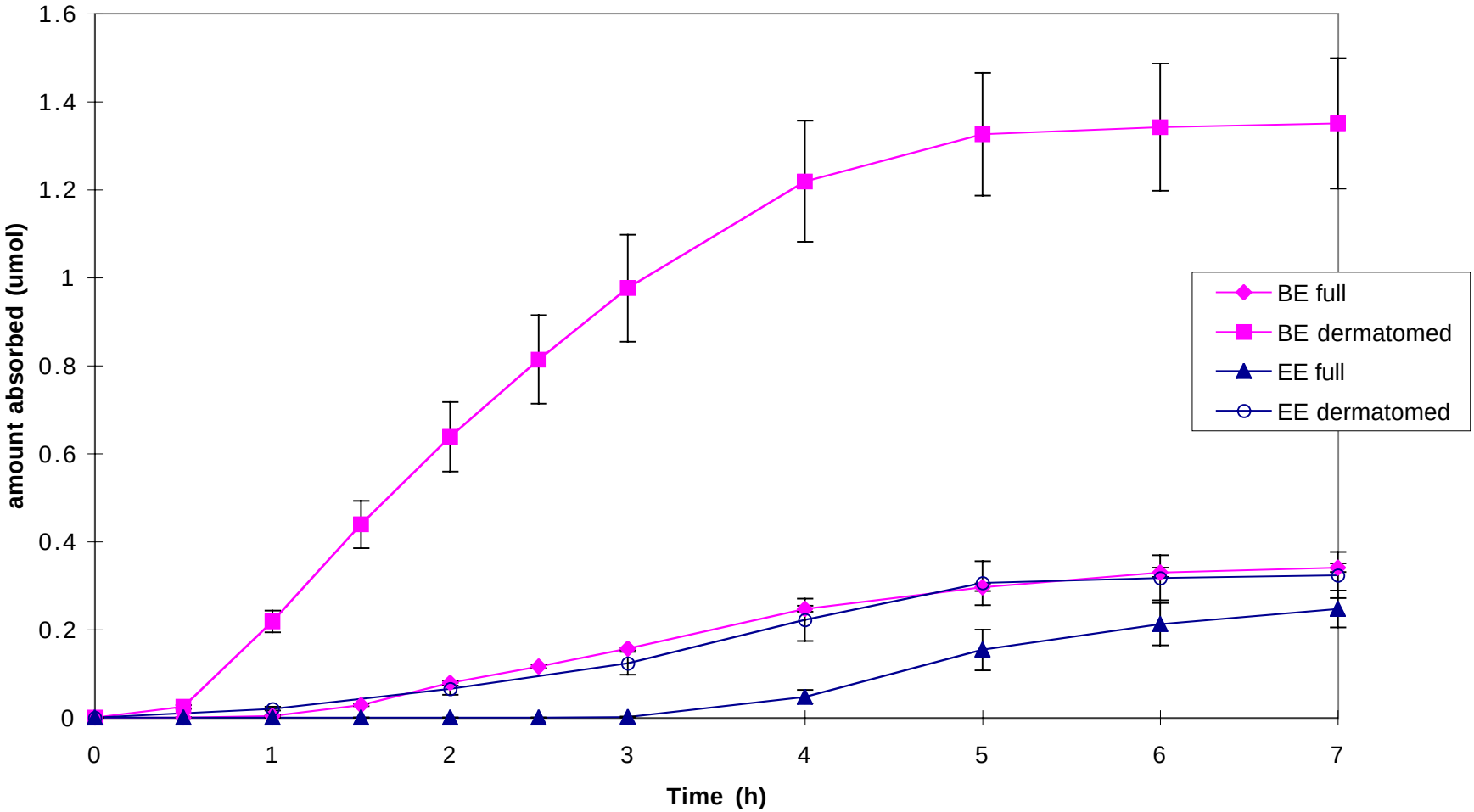

Points are means +/- SEM (n=4/5)

Fig 4.5 Influence of receptor fluid additions on penetration of 2-ethoxyethanol (3 mg/ml aqueous solution, 200 ul) through dermatomed human skin in vitro

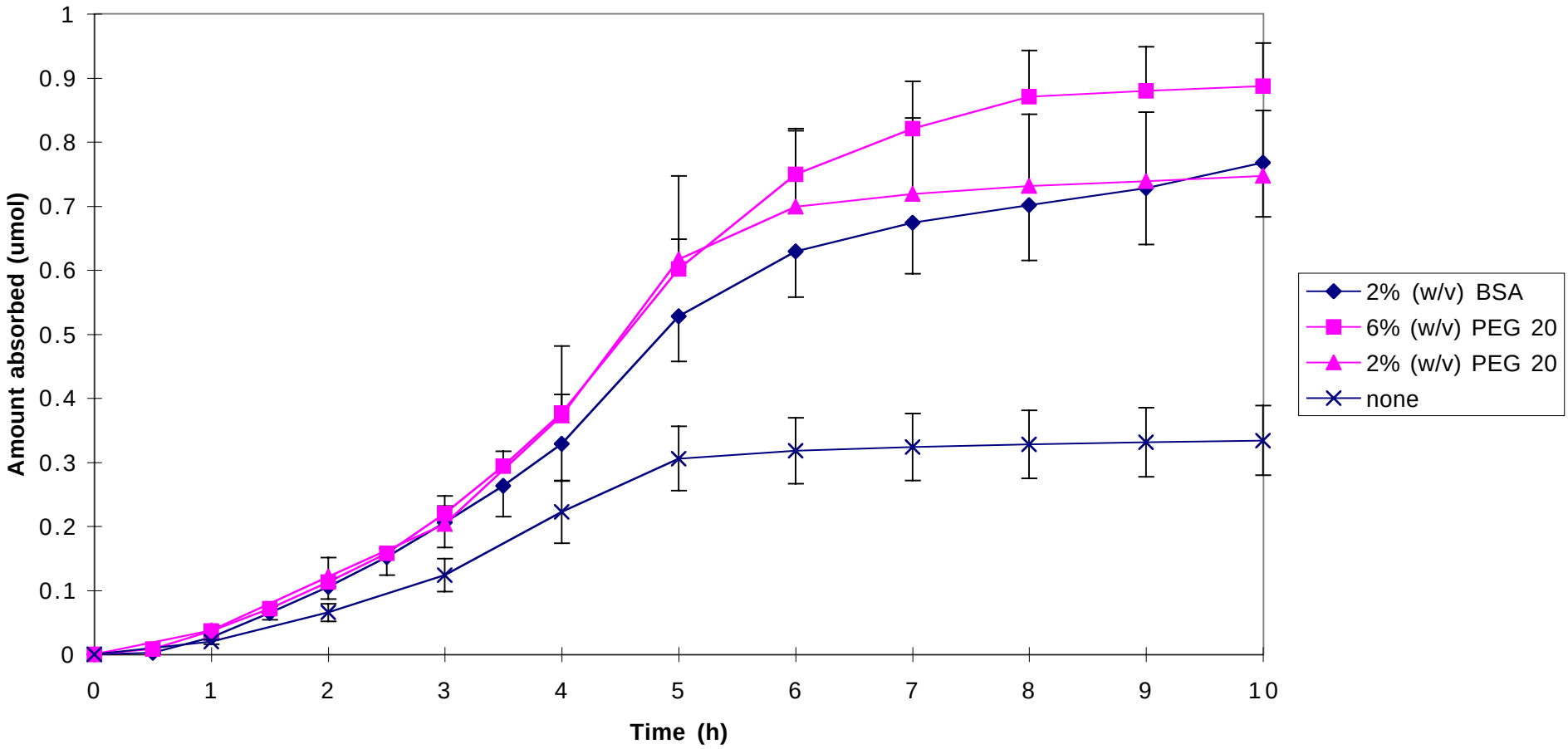

Points are means +/- SEM (n=5/6)

Fig 4.6 Penetration of neat glycol ethers (10.5 ul) through dermatomed human skin in vitro

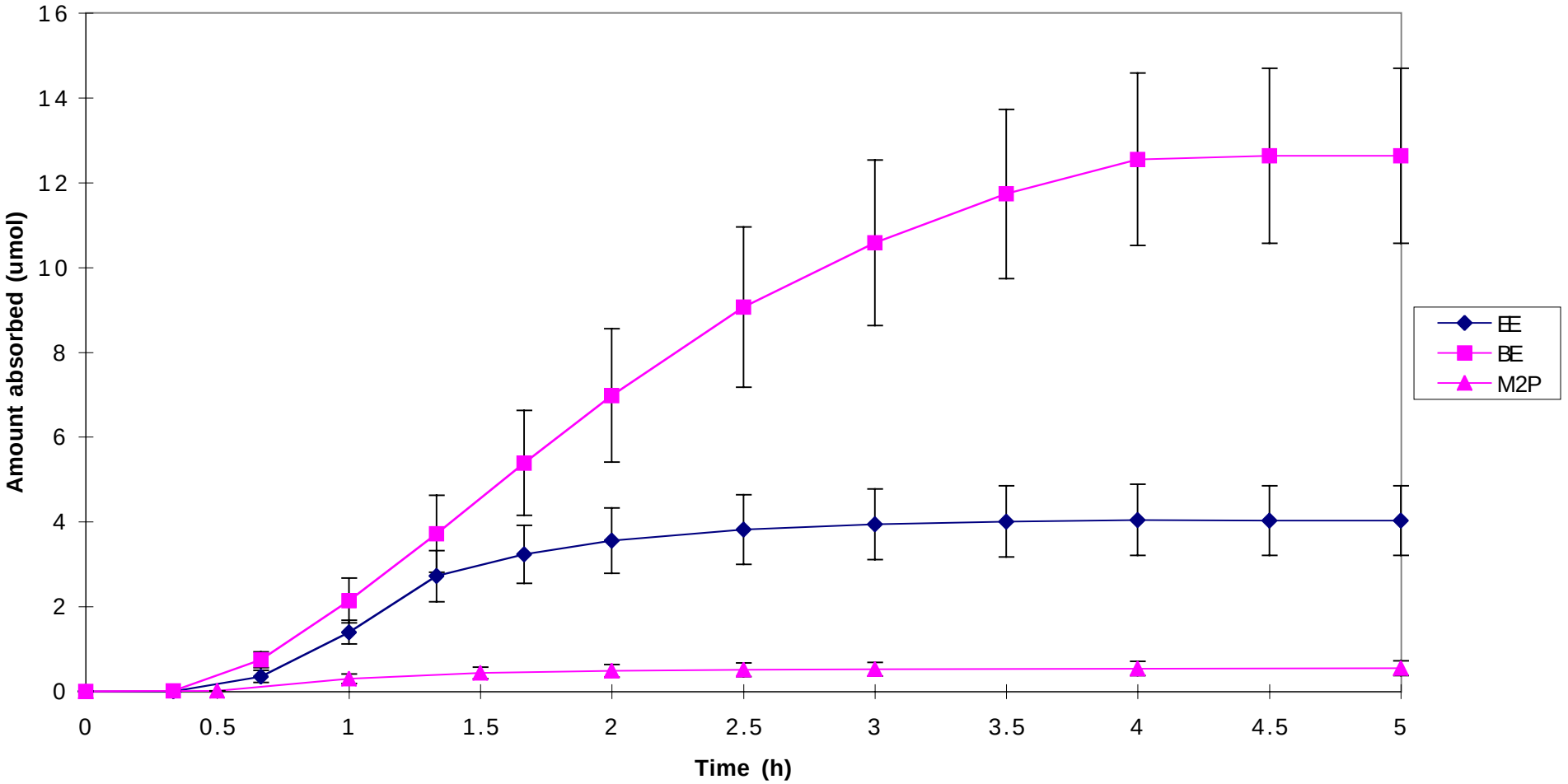

Points are means +/- SEM (n=4/5)

Fig 4.7 Penetration of neat glycol ethers (10.5 ul) through dermatomed human skin in vitro - 6% (w/v) PEG 20 in receptor fluid

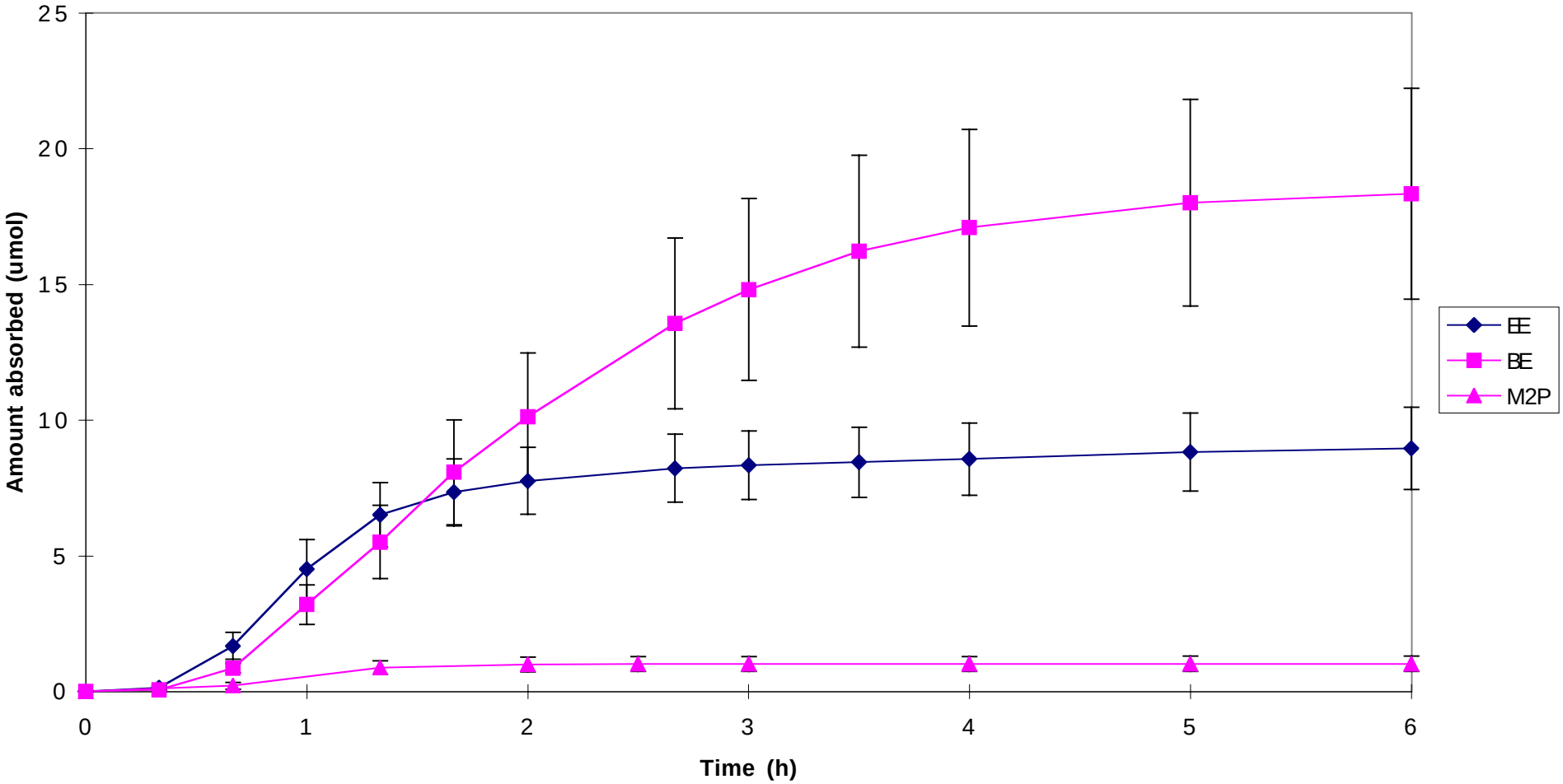

Points are means +/- SEM (n=4/5)

Fig 5.1 Penetration of neat MEK, THF and acetone (10.5 ul) through dermatomed human skin in vitro

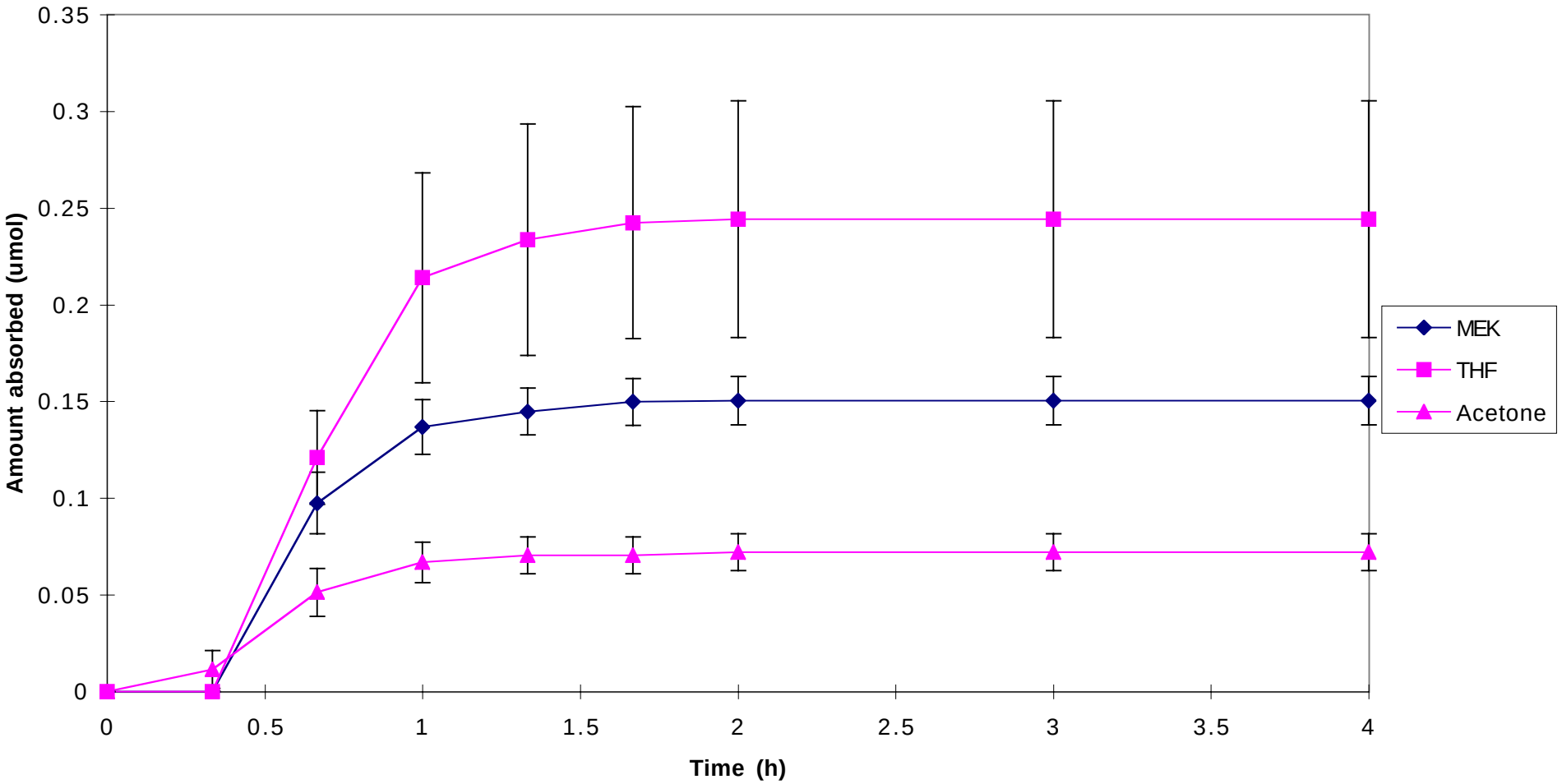

Points are means +/- SEM (n=4/5)

Fig 5.2 Penetration of MEK, THF and acetone in aqueous solution (200 ul, 3 mg/ml) through dermatomed human skin in vitro

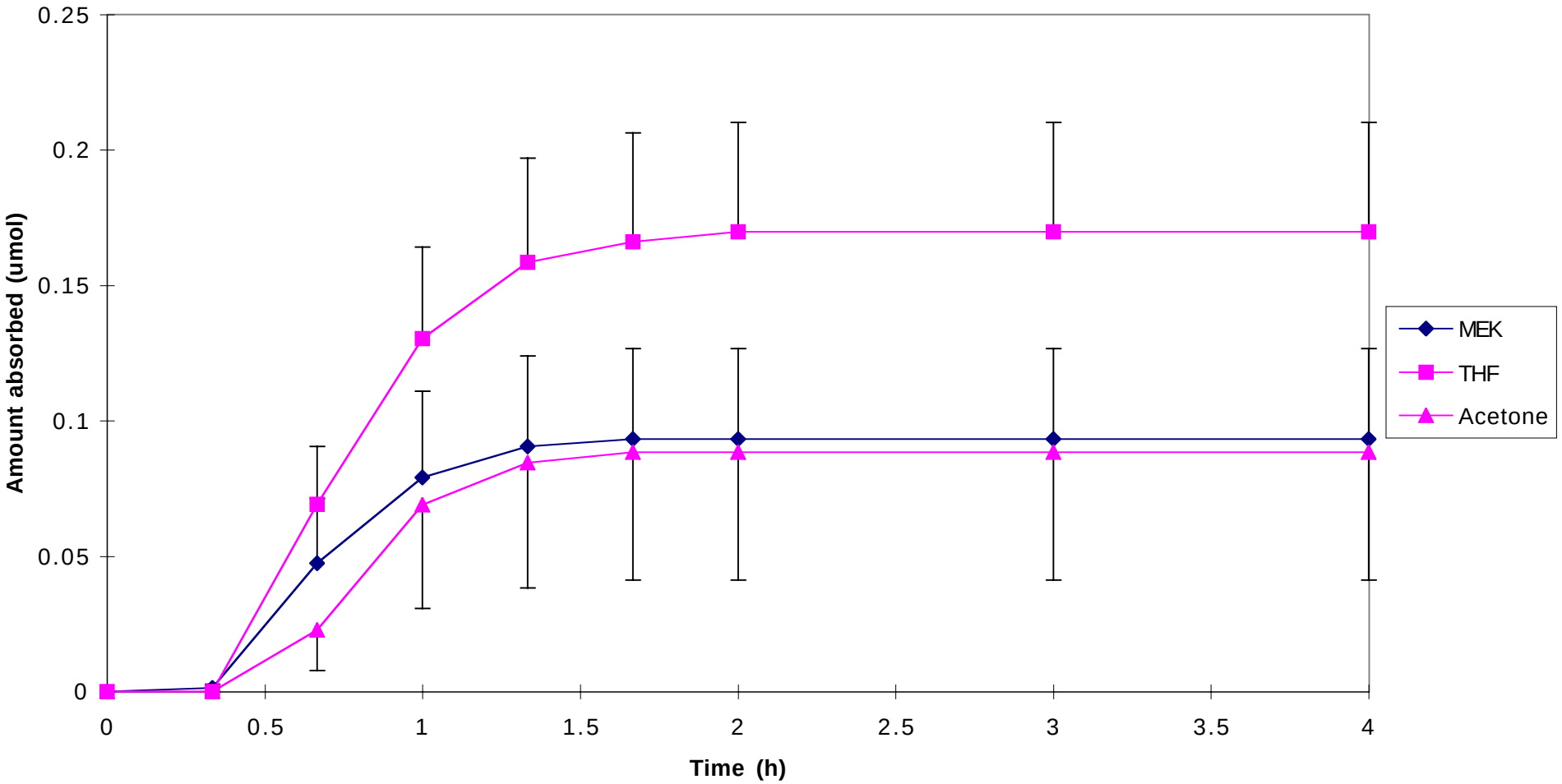

Points are means +/- SEM (n=4/5)

Fig 6.1 Penetration of neat toluene, m-xylene and o-xylene (10.5 ul) through dermatomed human skin in vitro

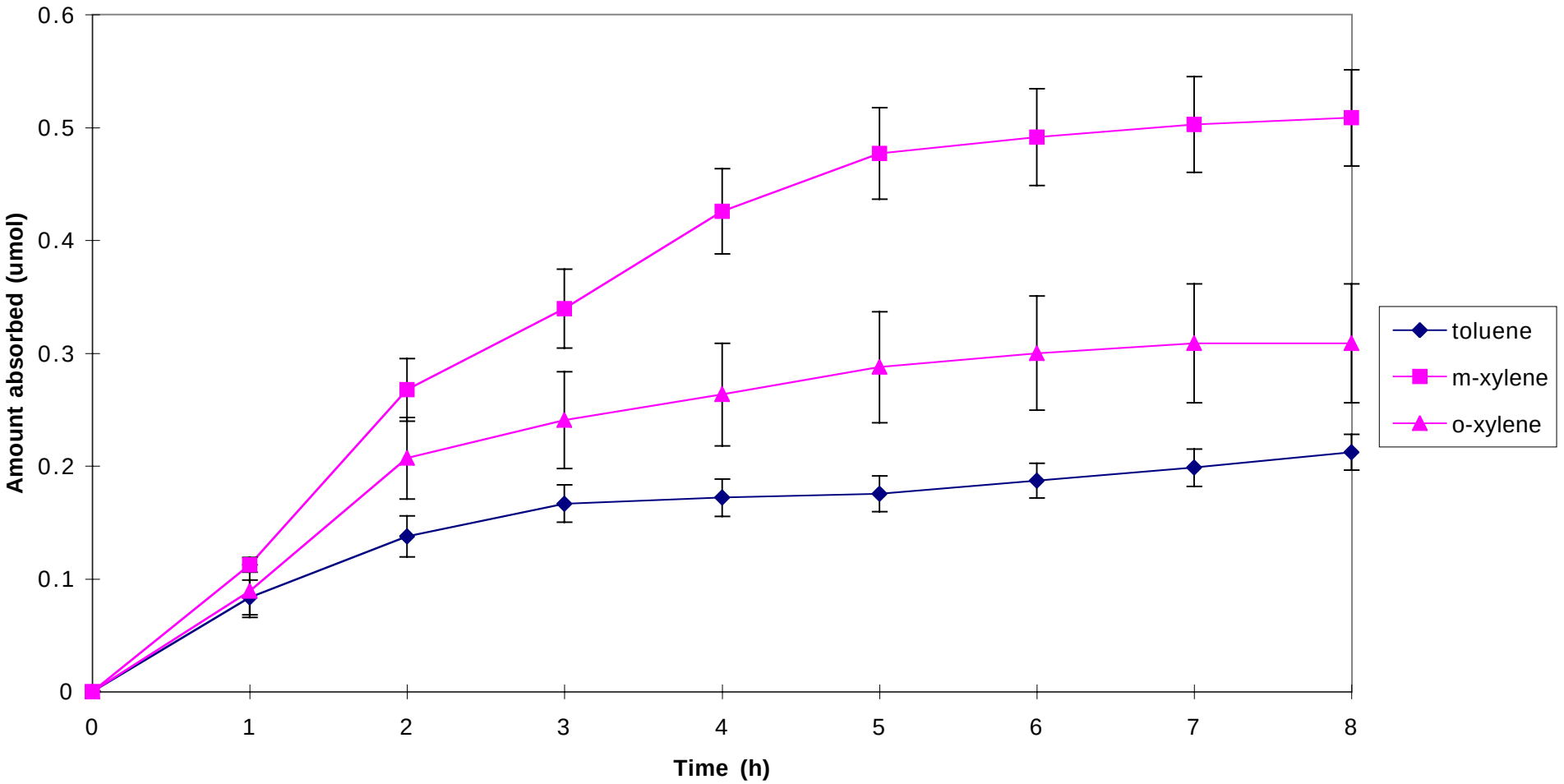

Points are means +/- SEM (n=4)

Fig 6.2 Penetration of toluene (211.8 uM), m-xylene (244.1 uM) and o-xylene (295.8 uM) in aqueous solution (200 ul) through dermatomed human skin in vitro

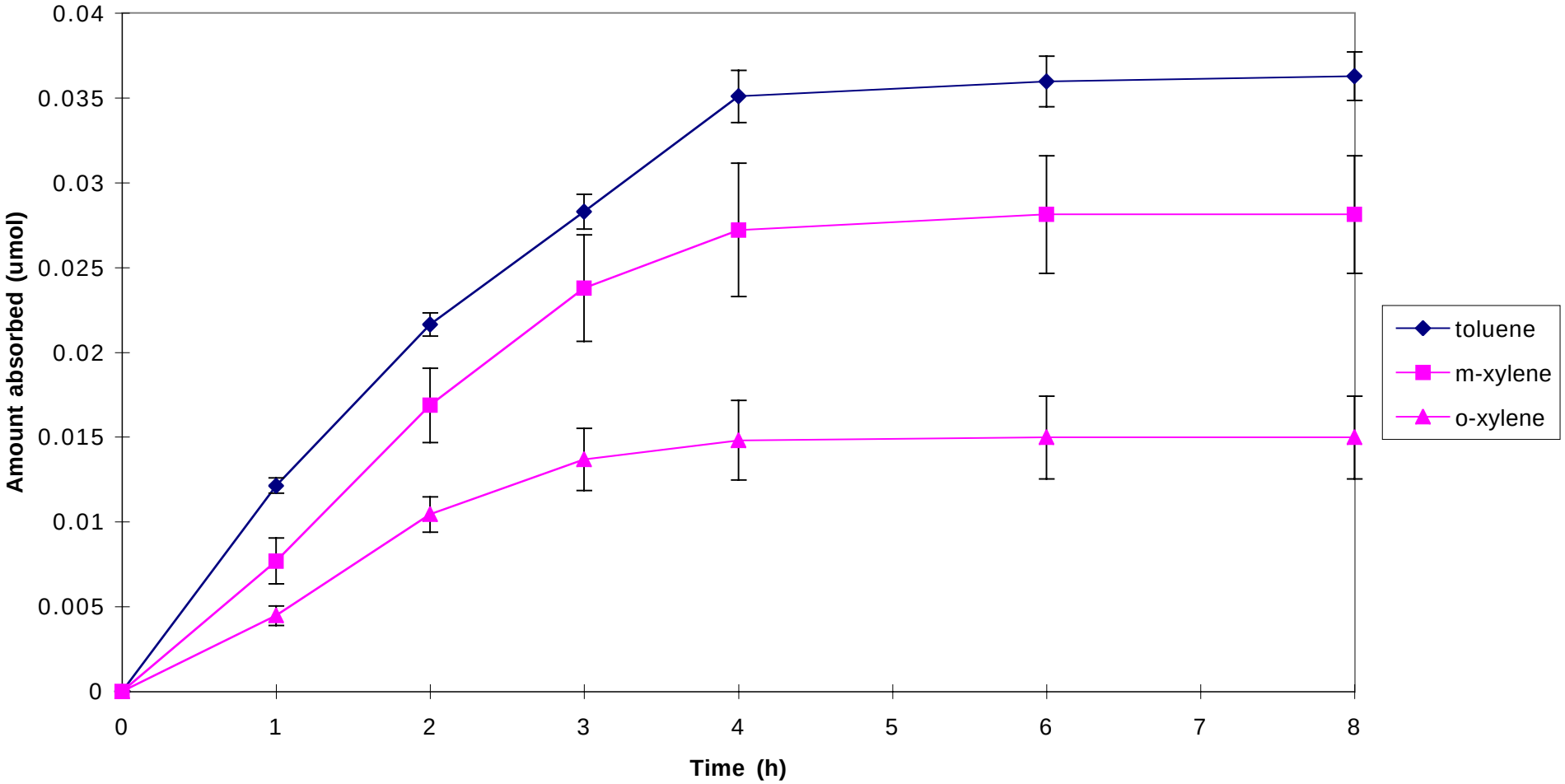

Points are means +/- SEM (n=4)

Fig S.3.1 Dermal absorption of pyridine in aqueous vehicle through human skin in vitro - influence of dose concentration

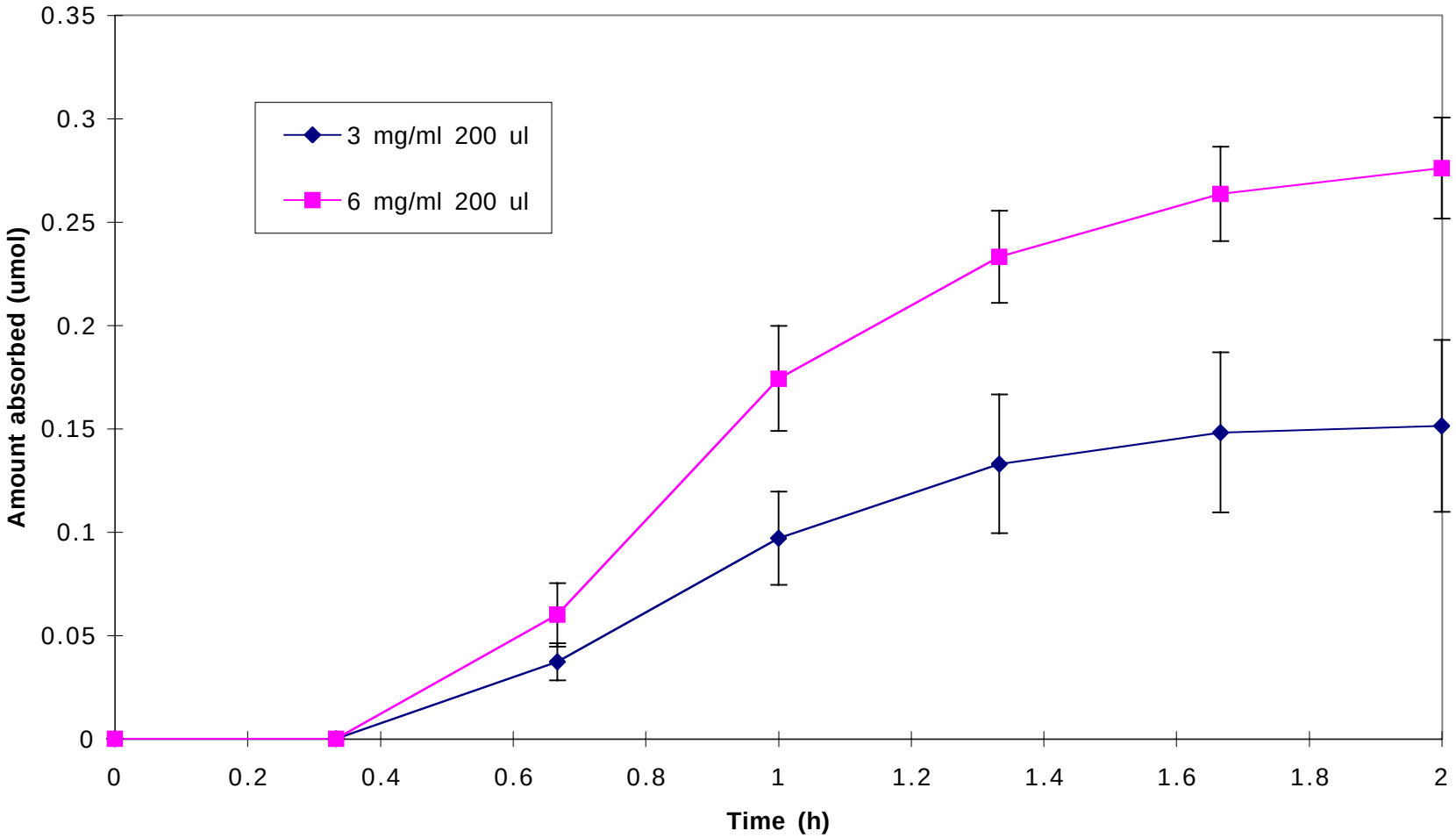

Fig S.3.2 Dermal absorption of aqueous pyridine and its derivatives (3 mg/ml, 200 ul) through dermatomed human skin in vitro

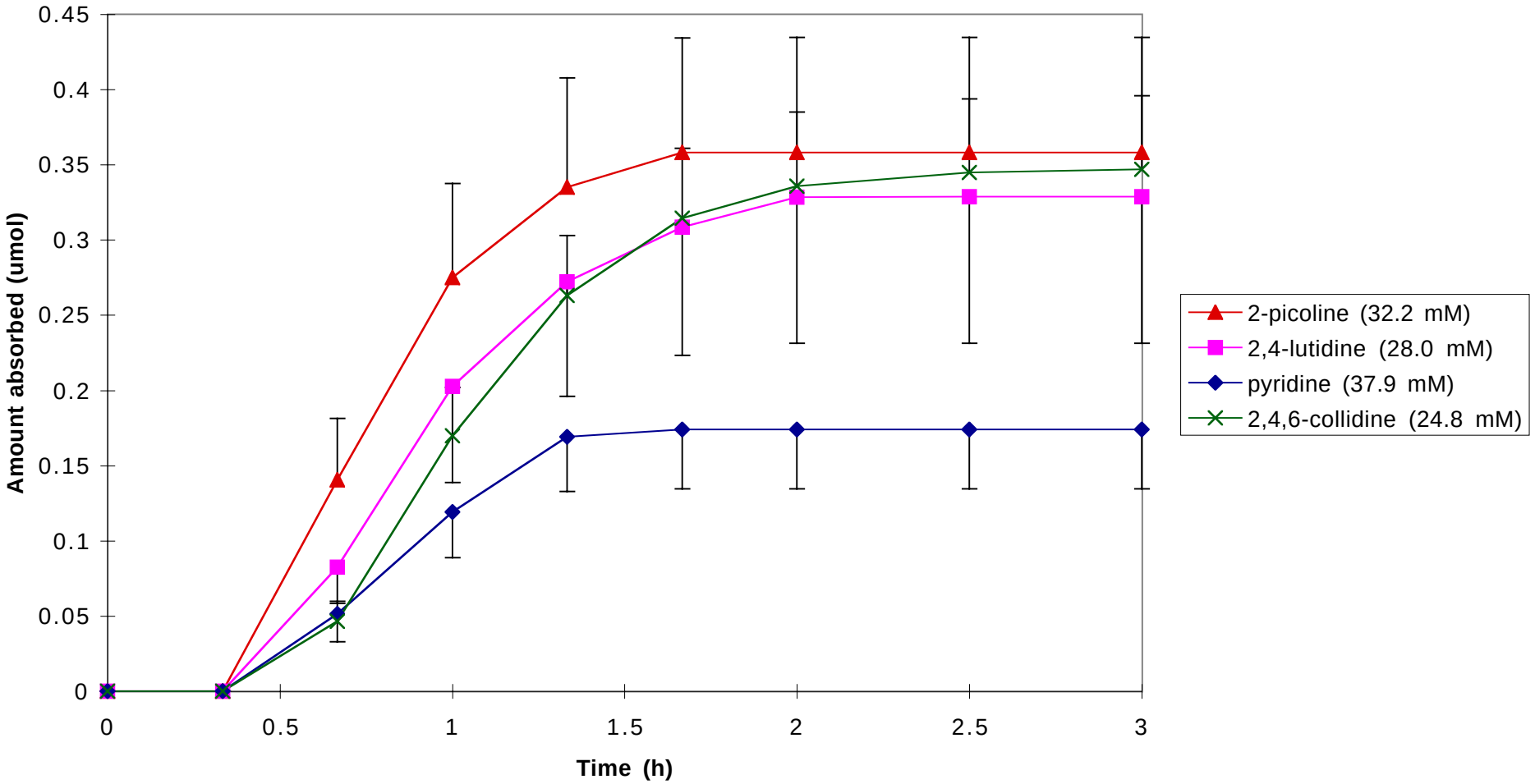

Fig S.3.3 Dermal penetration of neat finite (10 ul) pyridine and its derivatives through dermatomed human skin in vitro

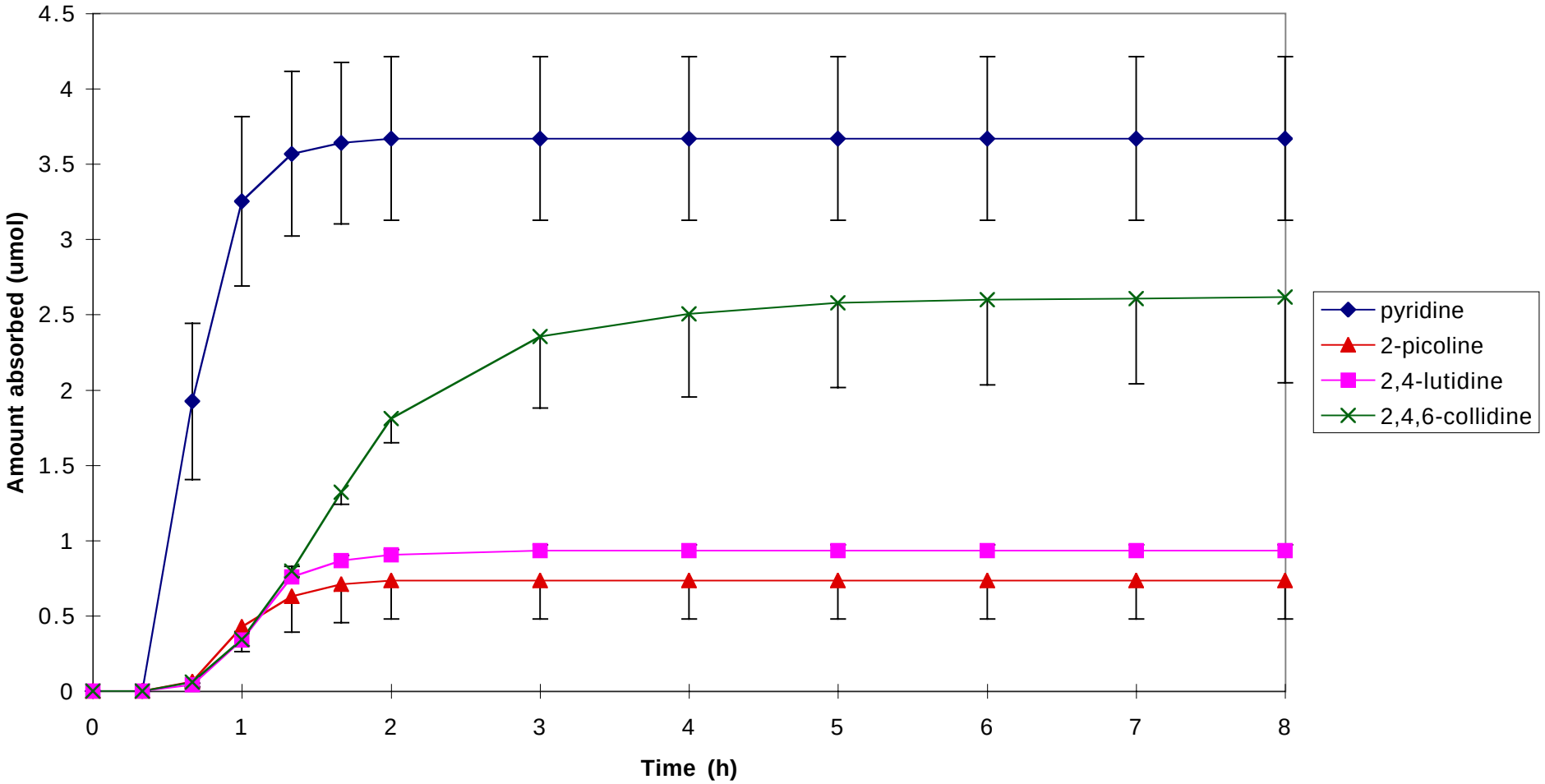

Fig S.4.1 Influence of log P on apparent permeability coefficient for a range of solvents from neat finite doses

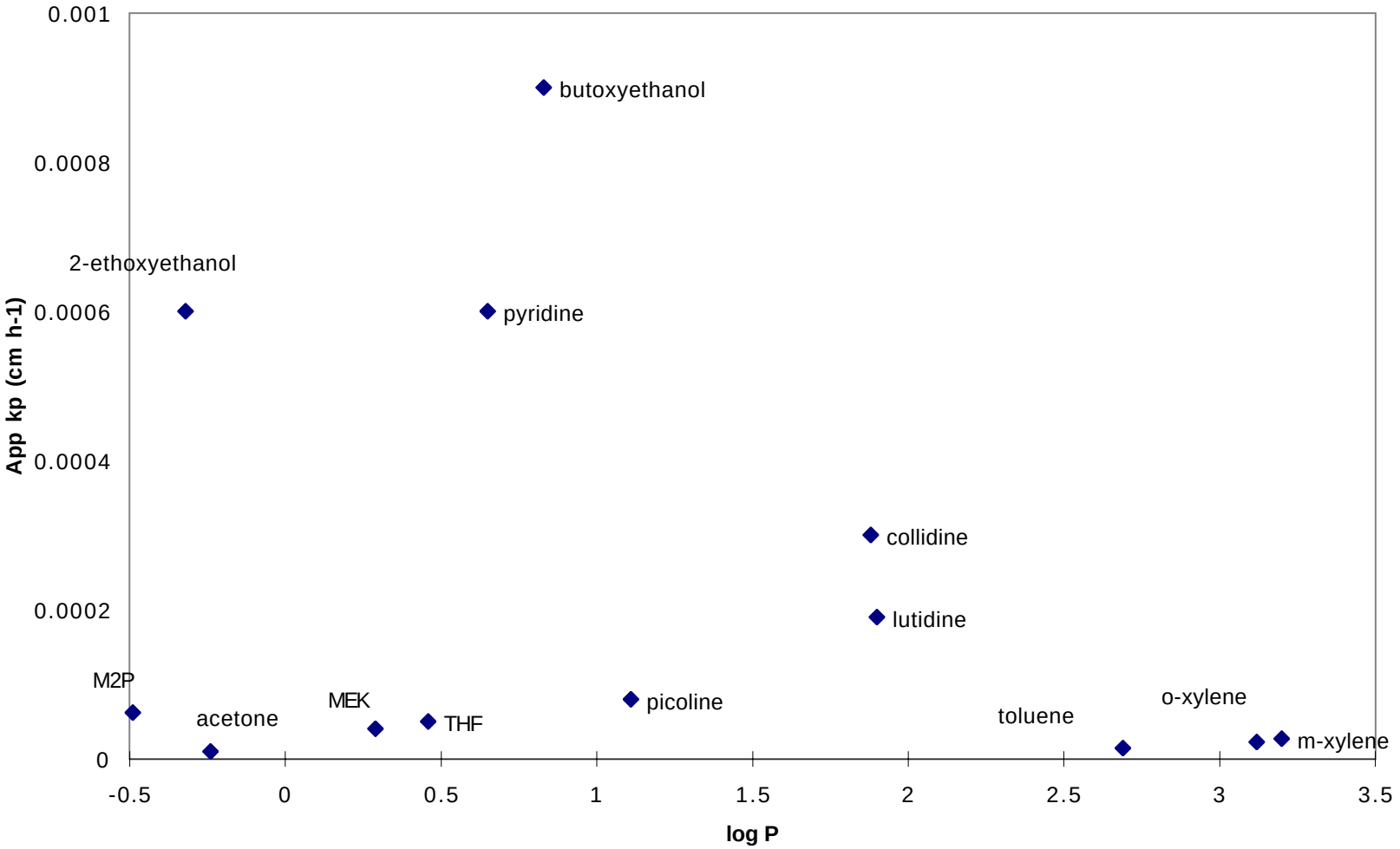

Fig S.4.2 Influence of log P on apparent permeability coefficient for a range of solvents from aqueous doses (3 mg/ml, 200 ul)

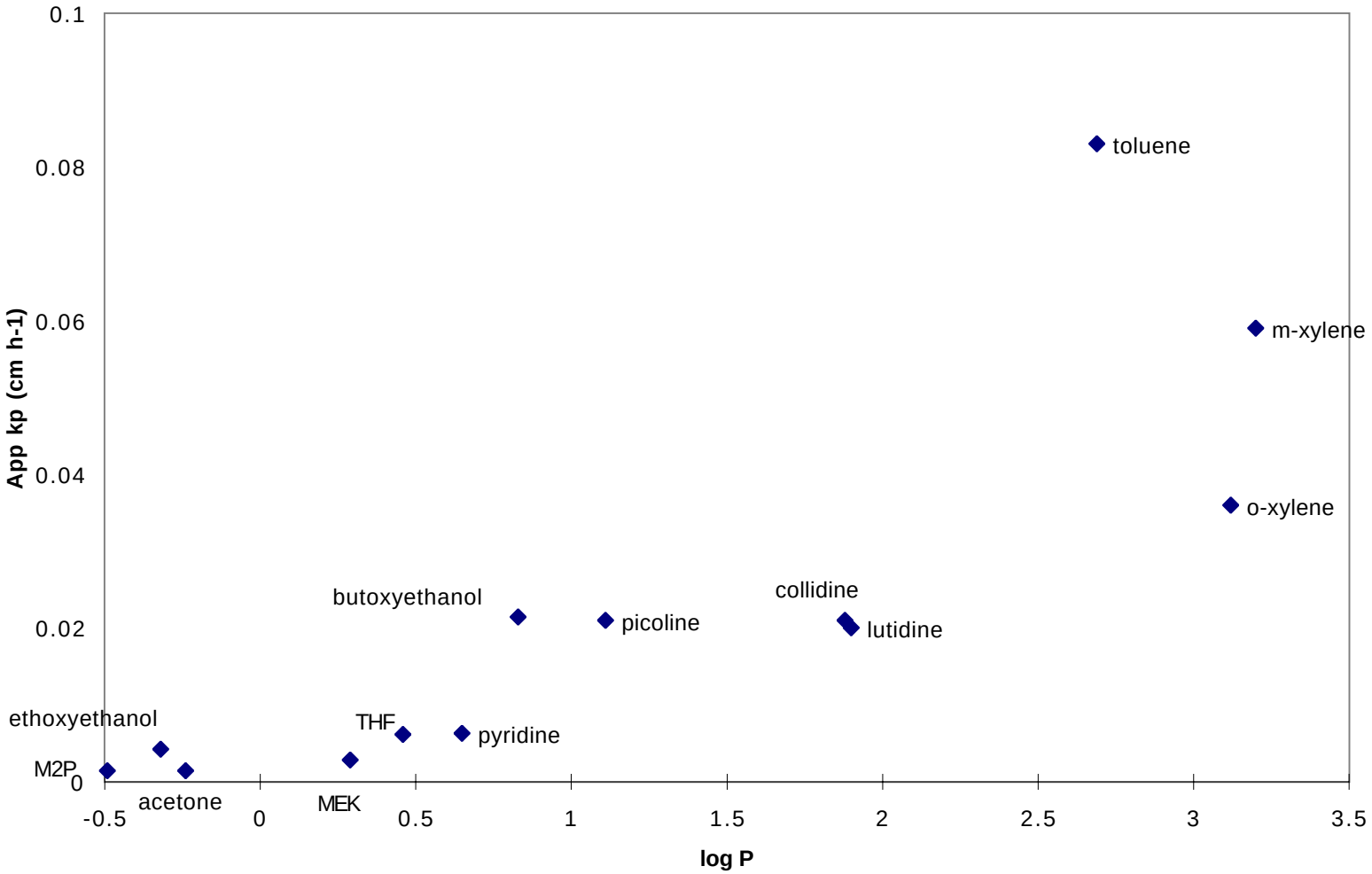

Printed and published by the Health and Safety Executive
C1 06/01

MAIL ORDER
HSE priced and free
publications are
available from:
HSE Books
PO Box 1999
Sudbury
Suffolk CO10 2WA
Tel: 01787 881165
Fax: 01787 313995
Website: www.hsebooks.co.uk

RETAIL
HSE priced publications
are available from booksellers

HEALTH AND SAFETY INFORMATION
HSE InfoLine
Tel: 08701 545500
Fax: 02920 859260
e-mail: hseinformationservices@natbrit.com
or write to:
HSE Information Services
Caerphilly Business Park
Caerphilly CF83 3GG

HSE website: www.hse.gov.uk

CRR 350

£25.00

ISBN 0-7176-2048-4

9 780717 620487